THE STELLAR COMPOSITION AND EVOLUTION OF IRREGULAR AND OTHER LATE-TYPE GALAXIES

Thesis by

William G. Bagnuolo, Jr.

In Partial Fulfillment of the Requirements

for the Degree of

Doctor of Philosophy

California Institute of Technology

Pasadena, California

1976

(Submitted January 23, 1976)

To My Parents, and E. T. O.

ACKNOWLEDGEMENTS

I wish to thank, first of all, my long- suffering advisor, Wal Sargent, who gave me advice and encouragement in every step of this project. Through him I got at least some notion of how research should be conducted. And although my use of English is still far below the "Orwell" level, this is not his fault! Hopefully, he can now get a new student with fresher ideas!

I also would like to thank Dr. Searle for his advice and ideas, and also for the thankless task of helping me prepare for the "Orals" a long time ago.

Earl Emery and Ray Ballard also deserve my thanks- Earl for building pieces of apparatus and Ray for unsnarling financial matters.

I also thank Caltech (RA's and TA's) and the U. S. Government (NASA Traineeship) for their generous financial assistance.

Martin Olsiewski and Taras Kiceniuk provided much-needed assistance during observing runs at Palomar.

Finally, I wish to thank anyone who, through my forgetfulness or ingratitude, was not mentioned above!

ABSTRACT

The stellar content and history of star formation of a number of Irregular and other late-type galaxies have been analyzed by means of 10-color photometery of the galaxies and a comparison of their colors to the calculated colors of a set of three-parameter models. The galaxy models are assumed to be composed of various amounts of "clusters" from 10^6 to 10^{10} years old, the colors of which were calculated from stellar-evolutionary tracks and observations of 102 stars of all spectral types. The colors of the model clusters were checked by comparison to the colors of 46 clusters in the Magellanic Clouds.

The first chapter of the thesis gives the principal results of the work, the analysis of the galaxies; the second gives a description of the cluster models and comparison to the cluster observations; the third presents the colors of the 102 calibrating stars.

In the first chapter the colors from 79 observations of 46 different Irregular and other late-type galaxies (mostly Sc's) are given first. The construction of model cluster colors and their behavior as a function of time, t, are briefly discussed. A principal component analysis of the galaxy colors indicates that only three parameters could explain most of the variation in galaxy colors.

Accordingly, a set of three-parameter models is

adopted to explain their colors. The three parameters chosen govern the star formation history of the galaxies. The Limber initial mass formation function is assumed. Various two-color plots of some of the galaxy models were made. It is found that the loci of the models agree well with observations. Finally, fits to individual galaxies in the three parameters are made, as well as estimates of the "uniqueness" of the fits. The average difference between the best-fitting parameters of Irregulars and Sc's is interpreted to mean that Irregulars have both relatively more star formation in the recent past and an initial mass formation function enriched in massive stars compared to the Sc's. An irregular rate of star formation in the recent past ($t < 10^8$ yr) is also indicated.

The second chapter describes the construction of cluster models and a comparison between the model colors and the colors of 46 clusters in the Magellanic Clouds. Cluster models are found to fit observations well in general. Furthermore, the observations permit estimates of n_b/n_r, the ratio of blue to red supergiants, to be obtained for stars of 3 to 20 solar masses.

The third chapter gives a description of the observation of 102 stars of all luminosity classes and spectral types from O5 to M6. The behavior of the colors of stars of different luminosity classes as functions of assumed $\log T_e$ and spectral type are discussed.

TABLE OF CONTENTS

INTRODUCTION

Because of the new Astronomy Department regulations, each chapter of this thesis is written in the form of a paper suitable for direct submission to the Astrophysical Journal. Therefore, there is some redundancy in the chapters.

This work is divided into three parts. The first chapter, which contains the bulk of this work, describes the analysis of observations of late-type galaxies in terms of three-parameter models of their star-formation history. Galaxies are regarded as being composed of "clusters" of various ages. The second chapter consists of a full description of the construction of cluster models which are used in Chapter 1. In Chapter 2 models and observed clusters are compared in several kinds of plots, and conclusions are drawn about properties of the clusters, chiefly n_b/n_r, the ratio of red to blue supergiants in younger clusters. Chapter 2 is a contribution to a larger paper by Searle and Bagnuolo, and will probably not be published separately. Chapter 3 presents the data that enable cluster colors to be calculated, the observations of 102 stars of various spectral types. The behavior of the colors of stars as functions of log T_e and spectral type is also discussed.

CHAPTER 1

MODELS OF THE STELLAR CONTENT AND EVOLUTION OF IRREGULAR AND OTHER LATE-TYPE GALAXIES

I. INTRODUCTION

The general purpose of the research presented in this paper was to investigate the stellar content of late-type galaxies, especially Type I (Magellanic) Irregulars. In particular, the systematic differences in the stellar content, if any, of Irregulars and Sc spirals were to be investigated. The Sc's could also be used as a control to which the Irregulars could be compared. The variation of the stellar content of galaxies of the same type could also be examined. The observational technique chosen was photometry with filters at different regions of the continuum and at prominent spectral lines. Calculations of model galaxies with various stellar contents determined the filters used.

There are several approaches to the analysis of galaxy colors in terms of stellar content. One approach is that of Wood (1966) and Spinrad and Taylor (1971) among others. The H-R diagram is divided into twenty to thirty star blocks such as "early A dwarfs" or "late K giants." Stars with different chemical abundances, such as "super metal rich" stars, can also be included. Galaxy colors are computed from the color intensities of the star blocks, and the relative numbers of stars in each block are adjusted until an adequate fit to the observed galaxy colors is obtained. In principle, if n

colors are observed, the numbers of stars in n blocks could be determined by a unique least-squares fit. Unfortunately, the number of colors is usually less than the number of star blocks. Moreover, in practice the number of independent parameters that can be determined is smaller still.

Martin and Bingham (1970) have analyzed the galaxies of Wood's (1966) photometry by means of principal component analysis and found that only three significant parameters could be extracted from the data. Therefore, if we attempt, like Wood, to obtain a unique fit to a galaxy using 23 stellar blocks, we must use 20 implicit or explicit constraints on the numbers of stars in the blocks. In principle, the final fit could be expressed as a function of three independent parameters. It is evident that in general such an analysis of stellar content will involve a small number of independent parameters and a large number of assumed constraints.

A number of constraints have been used by the authors cited, such as reasonable looking Hess and color-magnitude diagrams and mass-to-light ratios. Another possibility is to put in explicitly the constraints on the numbers of stars in the blocks. Then the problem of minimizing the squared difference between calculated and observed colors subject to the constraints could be solved by a Lagrange-multiplier technique. Other techniques of control theory

mentioned in Bryson and Ho (1969) might also be used.

One disadvantage of the approach using stellar blocks is that it is difficult to decide what reasonable constraints are. Suppose, for example, that we assume that the number of stars on the Main Sequence must increase monotonically with absolute magnitude. We would then misinterpret the colors of galaxies with a bulge of, say, A stars due to an irregular rate of star formation. Another disadvantage is that it is difficult to determine the "uniqueness" of the final fit.

The approach used in this paper is roughly as follows. A set of stellar-evolutionary tracks were used to calculate colors of clusters as a function of time. The computed colors were checked by comparison to observed clusters. (These results are given in another paper by Searle and Bagnuolo (1976), hereafter called SB.) Galaxy colors were computed from the cluster colors, since the galaxies were assumed to be composed of clusters of different epochs.

The general philosophy was to use as few parameters as possible to fit the galaxy colors. Several parameters could be used in making galaxy models. The creation rate of clusters with time could be described by one or more parameters. The initial mass formation function (IMFF) assumed for stars in the clusters could also be varied. Finally, a simple procedure was used to obtain a good fit

to the galaxies with the parameters adopted and to obtain an estimate of the "uniqueness" of the fit.

An advantage in this approach over the first approach discussed above is that the assumptions used are more explicit and the fitting procedure is more objective. A disadvantage is that the parameters used don't have the simple observational significance as the stellar blocks of the former approach do.

II. OBSERVATIONS

A set of eleven filters was used for the photometery of the galaxies and stars used for calibration. Five medium bandwidth filters designed originally by J. E. Gunn, designated by u, b, g, o, and r respectively, were used to measure the overall continuum over a wide frequency range and the Balmer Jump. The Gunn filters were constructed from a collection of Wratten filters and Schott glass. (See Bagnuolo (1976), hereafter called Paper I, for details.) It was felt that somewhat more information could be obtained about the shape of the integrated continuum of galaxies than with the wider UBVR system.

Three of the most prominent spectral features in late-type galaxies were expected to be the Hα line, especially in emission, the Mg b triplet, and the TiO bands. A set of filters was used to measure these features. The filters designated by Hα, Hα', and 66 measure Hα emission,

the latter two filters being especially useful for redshifts greater than 1000 km/s. The Mgb filter, centered on the Mg b triplet near λ 5175, is similar to that of Wood (1965). Stars later than G7 of different luminosity classes differ in (Mgb-g) by up to 0.3 mag. However, in late-type galaxies (Mgb-g) was found to be mainly useful in measuring the strength of the [O III] emission lines in filter g. The filter designated by TiO was intended to measure the TiO band at about λ 6200. It was found that light in TiO drops abruptly for stars later than M2. Finally, the IR filter, centered at about λ 7010, measures an emission-free continuum region somewhat redder than the r filter. Table 1 lists the properties of the photometric system defined by the above filters and S-20 phototubes.

Galaxies were selected in order to examine and extend the results of Searle, Sargent, and Bagnuolo (1973), hereafter referred to as SSB, concerning the history of star formation in late-type galaxies. Seventy-nine observations of fifty-one different galaxies were made, including 24 galaxies of type Irr I, 3 of Sc-Irr (transitional type), 22 Sc's and 2 Sb's. As many galaxies as possible described as Irr I or the equivalent by classifiers in de Vaucouleur's (1964) catalog were observed, although galaxies with listed radial velocities less than 1200 km/s were given priority. About half of all listed

Irregulars were observed, including most with listed magnitudes or radial velocities. A galaxy was considered to be a transitional type, Sc-Irr, if more classifiers listed in the catalog classified it as "Sc" or "SI," or equivalent, than "Irr." In addition, NGC 4861 appears to be connected to IC 3961, and the whole system is considered to be a transitional type. One galaxy, NGC 5253, was observed by Searle (1975) in the five Gunn filters and transformed to the color system of this paper. The main criteria for the choice of spirals were redshift and inclination. Nearly all have radial velocities less than 1100 km/s and major/minor axis ratios of less than three.

The galaxy observations were made on 25 nights during the period February 1973 to April 1974 with the 60" and 20" reflectors at Palomar and the 24" reflector at Table Mountain Observatory. A two-tube S-20 photometer was used for the Palomar observations and another S-20 photometer was used at Table Mountain. In both cases the number of counts was recorded digitally on paper tape or punched cards. At Palomar apertures of 3 to 6 mm were used, corresponding to 57" to 114" at the 60" and three times this at the 20". Three to six readings of ten to thirty seconds integration time were commonly used. Readings of the galaxy and sky were obtained, usually by taking successive readings with the galaxy in one tube, then the other. Typically, about 18,000 net counts (galaxy minus

sky) in the g filter were obtained in ten seconds for a galaxy with a visual magnitude of 13.0 with the 60". At Table Mountain a similar procedure was followed. Apertures of 2 to 6 mm were used (1' to 3' at the 24"). Measurements of the sky and galaxy were taken several times each, usually in a pattern of G-S-S-G or G-S-G-S-G, where G is a galaxy and S is a sky measurement. Ten thousand or more net counts in each filter was a goal throughout.

One hundred and two stars of all luminosity classes and spectral types O5 to M6 were observed in order to calculate colors of model galaxies for comparison with observations. Details of star observations are given in Paper I. A simple linear transformation, obtained from a least squares estimate from 19 stars observed at both Table Mountain and Palomar, was used to transform the Table Mountain colors to the standard Palomar system:

$$\begin{aligned} (i-g)_P &= a_i(i-g)_T + b_i \\ g_P &= a_g g_T + b_g(o-g)_T + c \end{aligned} \qquad (1)$$

where i is an arbitrary filter, P and T refer to Palomar and Table Mountain quantities respectively, and the a's, b's, and c are constants. No deviation from linearity in the plots defining the empirical transformation above could be detected. This is not surprising for transformations between similar systems. In the standard Palomar system, the colors of the A0 V equatorial standard of

Haug et al. (1967), "Z4A," are set at (i-g) = 0.00 for all $i \neq g$, and g = 7.00.

Several corrections were made to the observed galaxy colors. First, the galaxy colors were corrected for reddening by using a result of Holmberg (1958):

$$\Delta(P-V) = E(\csc B-1) + \beta(1-b/a) - 0.047 \qquad (2)$$

where $\Delta(P-V)$ is the reddening correction, E = 0.062, b/a is the ratio of minor to major axis, and β varies from 0.049 for type Irr I to 0.136 for Sc+ galaxies. The first two terms in the reddening correction are for reddening in our galaxy and the observed galaxy respectively. The factor 0.047 is the average reddening assumed for the clusters in the Magellanic Clouds which were used (see below) as an intermediate step in the construction of galaxy models. (Of course, either the observed or model colors could have been adjusted by 0.047 as long as they are consistant.) The differential reddening of color (i-g), designated by $\Delta(i-g)$, was found from $\Delta(P-V)$ by using Whitford's (1958) reddening law.

The colors (Hα-r) and (Hα'-r) were also corrected for redshift effects by calculating the transmission in the Hα and Hα' filters for different redshifts in the Hα and [N II] lines. A standard temperature of 5 ^{o}C was assumed. The typical ratio Hα/[N II] = 4 was used; however, the

corrections don't differ much from those of the pure Hα case. It was also assumed from calculated models and the colors of galaxies with the least emission that without emission lines (Hα-r) = -0.06 and (Hα'-r) = -0.04. The color corrections were assumed to be zero at a radial velocity of 500 km/s. In most cases the correction in (Hα-r) is less than 0.05 mag. (The largest corrections, about 0.4 mag for NGC 4532 observations, are probably accurate to only 0.1 mag, however.) In Table 2 the uncorrected colors of galaxies are listed first, then the corrected colors immediately below. Other galaxy data such as radial velocity, V_r, is also listed, of which G/S and d will be discussed below.

In the galaxies, particularly Irregulars with low surface brightness, the greatest source of error results from fluctuations in the sky brightness. In order to check the accuracy of the observations, a sample of 28 galaxy observations with different galaxy/sky ratios, G/S, was used. The sample observations have two galaxy and two sky readings, the typical case. The median and mean differences, or errors, between the colors obtained from the first set of galaxy-sky readings and the second set were obtained for three groups of galaxies with different values of G/S. In Table 3 the first column gives the range in G/S for each group. The second and third columns list the numbers of sample galaxies and total galaxies (n' and n) in

each group. In the headings of succeeding columns we write for brevity "Δi" for the median error in color (i-g). Mean errors are listed below the median errors. (IR, Hα', and 66 were almost never observed for low G/S/ galaxies; thus, no estimate of these errors was obtained.)

III. EMPIRICAL GALAXY COLORS

Before analyzing the galaxies, let us consider some plots of their colors to see what general tendencies occur. A number of two-color plots of the galaxy colors were made, the following of which are among the more interesting. Figure 1 is a plot of (g-o) and (b-g) and is an example of a typical plot. In Figure 1 the galaxies follow a well-defined sequence from the reddest galaxies at (g-o) $\sim$ 0.7 through galaxies with (g-o) $\sim$ 0.3, with a slight amount of fanning out of the bluer galaxies. Colors for galaxies with (g-o) redder than 0.3 appear to represent an overall color temperature, and the linear relation here between (b-g) and (g-o) is typical of the redder part of most of the plots. In the Figure it can also be seen that the Irregulars are generally bluer in (g-o) than the Spirals (which we shall hereafter refer to as "Sc's" unless otherwise noted). As will be seen, Irregulars are generally bluer in other plots also. Finally, there is a distinct turnoff in (b-g) for galaxies with (g-o) less than 0.3, which is probably due to strong emission lines, such as

λ4959 and λ5007 of [O III] and Hβ in filter g. To get an estimate of general emission line strength we can introduce a "reddening independent" parameter, Q_3, first defined in SB as: $Q_3 = (g-o) - 1.703(o-r)$. Q_3 is insensitive to reddening and also to redshifts (to V_r less than 2000 km/s). For most clusters (see SB) and galaxies, the value of Q_3 is close to zero; however, emission lines in filters g and r, chiefly [O III] and Hα, cause Q_3 to become strongly negative. Calculation of Q_3 indicates that there is significant emission ($Q_3 \leq -0.1$) in about thirty of the observations, showing that plots such as Figure 1 are indeed affected by emission lines.

Next, we consider a plot of (b-o) and (u-b) which is shown in Figure 2. The color (b-o) is a measure of overall color temperature, and other colors might have been used. The color (u-b) is intended to be a measure of the Balmer Jump similar to (U-B) in the UBV system. Generally speaking, the Irregulars are bluer in both (b-o) and (u-b) than the Sc's. There also appears to be a definite width of about 0.3 mag in (u-b) which might indicate differences in the numbers of massive Main Sequence stars, as will be discussed later.

Figure 3 is a plot of (b-o) against (Hα-r). Again, (b-o) is a measure of overall color temperature, while (Hα-r) is a measure of Hα emission. In the figure we see the following features. First, Irregulars are generally

bluer and have more Hα emission than the Sc's. Secondly, the locus of galaxies has a sail-like shape- there is a wider range in (Hα-r) for the bluer galaxies, although the average Hα emission is still stronger than that of the redder ones. A possible interpretation to be discussed later is that the bluer galaxies have more young stars and therefore a generally higher number of active H II regions. The spread in (Hα-r) is then due to irregular rates of recent star formation.

The main features of the color plots may be summarized as follows. First, the Irregulars are generally bluer and have more Hα emission than the Sc's. Secondly, the redder galaxies lie fairly closely along straight lines in the plots without much deviation in color. Thirdly, bluer galaxies show noticeable variations in (u-b) and (Hα-r), especially in the latter. Finally, the colors of the bluer galaxies are influenced by emission lines, particularly colors involving filters Hα, g, and r. In a later section we shall seek galaxy models that explain these observational features.

We can next consider whether any systematic relations exist between galaxy colors and the ratio of the aperture used to galaxy size. The aperture/ galaxy size ratio can be defined by $d = A/\sqrt{ab}$, where A is the size of the aperture used, and a and b are major and minor axes. Values of a and b are taken from Holmberg (1958), except

for a few southern galaxies where de Vaucouleur's (1964) catalog is used. The parameter d is thus a rough measure of the diameter of the aperture used to a characteristic size of a galaxy. Obviously, d is more meaningful for symmetrical galaxies than for some of the more unsymmetric Irregulars like NGC 4657. Figures 4 a, b, c are plots of the colors (b-o), (u-b), and (Hα-r) with log d. Plots of the colors as a function of d were also made but are not shown. In Figure 4a the Irregulars are generally bluer than the Sc's for all values of d. Furthermore, despite large scatter in the plot, there seems to be a tendency for Irregulars to become redder and Sc's bluer with increasing d. These trends were noted previously by de Vaucouleurs (1961) for (B-V) colors in late-type Spirals and Irregulars. In Figures 4b and 4c, which are plots of (u-b) and (Hα-r) respectively with log d, general tendencies are difficult to detect. A slight tendency toward convergence in the (Hα-r) colors of Irregulars and Sc's similar to that in (b-o) may exist, but this is not obvious. A similar comment may be made concerning Figure 4c. Therefore, there seems to be some tendency for central portions of galaxies to be somewhat bluer in (b-o) in Irregulars and redder in Sc's. However, in the other colors such tendencies are difficult to detect.

IV. CLUSTER MODELS

The calculation of cluster colors is an intermediate step in the calculation of models to be used in the analysis of the stellar content of galaxies. In this paper "clusters" are defined as systems in which star formation has occurred more or less instantaneously; "galaxies" are systems in which star formation has occurred over a period of time. If we assume, as in SSB, that galaxies are composed of clusters of various ages, then colors of galaxy models can be built up from cluster colors, depending on the star-formation history assumed.

Cluster colors can also be checked empirically. In SB cluster calculations were compared to observations of clusters in the Magellanic Clouds in the five Gunn filters. The cluster observations were particularly useful because the ratio of blue to red supergiants, n_b/n_r, of calculated evolutionary tracks for massive stars varies greatly depending on theoretical assumptions. More details of the cluster observations and calculations can be found in SB.

The following is a summary of the main steps in the calculation of model cluster colors. We seek to use a set of evolutionary tracks together with observations of a variety of stars (see Paper I) to calculate a reasonable set of cluster models. The set of calculated models should include those with different n_b/n_r and different initial

mass formation functions (IMFF's).

We start with the observations of 102 stars, including 18 supergiants corrected for reddening, given in Paper I. Plots of colors versus spectral type were transformed into color, log T_e plots by assuming log T_e, spectral type relations from Johnson (1966), Morton and Adams (1968), Morton (1969), and Lee (1970). Bolometric corrections (BC) as a function of log T_e were similarly obtained. The (g-V), log T_e relations were obtained from the over 60 stars with known visual magnitudes. The relations in color, log T_e; BC, log T_e; and (g-V), log T_e suffice to calculate color intensities produced by points along evolutionary tracks in the log L, log T_e plane.

Evolutionary tracks were assembled in the log L, log T_e plane for stars of from 60 to 0.08 solar masses. These tracks were based on models of Robertson (1971,1972) and those in SSB, the latter with portions of blue loops shifted to agree with more recent models. The upper mass models, 60 to 3 solar masses, were modified so that models with different n_b/n_r could be readily calculated. The positions and times along red-giant tips in 1.0 to 2.25 solar mass models were modified to agree with Sandage's (1962) observation of NGC 188, and Johnson and Sandage's (1955) of M 67.

The computation of model cluster colors was begun by generating a large number (up to 60) of evolutionary tracks

interpolated between the above model tracks in log L, log T_e, and log t, where t is the time. The time between t = 0 and t = 10^{10} years ago was divided into 41 "time slots," the upper boundaries of which are given by: log t_{imax} = .1(i-1) + 6.0 , where t_{imax} is the upper boundary of the i^{th} time slot. The use of time slots automatically averages out the colors of red giant excursions in the tracks and is an improvement on the computation method used in SSB. The color intensities of the tracks for each time slot were calculated by the relations mentioned previously and added together. Cluster colors were calculated for three different mass functions and for n_b/n_r = 0, 1, or infinity. It was found (see SB) that the colors of younger cluster models were mainly influenced by the value of n_b/n_r, regardless of IMFF assumed, because the light contributions of the highest mass stars dominate.

The calculation of the colors of the youngest clusters must be modified to take into account the presence of emission lines. The emission lines are assumed to arise from the absorption of ultraviolet photons of massive stars (greater than 15 solar masses) by the surrounding gas. Contributions to emission lines from within the stellar atmosphere were neglected. Also, perfect efficiency in degredation of the photons is assumed. It can be shown that:

$$F_i' \simeq F_i[1 + \sum_L (s_L/S_i)(1.27\times10^{11}/\Delta\upsilon_i)(F_\beta/F_i)\ W_\beta I_L] \quad (3)$$

where F_i' is the average flux density in the filter band i including the emission lines and is proportional to the number of counts per second. F_i and F_β are the mean continuum flux densities at the filter i band and Hβ respectively. W_β is the equivalent width of the H_β emission line in Å, and I_L is the intensity of emission line L relative to Hβ. $\Delta\upsilon_i$ is the bandwidth of the filter and 1.27×10^{11} is a conversion factor. s_L/S_i is the ratio of the sensitivity of the photometer at line L to the average sensitivity in the filter band i. Summation is taken over the number of lines than can affect the count in the filter. Relation (3) gives a corrected flux density in the presence of emission lines, and for no emission lines obviously $F_i' = F_i$.

Estimates of W_β, produced by O stars with T_e from 30,000 to 50,000 °K, given by Searle (1971), and estimates of I's for three H II regions of different temperatures- M 101 #2, NGC 604, and NGC 5471 are given by (Ibid.), Aller, Czyzak, and Walker (1968), and Searle and Sargent (1972) respectively. These quantities were used in (3) to calculate the color intensities of the hottest stars in the youngest clusters.

The cluster colors calculated above could now be compared to the colors of 46 clusters with widely differing

ages observed by Searle in the Magellanic Clouds. (see SB) In general, the calculated colors agree well with observations. In addition, the younger clusters were used to estimate n_b/n_r. These values of n_b/n_r were used in all later calculations of cluster and galaxy colors. Also, as a check on the youngest cluster models NGC 604 was observed in eight filters (see Table 2), and the colors appear to agree fairly well with a computed cluster with $t = 2 \times 10^6$ (Table 4).

Table 4 lists the adopted colors of clusters to be used in the construction of galaxy models. These colors are substantially the same as the calculated cluster models, except for slight adjustments in the colors of the last six time slots, to better fit observed oldest clusters and reddest galaxies. An IMFF from Limber (1960) and the values of n_b/n_r obtained above were assumed. The first column in Table 4 gives the number of the time slot; the second, the upper boundary in time of the interval, log t_{imax}. Succeeding columns give the average colors of clusters in the time slots. For brevity, at the top of the column we write "i" for color "(i-g)." The last column gives relative absolute g magnitudes. The run of cluster colors with time appears to fall into five groups:

i) log $t \leq 6.2$ The youngest clusters have high Hα and [O III] emission, as can be seen by the values of (Hα-r) and (Mgb-g). Also, (u-g) is weaker than at maximum (in the

sense of being less negative in value).

ii) $6.6 \geq \log t > 6.2$ Clusters have Hα emission, but little [O III] emission; (u-g) gets stronger.

iii) $8.0 \geq \log t > 6.6$ Clusters have strong (u-g), little Hα emission, and are generally "blue."

iv) $9.3 \geq \log t > 8.0$ This is a transition region in which clusters become generally redder in (u-g) and (b-g), and to a lesser extent in (r-g).

v) $10.0 \geq \log t > 9.3$ These are the reddest clusters, very red in (r-g), etc.

In the next section, models of the stellar content of galaxies will be made by adding up light contributions of clusters of various ages. However, it already appears that only about five different types of clusters could be used in building galaxies. Therefore, probably no more than four or five parameters should be used in the galaxy models.

V. GALAXY MODELS

A. Principal Component Analysis of Galaxies

The problem here is to explain the observed galaxy colors by means of some formation history of the clusters in the most economical manner. To avoid redundancy in the models, we must first estimate the number and nature of independent parameters given by the observations. A mathematical technique, principal component analysis, may be applied here. Methods in principal component analysis

are discussed in Deeming (1964,1968), Martin and Bingham (1970) for astronomical applications, and in Kendall (1968) and Kendall and Stuart (1966) in greater detail.

In making a principal component analysis we regard each galaxy observation geometrically as a point in an n-dimensional color space. The n galaxy colors are standardized by a simple linear transformation to having zero mean and unit variance. Then the axis is found about which the points vary least- that is, we seek to minimize $\sum d_i^2$, where d_i is the length of a perpendicular from point i to the axis. It can be shown that this is the axis <u>along</u> which the variation of the points is the greatest. Next, another axis minimizing the variation is found perpendicular to the first and so on. For example, if the observations formed an ellipse, the procedure would find the major and minor axes. Finally, the number of effective dimensions in the space, "significant parameters," can be estimated by comparing the variation along each axis with the variation expected from observational error alone.

Mathematically, we find the eigenvectors and eigenvalues of the correlation matrix C_{ij}, defined by:

$$C_{ij} = 1/p \sum_{k=1}^{p} x'_{ik}\, x'_{jk} \qquad (4)$$

where x'_{ik} is the standardized observation of the k^{th} object in the i^{th} color and summation is taken over the p objects observed. The eigenvalues are the variances along the

new axes (which are ξ_i, the eigenvectors) and can be compared to the variance expected from observational errors alone. A test given by Deeming (1964) for significance of the variation along ξ_i is that the ratio $F = (\delta\xi_i)^2/\lambda_i$ follows the F distribution, where $(\delta\xi_i)^2$ is the expected variation along ξ_i due to observational errors and λ_i is the eigenvalue.

In analyzing the galaxy data of Table 2 the problem of how to treat missing data arises, since observations in a few filters, notably Hα', were made in only 50-70% of the galaxies. One way is to form the correlation matrix using only the existing data, i.e. in (4) sum over only the p' galaxies where both filters i and j are observed and divide by p'. This method produced some small negative (non-physical) eigenvalues because different terms in the correlation matrix were calculated using somewhat different sets of galaxies. (However, the largest three eigenvalues and eigenvectors agree well with those of the method below.)

A better approach seemed to be to estimate missing observations from the existing data first, then calculate the correlation matrix using estimated observations. Estimates of missing data were obtained from:

$$x_{jk} \simeq X_j + \frac{\sum_i (x_{ik}-X_{i,j})(\sigma_{j,i}/\sigma_{i,j})\ r_{ij}^2\ \mathrm{sgn}(r_{ij})}{\sum_i r_{ij}^2} \qquad (5)$$

where x_{jk} is the estimate of the j^{th} color of the k^{th} galaxy, X_j is the average value of the j^{th} color. $X_{i,j}$ is the average value of the i^{th} color when color j is also observed, and $X_{i,j} \simeq X_i$. Similarly, $\sigma_{i,j}$ is the standard deviation of the i^{th} color when j is also observed, etc. Using these conditional means and standard deviations seemed more accurate than using simple means and standard deviations. $\mathrm{sgn}(r_{ij})$ is the arithmetic sign of the correlation coefficient r_{ij}. Summation is taken over all colors observed in the k^{th} galaxy.

The meaning of (5) becomes apparent by taking as an example an estimate of a missing color x_{jk} from an observed color x_{ik}. We have: $x_{jk} \simeq X_j + (x_{ik} - X_{i,j})(\sigma_{j,i}/\sigma_{i,j})\mathrm{sgn}(r_{ij})$ Here, $\sigma_{j,i}/\sigma_{i,j}$ is simply the slope of a fit to the data in the i, j plane. In (5) such estimates are weighted by a factor of r_{ij}^2. As a check on (5) points with estimated (Hα'-g) were plotted in the (Hα'-g), (Hα-g) plane and seemed indistinguishable from the "real" points.

A ten-color principal component analysis was done including estimated colors of missing observations. The four largest eigenvalues and corresponding eigenvectors are listed in Table 5. The first column of Table 5 gives the eigenvalues; columns 3-12 give the components of the eigenvectors in the colors (i-g), written here as i for short, for all i. The second column gives the values of

$F = (\delta\xi_i)^2/\lambda_i$, assuming errors of 0.05 in all colors, for comparison with the F-test. It can be seen that three parameters account for 79% of the variation in the ten-color analysis. Also, according to the F-test, while the first three eigenvalues are significant to 0.1%, none of the other eigenvalues are significant to 5%. A similar analysis was done using only the first six colors, which are observed in the great majority of galaxies. The results are very similar to those of the ten-color case, as can be seen from the lower part of Table 5.

The eigenvectors corresponding to the first three eigenvalues can now be examined for possible physical significance. The first eigenvector, the direction of greatest variation, clearly seems to represent an overall color of galaxies from blue to red. The second, which has large positive components in (Hα-g) and (Hα'-g), clearly represents Hα emission. The third, which has large positive components in (u-g) and (b-g) and smaller components in (o-g) and (Mgb-g), lacks the obvious physical significance of the first two eigenvectors. However, it seems possible that the third eigenvector represents the combined effects of the ultraviolet continuum and [O III] emission, and should be strongly influenced by clusters in time regions i or iii. ($6.2 \geq \log t$ or $8.0 \geq \log t > 6.6$)

The main conclusions to be drawn from these analyses

is that there exist three parameters that explain most of the variation in galaxy colors. Galaxy models should be built with only three parameters, since more information about the stellar content of the galaxies cannot be obtained. Finally, these models should explain overall color, Hα emission, and the ultraviolet continuum and/or [O III] emission.

Because only three parameters can be estimated from the data, it is worth considering whether most of the information about the galaxies could have been obtained with observations of only three colors (four filters). If so, what is the optimum set of filters? In Table 5 the three principal eigenvectors have low components in 66, Mgb, and TiO, and the information in the Hα' filter largely duplicates that of the Hα filter. Principal component analysis of the most promising four-filter combinations of the remaining seven filters were done, and the results are presented in Table 6. In each set of four filters the second filter, f2 say, was chosen in forming colors (i-f2), where i is an arbitrary filter. The analysis proceeded exactly as before, except that three colors were used instead of ten. In Table 6 the filters chosen for each analysis are given in the first column. The next six columns give the values of the three eigenvalues and corresponding F values. We adopt as a reasonable figure of merit the product of the three F values

as a measure of the volume occupied by the observations in each three-dimensional color space. In order of F products, according to Table 6, the best choices for filter sets are: (u, g, o, Hα), (u, g, Hα, IR), (u, g, r, Hα), and (b, g, o, Hα). In the best set, the three eigenvalues are significant to 2% or better in the F-test; however, the errors in obtaining the colors could be significantly less than in the ten-color case. It seems that three parameters could be observed in the (u, g, o, Hα) nearly as well as in the original ten-color system.

The eigenvectors for this three-color system, given as components in (u-g), (o-g), and (Hα-g) are in order of eigenvalue size: (0.665, -0.521, 0.536), (0.112, 0.816, 0.567), and (0.789, 0.322, -0.523). These eigenvectors lack the physical significance of those discovered for the ten-color or six-color cases, since the effects of overall color, Hα and [O III] emission, and ultraviolet color seem to be mixed.

Three plots of the colors of this system were made, of which (u-g), (o-g) and (u-g), (Hα-o) are the most interesting and are plotted in Figures 5 and 6 respectively. The plot of the other color combination (o-g), (Hα-o) resembles that of (b-o), (Hα-r) in Figure 3, although contracted in the x direction. All three plots show a good two-dimensional scatter in the points, as should be the case. Figure 5 is similar to Figure 1, (b-g), (g-o).

The plot in Figure 6 combines the effects of overall color, Hα and [O III] emission, and ultraviolet. One isolated point is from a low-accuracy observation of NGC 3447B, which merits re-examination.

B. Construction of Galaxy Models

The following set of three-parameter models were constructed to take into account the results of the last section. We assume, as in SSB, that the galaxies are 10^{10} years old; the question of "young galaxies" will be discussed later. Also, as in SSB let $\phi(m,t)dmdt$ be the number of stars formed in the mass range m to m+dm during the time interval t to t+dt. Then, we shall assume that the formation history of stars can be given by:

$$\begin{aligned}\phi(m,t) &= C\ f(m)\ e^{-\beta t'} \quad \text{if} \quad 10.0 \geq \log t > 8.0 \\ &= C\ f(m)\ e^{-\beta t'}\ B_1 \quad \text{if} \quad 6.4 \geq \log t \\ &= C\ f(m)\ e^{-\beta t'}\ B_2 \quad \text{if} \quad 8.0 \geq \log t > 6.4\end{aligned} \tag{6}$$

where t' is the time since galaxy formation in units of its present age (10^{10} years), C is a constant, f(m) is the IMFF, assumed for now to be that of Limber (1960). β, B_1, and B_2 are the three independent parameters that determine each model. B_1 and B_2 are "burst parameters," similar to that of SSB and control the relative numbers of "very young" and "young" clusters respectively. β controls the relative numbers of oldest clusters ($t \geq 3 \times 10^9$ yrs.),

and was previously used in SSB. (6) is used, together with the cluster colors of Table 4 to calculate model galaxy colors.

From the cluster colors it can be seen that B_1 and B_2 strongly influence Hα and u intensities respectively, and β influences the overall color. Thus, the parameters adopted are roughly similar to the purely empirical parameters (eigenvectors) obtained from principal component analysis. Other models might have been used. A four-parameter model could adjust the relative numbers of clusters in the five regions in time discussed earlier, but would be redundant. An alternative set of three-parameter models could be constructed with the boundary of the bursts at log t = 6.2 instead of 6.4. Such models would explain more of the variation in the (Hα-o), (g-o) plane, i.e. the relative strengths of [O III] and Hα. However, these models would explain less of the variation in the ultraviolet, as in (u-b), considered more important.

The contribution of stars of various masses to the light of the bursts is worth considering for future reference. In the following calculation the star formation within the bursts is considered constant, and the term $e^{-\beta t'}$ is ignored for $10^8 \geq t$. Table 7 gives the percentages of light in the filters contributed by stars of different masses to the two bursts. In the first column the mass range of the stars is given; succeeding columns give

the relative intensities in the filters. The two top sections of Table 7 give the contribution of stars to the "B_1" and "B_2" bursts respectively. The bottom section gives the intensities contributed by stars 10^8 to 10^{10} years old, assuming a constant rate of star formation ($\beta = 0$). (i.e. These stars contribute light to a 10^8-10^{10} yr. "burst.") The bottom line of each section gives relative intensities in the filters (i.e. the intensities of the standard A0 V star would all be equal.) Here 1.0×10^6 is written 1.00(6), etc.

In Table 7 light in all filters of the B_1 burst is dominated by stars of greater than 30 solar masses. In the B_2 burst 65-80% of the light is produced by stars of 2.5 to 20 solar masses, 30-44% from those between 5 and 10 solar masses. In the 10^8-10^{10} yr. "burst," over 70% of the light comes from stars of 1.0 to 2.5 solar masses. The light contribution of lower Main Sequence stars of less than one solar mass is less than 15%. The masses above which half of the light is contributed, the "median masses," are about 35 and 8 solar masses respectively for the B_1 and B_2 bursts. The median mass of the 10^8-10^{10} yr. "burst" is about 1.9. For cases in which more stars were formed in the past ($\beta > 0$), the median mass would be still lower. Finally, except for Hα and Hα', more light is produced by the B_2 burst and the B_1, and the 10^8-10^{10} yr. "burst" produces more than either. For this constant-creation

galaxy model the latter produces 69% of the g light; the B_1 and B_2 bursts produce 6.8% and 24.2% respectively.

Several conclusions can be drawn from the above. First, the light in the B_1, B_2, and 10^8-10^{10} yr. bursts comes from stars of largely distinct masses (with median masses of about 35, 8, and 1.9 respectively). Secondly, that consequently, changes in the recent IMFF, f(m), would have much the same effect as changes in B_1 or B_2. For example, enriching f(m) with stars of about 35 solar masses would have a similar effect on galaxy colors as a large B_1 burst. Thirdly, that in the constant-creation case most of the light is still contributed by stars older than 10^8 years. Finally, that stars on the lower Main Sequence do not contribute a significant amount of light to the galaxies.

VI. ANALYSIS OF GALAXIES IN TERMS OF MODELS

A. The Colors of Models

The three-parameter galaxy models can now be compared with the observations. Each model is specified by the values of the three parameters governing the star formation history, (β, B_1, B_2). A 7 x 7 x 7 grid of these models was generated. The values of β, B_1, and B_2 chosen for this set of models were: (-2, 0, 1, 2, 3, 4, 6), (0, 1, 2, 4, 8, 16, 31), and (0, 0.5, 1, 2, 3, 5, 12) respectively. These values were chosen to provide a reasonably even

and complete coverage of the galaxy observations. For ease of reference and later computation, the models are denoted by three numbers running from 1 to 7. For example, a model with (β, B_1, B_2) = (0.0, 8.0, 0.5) will be designated by (2, 5, 2), a model with (β, B_1, B_2) = (-2.0, 0.0, 0.0) by (1, 1, 1) etc.

Let us now consider some overall properties of this set of models and make a general comparison of models with observations before undertaking more detailed analysis. In Figures 7, 8, and 9 thirty-five models are plotted in the same colors as in Figures 1, 2, and 3 respectively. For each of the seven values of β assumed, five models are plotted: (β, 1, 1), (β, 7, 1), (β, 1, 7), (β, 7, 7), and (β, 2, 3). The last are models in which the numerical values of B_1 and B_2 are unity; i.e. no "unusual" star formation takes place in the last 10^8 years. The colors of these models are plotted with filled circles in the Figure. The other four models represent extreme bursts for given β, and should give the extremes in color of the set of models. These models are plotted with unfilled circles and are the vertices of four-sided figures formed by connecting these points in the order: (β, 1, 1), (β, 7, 1), (β, 7, 7), and (β, 1, 7). To enable individual models to be identified, the line segment between models (β, 7, 1) and (β, 7, 7) is marked with an arrow pointing toward the latter point. Finally, the general loci of the galaxies

in the Figures is indicated by the areas inside dotted lines.

Certain general properties of the models can be seen in Figure 7. In this Figure the rightmost and smallest quadrilateral has the highest β, while the leftmost and larger quadrilateral has the lowest β. Evidently, the high β models are dominated by the oldest stars, and the colors of high β models change only slightly even with large bursts. Another property of the models in Figure 7 is that models with high B_1, the (β, 7, 1) models, are located downward and to the left of models with the same β but a big B_2 burst, (β, 1, 7). The explanation is that here the youngest clusters in the B_1 burst have strong emission lines in filter g.

Turning our attention to the comparison of the models with the locus of observed galaxies, we see that galaxy colors in Figure 7 appear to be well "explained" by the set of models. The red and blue limits in (b-g) are about the same for observations and models. Also, the "turnoff" for galaxies bluer than (o-g) $\sim$ 0.3 can be explained by large B_1 bursts. It is significant that none of the models with unity bursts are bluer than (o-g) = 0.25, thus, bluer galaxies (all Irregulars) must be undergoing a higher rate of star formation that 10^8 or more years ago.

Figure 8 is a plot of (b-o) and (u-b) similar to that of Figure 2. The overall effect of both types of bursts

in Figure 8 is to make the models bluer in both colors in almost the same direction. Thus, there is not much overlapping of models of different β, and β could be estimated for galaxies from this plot. (In the Figure the redder models have higher β.) In general, the models fit the observations well, although some galaxies are somewhat bluer in (u-b) than the models. The blue and red limits of the models and observations correspond closely. The observed variation of galaxies in (u-b) is explained by varying burst parameters, particularly B_2.

Finally, Figure 9 is a plot of (b-o) and (Hα-r) similar to that of Figure 3. The effects of B_1 and B_2 bursts are quite different. An increase in B_1 mainly increases Hα emission in (Hα-r), while an increase in B_2 mainly makes models bluer in (b-o). The youngest stars contribute most of the Hα emission. As in the previous Figures, the high β quadrilaterals are smaller and redder in Figure 9. The agreement in the color limits of galaxies and models appears reasonable, and the sail-shape of the locus of galaxies is matched by that of the models.

The following conclusions can be drawn from the analysis of Figures 7, 8, and 9. First, the color limits and general appearance of model points resembles that of the galaxies. Secondly, that the spread of galaxies in the plots may be interpreted as being due to fluctuations in recent star formation. Thirdly, that the effects on the

colors of varying B_1, B_2, and β are different. This may make it possible to determine of fairly "unique" fit of these parameters for each galaxy.

B. Fit of Models to Individual Galaxies

Because a good overall agreement between galaxies and models was found, we next try to find the best fit in (β, B_1, B_2) for each galaxy. The following fitting proce - dure was used. Let c_i be the i^{th} observed color of a galaxy. Then, for each model j an error function, E_j, was evaluated as follows:

$$E_j = \sum_i (c_i - a_{ij})^2 \qquad (7)$$

where the number of models j is 7^3 or 343, a_{ij} is the i^{th} color calculated in the j^{th} model, and summation is over the colors i. E_j is simply the sum of the squared diff- erences between the observed galaxy and the j^{th} calculated one. Geometrically, it is a squared distance in a color space. The models closest to the observed galaxy, those with the smallest E's, were found.

Let us consider only the models j with $E_j \leq E_{min} + N\delta^2$, where E_{min} is the E for the best fitting model, N is the number of colors used, δ is a parameter. For a given δ these closest models define a volume V in the three- parameter space (β, B_1, B_2) where the observation is best fit. Clearly, the size of this volume is a measure of the

"uniqueness" of the fit- the smaller the volume the "more unique" the fit. If δ^2 is comparable to the average squared error of the colors, then V should include the set of models that could be the best fit if the observation were repeated. V is thus a measure of the uncertainty of a fit in (β, B_1, B_2).

The centers of the error volumes (CEV's) were estimated by simply averaging the numbers denoting the closest models. For example, if the closest models are (2, 1, 1), (1, 1, 2), and (1, 1, 1), then the CEV is (1.33, 1.00, 1.33). The CEV's were used as an estimate of the best fits to the observations. More sophisticated methods to find the best fit, such as first and second order gradient methods, seemed uneconomical in view of the fairly large uncertainties in the fits (error volumes).

The galaxies were compared to the models in the following colors: (u-g), (b-g), (o-g), (r-g), (Hα-r), and (Mgb-g), since the first seven filters are the most frequently observed and because the last four filters contribute little additional information. (A ten-color analysis, however, gave results similar to that of this six-color analysis.) Estimates of missing colors obtained earlier were used; this was particularly useful in five cases where Hα' but not Hα was observed. Table 8 summarizes the results obtained. The second column gives the aperture/size ratio, and the next three columns give the

numbers (β, B_1, B_2) designating the closest model to the observation. The fourth column gives E_{min} for this model. The last column gives the number N_c of closest models with $E \leq E_{min} + 0.01$ (here, the δ assumed is slightly greater than 0.04). The seventh, eighth, and ninth columns give the (β, B_1, B_2) of the CEV. The model numbers of the CEV's were converted into numerical values of the parameters by means of linear interpolation. For example, a model number of $\beta = 2.5$ means that the numerical value of β is halfway between the second and third β's of the grid, 0. and 1., or 0.5. The E's obtained by comparing the CEV's with observations are listed under E' in the second-to-last column of Table 8. E' is generally slightly smaller than E_{min}, as expected.

Several observations can be made from Table 8. E_{min} and E' are upper estimates of how close the fits are to observations. An E_{min} of 0.06 corresponds to a difference of 0.10 mag between observations and models in each color, and 67 galaxies (84.8%) have $E_{min} < 0.06$. Similarly, E_{min} values of 0.03 and 0.015 correspond to differences of 0.071 and 0.05 in each color, and 56 (70.9%) and 41 (51.9%) galaxies respectively have E_{min} less than these limits. Thus, the colors of most of the galaxies can be reasonably well fitted by the models. Four observations have $E_{min} \geq 0.24$ (differences of 0.2 mag in each color). Of these, one is a low-accuracy observation of

A0957, a better observation of which is well fit; and two are observations of NGC 2366 which have very strong emission lines and are a little beyond the limits of the grid of models on some plots. The last is a low-accuracy observation of NGC 3447B mentioned before. The average number of closest models is 4.06, which is a measure of the "uniqueness" of the fit; that is, about 4 out of 343 models are within the error volume of a typical observation.

Figures 10, 11, and 12 are plots of the β, B_1, and B_2 of CEV's listed in Table 8. In these Figures Irregulars and Sc's with aperture/size ratios greater than 0.6 and 0.7 respectively, are plotted with filled symbols (which does not imply greater accuracy for these observations). Also, some average error volumes, obtained from the sets of closest models of a number of galaxies, are plotted in each Figure. The larger numbers along the axes denote model numbers, the smaller numbers in parentheses are the corresponding numerical values of β, B_1, or B_2. To avoid confusion, we will denote numerical values of parameters by parentheses from now on.

The following observations may be made from the Figures:

i) β represents an overall rate of star formation. Galaxies with $\beta > (0.)$ have had a higher rate of star formation in the past, and galaxies with $\beta \sim (6.)$ have had almost all star formation $\sim 10^{10}$ years ago.

"Young galaxies" with most or all of the star formation less than 10^{10} years ago should have $\beta < (0.)$. Almost all galaxies in Figures 10, 11 have $\beta \geq (0.)$. The three with $\beta < (0.)$ are low-accuracy observations of NGC 4656, A0957, and IC 1613. Moreover, A0957 has $\beta > (0.)$ in a more accurate observation, as does NGC 4656-7 (a composite galaxy). Therefore, it seems unlikely that any young galaxies were unambiguously observed, although IC 1613 is the best candidate. As in SSB, variations in galaxy colors can be better explained in terms of "flashing galaxies" than "young galaxies."

ii) The Irregulars and Sc's generally occupy different regions in the β, B_1 and β, B_2 planes (Figures 10 and 11). Irregulars occupy a region left of and above the Sc's in both Figures. In particular, Irregulars have lower β's and thus generally have had a relatively higher rate of recent star formation, compared to that of $\sim 10^{10}$ years ago, than the Sc's. Table 9 lists the average model numbers of different groups of galaxies. The second column gives the number of galaxies in each class, and the last three columns give the average model numbers. The average value of β is 3.54 for Irregulars and 5.31 for Sc's, a difference of 1.77. (In Table 9 for greater clarity we distinguish again between "Spirals" and "Sc's," although there are only small differences in color between them.) This difference in model numbers means that the

ratio of present star formation to that 10^{10} years ago is roughly exp(1.77) or 5.9 times greater for Irregulars than Sc's.

iii) Also, it appears that among galaxies with similar β's the Irregulars have generally higher B_1 and B_2 than the Sc's. In order to see this more clearly, let us consider the average model numbers of galaxies in the broad region in β in which Irregulars and Sc's overlap ($3 \leq \beta \leq 6$). From the bottom of Table 9 we see that the difference in $\langle\beta\rangle$ between Sc's and Irregulars in this region is much reduced. There is a difference in $\langle B_1 \rangle$ and $\langle B_2 \rangle$ of 0.92 and 0.98 respectively between Irregulars and Sc's. These differences in burst parameters are significant to 4-5 σ, judging from the estimated errors in the Figures. (The error regions are roughly parallel to the boundary between Irregulars and Sc's, so that the separation of galaxy types in the diagrams is very certain.)

In order to explain such a systematic difference in burst parameters, it is probably necessary to abandon the assumption that all galaxies have the same IMFF for the following reasons. Previously we have seen that the light in the two bursts is dominated by stars of >25 and 2.5-20 solar masses respectively. Also, that for any <u>individual</u> observation one cannot determine whether a galaxy has had a recent burst of star formation or has an IMff enriched in massive stars. However, the effects of bursts should

tend to average out over a large number of observations. Therefore it seems probable that the Irregulars are enriched in massive stars compared to Sc's.

If we attribute the difference in average burst parameters solely to the effects of different IMFF's, we can estimate how much the IMFF of Sc's and Irregulars should differ. In SSB the IMFF was assumed to be:

$$\begin{aligned} f(m) &= C\, m^{-\alpha}, \quad \text{if} \quad 35\ M_\odot \geq m \geq 0.25\ M_\odot \\ &= 0 \qquad\qquad \text{otherwise} \end{aligned} \tag{8}$$

where m is in solar mass units and C is a constant. An f(m) with $\alpha = 2.45$, an approximation to the IMFF's of Saltpeter (1955) and Limber (1960), was found to fit the UBV colors of Sc's. The UBV colors of Irregulars could be explained by $\alpha \simeq 2.0$. Now, the median masses for the bursts are about 35 and 8, and about 2 for older stars. We can therefore estimate the relative enrichment of galaxies with different α's in massive stars by the ratios of the numbers of 35 and 8 $M_\odot$ stars to 2 $M_\odot$ stars. Let:

$$r(m,\alpha) = \frac{f(m,\alpha)\ f(2,2.45)}{f(2,\alpha)\ f(m,2.45)} \simeq (m/2)^{(2.45-\alpha)} \tag{9}$$

where $f(m,\alpha)/f(2,\alpha)$ is the ratio of the number of stars of mass m to those of 2 $M_\odot$ for an IMFF with α; $f(m,2.45)/f(2,2.45)$ is the same ratio for the standard case of $\alpha = 2.45$. The "relative enrichment," $r(m,\alpha)$, is

the ratio of these quantities. Obviously, r(m, 2.45) = 1.0 for all m. For the case α = 2.0, which fit the UBV colors of Irregulars, we get: r(35,2.0) = 3.63 and r(8,2.0)=1.87. Thus, Irregulars should have several times as many higher mass stars as the Sc's.

In this paper the differences of about one unit in model number in the average burst parameters correspond roughly to differences of factors of two in massive stars in Irregulars and Sc's. This enrichment is comparable to that of the α = 2.0 case of SSB discussed above. Therefore, the difference in average burst parameters can be explained by a difference in α of 0.45, or slightly less, between Irregulars and Sc's, as in SSB.

iv) There is a tendency, mentioned previously, for B_1 and B_2 to increase with increasing β in Figures 10 and 11. As noted in a previous section, model galaxies with high β tend to have similar colors regardless of burst parameters. Because of this convergence of the model colors, B_1 and B_2, especially for low values of these parameters, should become more inaccurate for galaxies of high β. (See error estimates in the Figures.) More importantly, if the reddest galaxies are not fit exactly by the unity burst, (β, 2, 3), models, the estimated B_1 and B_2 will tend toward either 1 or 7. In Figure 9, for example, (Hα-r) of the reddest galaxies is a bit higher than that of the unity burst models. Thus, we should

expect that high β galaxies have high B_1 parameters, as in fact they do. It is difficult, therefore, to obtain accurate absolute values of B_1 and B_2 for galaxies with high β; although relative differences in the burst parameters for galaxies of similar β may be obtained. It is also difficult to determine whether the high burst parameters of high β galaxies are real or caused by small errors in the colors of the models. Probably the latter is the case.

v) The Irregulars and Sc's have been divided into two roughly equal groups according to aperture/size ratios. In Table 9 (and Figures 10 and 11) Sc's with larger aperture/ size ratios have higher β. Apparently, outer regions of Sc's have a higher rate of star formation than inner regions. Since β is strongly affected by overall color, it is not surprising that β should decrease for higher aperture/ size ratios; for, in Figure 4 (b-o) becomes redder with increasing d. A much smaller tendency in the opposite direction may exist for Irregulars. Finally, some narrowing of the separation between Sc's and Irregulars with high aperture/ size ratios is also apparent in the Figures.

vi) Figure 11 is a plot of B_1 and B_2. The most important feature of Figure 11 is the partial correlation between the bursts. The width of the scatter in the plot appears about three times the size of the errors.

Therefore, the scatter in the plot must be mainly due to irregular rates of star formation in the recent past. Finally, we note that the points fall fairly evenly around a dotted line in Figure 11 which denotes equal numerical values of B_1 and B_2.

The principal results found in this section may be summarized as follows. Sc's have higher average β's than Irregulars, indicating more older stars. Also, Sc's with higher aperture/ size ratios have higher β, which indicates that the central parts of these galaxies have more older stars. For galaxies of similar β, Irregulars have higher burst parameters than Sc's, which can be interpreted as an enrichment in massive stars of the IMFF of the former. Such an enrichment is consistent with the difference in the parameter α of SSB. The higher burst parameters for high β galaxies seems due to fairly small differences between models and galaxies. Finally, there appears to be only a partial correlation between B_1 and B_2, which indicates that the rate of star formation in the recent past is irregular.

VII. SUMMARY AND CONCLUSIONS

In this paper the results of observations of late-type galaxies were presented, and the loci of galaxies in several two-color plots were discussed. Irregulars appeared to be generally bluer in most colors and to have

more Hα emission than Sc's. It was also found that the colors of some galaxies (up to 30) are affected by emission lines. Three colors were plotted versus aperture/ size ratio, and it was found that Sc's with higher log d become bluer in (b-o), and to a lesser extent Irregulars become redder.

The construction of model cluster colors, and their behavior as a function of time, t, were discussed next. In a table of colors and log t, the clusters appeared to fall into roughly five groups. Thus, seemingly at most four or five parameters could explain the galaxy colors. A principal component analysis indicated that three parameters could explain most of the variation in galaxy colors. The three empirical parameters (eigenvectors) found by the analysis were an overall color temperature, Hα emission, and a combination of colors, (u-g) the strongest, which appeared to represent the effects of ultraviolet intensity and emission lines in filter g. It was found that some of the filters were redundant and that most of the information could have been obtained with a set of four filters: u, g, o, and Hα.

A set of three parameter models of the stellar content of galaxies was adopted to explain their colors. The three parameters chosen govern the star formation history of model galaxies. The Limber IMFF was assumed. The overall rate of star formation was assumed to vary as

$\exp(-\beta t_{10})$, where t_{10} is the number of years ago in units of 10^{10} years. Thus, β controls the relative number of very old stars. The parameters B_1 and B_2 govern the numbers of stars created in the intervals $\log t \leq 6.4$ and $6.4 < \log t \leq 8.0$ respectively. These time intervals were chosen to explain variations in Hα emission and ultraviolet intensity, which appeared significant in the principal component analysis.

The colors of some 35 models with different β, B_1, and B_2 were plotted on three two-color plots. It was found that the loci of the models agree well with observations. The features of plots of observations, such as the sail-like shape in the (b-o), (Hα-r) plane, could be explained by models with varying parameters. The properties of models in the plots were discussed. It was found that, as expected, overall colors, such as (b-o), were strongly affected by changes in β. Changes in B_1 and B_2 similarly affected (Hα-r) and (u-b) respectively. The contributions of stars of various masses to the bursts and to the light of stars older than 10^8 years were computed for the constant creation case. It was found that most of the light in these three regions in time comes from stars of different masses. The masses of stars above which half the light is contributed was found to be about 35, 8, and 2 $M_\odot$ respectively.

Finally, fits to individual galaxies in the three

parameters were made, as were estimates of the "uniqueness" of the fits. The procedure used was described in detail. The largest systematic difference between Irregulars and Sc's is that in the average β model number of 1.77. This difference implies that the ratio of star formation 10^{10} years ago to recently is roughly six times higher on average for Sc's than Irregulars. It was also found that for galaxies with similar β's Irregulars have higher average B_1 and B_2 than Sc's. Irregulars seem to be enriched in massive stars compared to Sc's. The ratio in the IMFF of stars of 8-30 $M_\odot$ to stars of 2 $M_\odot$ seems about a factor of two higher in Irregulars than Sc's. This enrichment corresponds roughly to the difference in parameter α of the IMFF's in SSB ($\alpha = 2.0$ versus $\alpha = 2.45$).

Among other features noted was the tendency for high β galaxies to have high B_1 and B_2, which can be explained by relatively small differences between models and observations for the reddest galaxies. (These differences may be due to errors in the cluster colors assumed or the neglect of Population II stars, etc.) Also noted was that the B_1, B_2 plot indicates only a partial correlation between star formation rates in the time periods of the bursts. Irregular rates of star formation in the recent past is indicated. Finally, the Sc's with lower aperture/ size ratios have higher average β's, implying that the central portions of Sc's have more older stars. A much smaller

reverse tendency may exist for Irregulars.

REFERENCES

Aller, L. H., Czyzak, S. J., and Walker, M. F. 1968, Ap. J., 151, 491.

Bagnuolo, W. G. 1976, to be published.

Bryson, A. E. Jr., and Ho, Y. 1969, Applied Optimal Control; Waltham Mass., Ginn and Co.

Deeming, T. J. 1964, M. N., 127, 35.
———. 1968, Vistas in Astronomy, 10, 125.

de Vaucouleurs, G. 1961, Ap. J. Supp., 5, 233.

de Vaucouleurs, G. and A. 1964, Reference Catalog of Bright Galaxies; Austin, Univ. of Texas Press.

Haug, U., Dachs, T., Pesch, J., and Pfleiderer, J. 1967, Z. Astrophys., 66, 433.

Holmberg, E. 1958, Medd. Lunds. Astr. Obs., Ser. II, No. 136.

Johnson, H. L. 1966, Ann. Rev. Astr. and Ap., 4, 193.

Johnson, H. L., and Sandage, A. 1955, Ap. J., 121, 616.

Kendall, M. G. 1968, A Course in Multivariate Analysis; London, Griffin and Co., 2nd ed.

Kendall, M. G., and Stuart, A. 1966, The Advanced Theory of Statistics, Vol. 3; New York, Hafner Pub. Co.

Lee, T. A., 1970, Ap. J., 162, 217.

Limber, D. N. 1960, Ap. J., 131, 168.

Martin, W. L., and Bingham, R. G. 1970, Observatory, 99, 13.

Morton, D. C. 1969, Ap. J., 158, 629.

Morton, D. C., and Adams, T. F. 1968, Ap. J., 151, 611.

Robertson, J. W. 1971, Ap. J., 170, 353.
———. 1972, Ap. J., 177, 473.

Saltpeter, E. E. 1955, Ap. J., 121, 161.

Sandage, A. 1962, Ap. J., 135, 333.

Searle, L. 1971, Ap. J., 168, 327.
———. 1975, private communication.

Searle, L., and Bagnuolo, W. G. 1976, to be published.

Searle, L., and Sargent, W. L. W. 1972, Ap. J., 173, 25.

Searle, L., Sargent, W. L. W., and Bagnuolo, W. G. 1973, Ap. J., 179, 427.

Spinrad, H., and Taylor, B. J. 1971, Ap. J. Supp., 22, 445.

Whitford, A. E. 1958, A. J., 63, 201.

Wood, D. B. 1965, A. J., 74, 177.
———. 1966, Ap. J., 145, 36.

TABLE 1

PROPERTIES OF THE PHOTOMETRIC SYSTEM

Filter	$\bar{\lambda}$(Å)	λ_{MAX}(Å)	h.p. Bandwidth (Å)
u	3545	3570	375
b	3970	3945	455
g	4930	4910	723
o	5975	5850	542
r	6750	6505	765
Hα	6572	6572	65
Mgb	5175	5173	66
IR	7005	6950	253
TiO	6210	6197	109
Hα′	6587	6590	95
66	6583	6583	207

TABLE 2

GALAXY OBSERVATIONS

Name	Type	AP	Tel.	(G/S)	d	u	b	o	r	Hα	Mg	IR	Ti	Hα′	66	V_R
						"corrected" colors										
N1140	IRR	1′	60"	1.01	.87	-.41	.30	-.21	-.56	-1.08	...	-.46	...	-1.15	...	1544
						-.42	.30	-.21	-.55	-1.34	...	-.45	...	-1.15	...	...
N1156	IRR	1.4′	60"	1.17	.42	-.14	.41	-.44	-.80	-1.42	-.03	-.74	-.46	-1.10	...	405
						-.17	.39	-.42	-.76	-1.39	-.02	-.70	-.44	-1.07	...	...
N1569	IRR	2′	60"	.62	.88	.02	.74	-.60	-1.13	-2.27	.15	...	...	...	-1.45	-42
						-.35	.48	-.36	-.76	-1.89	.21	...	...	...	-1.09	...
N2366	IRR	2′	60"	.38	.57	.18	.92	.61	-.26	-1.84	.68	...	...	...	- .88	145
						.14	.90	.63	-.23	-1.77	.69	...	...	...	- .84	
N2366	IRR	2x1.4′	60"	.69	.57	-.06	.56	.31	.15	-1.81	.69	.38	.45	-1.43	...	145
						-.10	.53	.33	.19	-1.74	.69	.42	.48	-1.45	...	...
N2537	IIR	1′	24"	1.94	.67	-.02	.55	-.47	-.81	-1.25	.00	-.80	-.48	...	- .91	404
						-.03	.54	-.46	-.80	-.124	.00	-.79	-.48	...	- .90	...
N2537	IRR	2′	60"	1.09	1.33	-.05	.45	-.32	-.75	-1.18	.08	...	...	...	- .76	404
						-.06	.45	-.32	-.74	-1.16	.08	...	...	...	- .76	...
N2552	IRR	1.4′	60"	.39	.46	-.06	.28	-.39	-.83	...	...	...	...	- .79	- .77	...
						-.06	.27	-.39	-.83	...	...	...	...	- .79	- .77	...
N2552	IRR	2′	60"	.31	.66	.02	.43	.00	-.54	- .89	.12	...	...	...	- .53	...
						.02	.42	.00	-.53	- .89	.12	...	...	...	- .52	...
N2552	IRR	1′	24"	1.74	.33	-.33	.25	-.26	-.54	- .98	.00	-.44	-.30	...	- .57	...
						-.33	.25	-.26	-.54	- .98	.00	-.44	-.30	...	- .57	...
N3109	IRR	6′	20"	.26	.43	-.06	.46	-.44	-.69	-1.05	...	...	...	...	...	403
						-.15	.40	-.39	-.60	- .96	...	...	...	...	...	...
N3396	IRR	2′	60"	1.09	.88	-.35	.23	-.13	-.58	- .98	...	...	...	...	...	1645
						-.28	.28	-.18	-.65	-1.29	...	...	...	...	...	...
N3396	IRR	2′	60"	.68	.88	-.42	.20	-.30	-.76	...	...	-.59	-.33	-1.06	...	1645
						-.35	.25	-.35	-.83	...	...	-.67	-.38	-1.15	...	...
N3447B	IRR	2′	60"	.26	1.71	.13	.37	.40	-.51	- .90	.29	...	...	...	- .20	855
						.20	.42	.36	-.58	-1.00	.28	...	...	...	- .27	...

TABLE 2 (CONT'D)

Name	Type	AP	Tel.	(G/S)	d	u	b	o	r	Hα	Mg	IR	Ti	Hα′	66	V_R
						"corrected" colors										
N3738	IRR	1′	24"	2.40	.31	-.29	.28	-.27	-.56	-1.01	.00	-.55	-.32	...	- .63	...
						-.22	.32	-.31	-.63	-1.07	-.01	-.62	-.37	...	- .69	...
N3738	IRR	2′	24"	.85	.62	-.26	.39	-.33	-.53	- .76	.00	-.32	-.27	...	- .54	...
						-.19	.44	-.37	-.60	- .82	-.01	-.39	-.32	...	- .60	...
N4032	IEE	1.4′	60"	1.42	1.90	-.07	.44	-.37	-.73	- .90	.04	-.65	-.38	- .77	- .66	...
						.00	.49	-.42	-.80	- .96	.03	-.73	-.43	- .83	- .73	...
N4038	IRR	6′	20"	.56	.85	-.01	.53	-.54	-.88	-1.23	-.02	-.84	-.56	...	-1.04	1650
						-.19	.40	-.42	-.70	-1.29	.00	-.64	-.42	...	- .87	...
N4190	IRR	2′	60"	.44	1.18	-.25	.28	-.28	-.49	- .87	.00	-.66	-.33	- .77	- .56	...
						-.17	.34	-.33	-.57	- .95	-.02	-.75	-.39	- .85	- .64	...
N4214	IRR	1.4′	60"	3.39	.16	-.51	.27	-.21	-.60	-1.57	.15	-.42	-.17	-1.28	...	290
						-.43	.32	-.27	-.68	-1.62	.14	-.52	-.24	-1.38	...	...
N4214	IRR	6′	20"	1.02	.67	-.36	.27	-.34	-.63	-1.28	.04	-.50	-.33	-1.07	- .66	290
						-.28	.33	-.39	-.71	-1.34	.03	-.59	-.39	-1.16	- .74	...
N4214	IRR	2′	60"	3.57	.22	-.37	.30	-.22	-.60	-1.44	.15	...	...	...	- .79	290
						-.28	.36	-.28	-.68	-1.52	.13	...	...	...	- .86	...
N4449	IRR	6′	20"	2.05	1.22	-.46	.20	-.28	-.53	-1.31	.08	-.45	-.27	- .99	- .75	207
						-.38	.26	-.33	-.61	-1.36	.06	-.54	-.33	-1.08	- .82	...
N4449	IRR	1.4′	60"	9.42	.29	-.45	.20	-.24	-.56	-1.28	.06	-.44	-.24	-1.01	...	207
						-.37	.25	-.29	-.64	-1.33	.04	-.53	-.29	-1.10	...	...
N4449	IRR	2′	60"	1.11	.41	-.44	.19	-.26	-.56	-1.25	.04	-.41	-.27	...	- .71	207
						-.36	.25	-.31	-.64	-1.30	.03	-.50	-.32	...	- .78	...
N4449	IRR	2′	24"	3.04	.41	-.44	.28	-.25	-.59	-1.28	.03	-.52	-.30	...	- .75	207
						-.36	.33	-.30	-.67	-1.34	.02	-.61	-.36	...	- .83	...
N4485	IRR	1′	24"	2.01	.40	-.29	.26	-.29	-.50	- .78	.01	-.50	-.34	...	...	795
						-.22	.32	-.34	-.58	- .86	.00	-.58	-.39	...	...	...
N4532	IRR	2′	24"	.52	1.01	-.49	.32	-.42	-.78	-1.04	-.02	-.71	-.36	...	- .90	2145
						-.42	.38	-.47	-.86	-1.52	-.03	-.80	-.41	...	- .98	...
N4532	IRR	1′	24"	1.16	.50	-.68	.17	-.22	-.63	- .98	.09	-.55	-.31	...	- .83	2145
						-.61	.22	-.27	-.71	-1.56	.08	-.64	-.37	...	- .91	...

TABLE 2 (CONT'D)

Name	Type	AP	Tel.	(G/S)	d	u	b	o	r	Hα	Mg	IR	Ti	Hα′	66	V_R
						"corrected" colors										
N4532	IRR	2′	24"	.43	1.01	-.40	.29	-.34	-.69	- .92	.00	-.49	-.30	...	- .80	2145
						-.32	.34	-.39	-.77	-1.33	-.02	-.58	-.36	...	- .88	...
N4656	IRR	2′	60"	.52	.32	-.81	-.03	-.02	-.33	-1.41	.15	-.02	...	...	- .76	755
						-.72	.03	-.07	-.41	-1.53	.13	-.12	...	...	- .84	...
N4657	IRR	3′	24"	.45	.48	-.45	.34	-.06	-.45	-1.38	.13	-.37	-.15	...	- .69	755
						-.37	.40	-.11	-.54	-1.50	.12	-.47	-.21	...	- .77	...
N4657	IRR	1′	24"	2.12	.16	-.50	.22	-.24	-.50	-1.15	.07	-.43	-.18	...	- .62	755
						-.42	.28	-.30	-.58	-1.26	.06	-.53	-.29	...	- .70	...
N4657	IRR	3′	24"	.46	.48	-.36	.31	-.23	-.52	-1.14	.01	-.53	-.40	...	- .68	755
						-.27	.37	-.28	-.60	-1.25	.00	-.61	-.46	...	- .76	...
N4668	IRR	1.4′	60"	.80	1.72	-.30	.34	-.31	-.51	- .85	-.01	-.58	-.32	- .88	- .68	...
						-.23	.39	-.35	-.58	- .92	-.02	-.65	-.37	- .95	- .75	...
N5253	IRR	...	40"	...	...	-.39	.39	-.07	-.48	...	...	...	...	...	...	403
						-.42	.37	-.06	-.46	...	...	...	...	...	...	...
A0957	IRR	1.4′	60"	.56	.29	-.27	.25	-.30	-.54	- .84	-.01	-.50	-.32	- .71	...	...
						-.23	.27	-.32	-.57	- .87	-.01	-.53	-.35	- .74	...	...
A0957	IRR	2′	60"	.33	.41	.02	.18	.22	-.47	- .64	.16	...	...	...	- .18	...
						.05	.21	.20	-.50	- .67	.16	...	...	...	- .21	...
I2574	IRR	.6′	20"	.12	.48	-.60	.17	-.52	-.74	-1.31	...	...	...	...	...	46
						-.56	.19	-.54	-.77	-1.37	...	...	...	...	...	...
I1613	IRR	4.2′	20"	.07	.37	-.57	.01	-.60	...	-1.21	...	...	...	...	...	-236
						-.50	.06	-.64	...	-1.27	...	...	...	...	...	...
N3259	IRR-Sc	1.4′	60"	.80	.99	.03	.54	-.52	-.88	...	...	...	...	-1.09	...	1866
						.07	.57	-.55	-.92	...	...	...	...	-1.13	...	...
N3259	IRR-Sc	1.4′	60"	.96	.99	.01	.55	-.50	-.82	-1.02	...	-.83	...	-1.07	...	1866
						.05	.58	-.52	-.86	-1.25	...	-.87	...	-1.12	...	...
N3259	IRR-Sc	2′	60"	.24	1.41	.20	.56	-.51	-1.03	...	...	...	...	-1.01	...	1866
						.25	.59	-.53	-1.08	...	...	...	...	-1.11	...	...
N4861-IC3961	IRR-Sc	1.4′	60"	.42	.55	-.38	.24	-.13	-.54	...	...	-.31	-.12	- .91	- .66	790
						-.29	.30	-.19	-.63	...	...	-.40	-.18	- .98	- .74	...

TABLE 2 (CONT'D)

Name	Type	AP	Tel.	(G/S)	d	u	b	o	r	Hα	Mg	IR	Ti	Hα′	66	V_R
						"corrected" colors										
N4861-	IRR-	1.4′	60"	.24	.55	-.23	...	-.27	-.64	-1.23	.03	...	...	...	...	790
IC3961	Sc					-.15	...	-.33	-.73	-1.34	.01	...	...	...	...	...
N5204	IRR-	2′	24"	.76	.50	-.41	.28	-.32	-.61	-1.19	-.03	-.60	-.37	...	- .72	...
	SC					-.39	.30	-.33	-.63	-1.21	-.03	-.63	-.39	...	- .74	...
N604	H II	7′	60"	3.32	...	-1.16	.06	.27	-.62	-2.90	...	.47	...	-2.39	...	-186
	Region					-1.21	.02	.30	-.57	-2.84	...	.52	...	-2.48	...	...
M33	Sc	2x4.2′	20"	2.38	~.16	-.07	-.47	-.55	-.86	-1.19	-.06	-.93	...	...	...	-186
						-.12	-.44	-.52	-.81	-1.14	-.05	-.89	...	...	...	...
N628	Sc	4.2′	20"	1.07	.40	.00	...	-.60	-.92	-1.13	-.05	-.95	...	...	...	653
						.04	...	-.63	-.96	-1.17	-.05	-1.00	...	...	...	...
N672	Sc	3′	20"	.76	.66	.00	.45	-.49	-.80	-1.14	.21	-.84	...	- .67	...	340
						-.07	.41	-.45	-.79	-1.08	.22	-.78	...	- .61	...	...
N1084	Sc	3′	20"	1.32	1.14	-.09	.39	-.50	-.84	-1.29	-.06	-.82	...	-1.22	...	1465
						-.17	.34	-.44	-.76	-1.40	-.05	-.73	...	-1.14	...	...
N1637	Sc	4.2′	20"	.62	1.08	.20	.67	-.30	-.62	- .99	-.03	-.61	...	- .88	...	661
						.23	.70	-.32	-.65	-1.03	-.03	-.65	...	- .91	...	...
N2403	Sc	6′	20"	2.01	.36	.08	.55	-.48	-.74	-1.09	-.04	-.73	-.51	- .91	- .81	136
						.00	.50	-.43	-.66	-1.01	-.03	-.64	-.45	- .84	- .74	...
N2903	Sc	6′	20"	1.69	.69	.21	.63	-.59	-.90	-1.23	-.06	-.90	-.64	-1.07	- .97	644
						.17	.60	-.56	-.87	-1.21	-.05	-.86	-.61	-1.04	- .94	...
N3184	Sc	6′	20"	.68	.77	.11	.57	-.54	-.79	-1.09	-.08	-.78	-.58	- .95	- .82	418
						.17	.61	-.58	-.85	-1.14	-.09	-.84	-.63	-1.01	- .88	...
N3198	Sc	6′	20"	.38	1.17	.03	.46	-.49	-.79	-1.04	-.02	-.72	-.52	- .96	- .79	649
						-.06	.40	-.43	-.65	- .96	.00	-.63	-.45	- .87	- .71	...
N3198	Sc	4.2′	20"	.93	.82	.09	.51	-.52	-.83	-1.11	-.02	-.90	-.58	-1.03	...	649
						.01	.45	-.46	-.75	-1.04	-.01	-.81	-.52	- .95	...	...
N3486	Sc	3′	20"	.96	.50	-.08	.45	-.48	-.79	-1.24	.01	-.81	-.48	-1.06	...	1116
						-.07	.46	-.49	-.80	-1.33	.01	-.82	-.49	-1.06	...	...
N3486	Sc	3′	24"	.36	.50	-.17	.47	-.40	-.73	-1.18	.00	-.68	-.53	...	- .85	1116
						-.16	.48	-.40	-.74	-1.27	.00	-.69	-.53	...	- .86	...
N3521	Sb	6′	20"	1.42	.63	.44	.77	-.64	-.98	-1.22	-.07	-1.02	-.72	-1.13	-1.01	790
						.27	.66	-.53	-.82	-1.08	-.04	-.84	-.60	- .97	- .85	...

TABLE 2 (CONT'D)

Name	Type	AP	Tel.	(G/S)	d	u	b	o	r	Hα	Mg	IR	Ti	Hα′	66	V_R
						"corrected" colors										
N3631	Sc	4.2′	20"	1.06	.84	-.08	.44	-.47	-.77	-1.10	-.04	-.80	-.47	-1.05	...	1087
						-.02	.48	-.51	-.84	-1.21	-.06	-.88	-.52	-1.11	...	...
N3631	Sc	4.2′	20"	.94	.84	-.10	.41	-.46	-.74	-1.08	-.02	-.74	-.49	-1.04	- .81	1087
						-.03	.46	-.50	-.81	-1.20	-.03	-.82	-.54	-1.10	- .87	...
N3810	Sc	4.2′	20"	.88	1.24	-.08	.43	-.50	-.83	-1.22	-.05	-.82	-.52	-1.13	- .90	988
						-.09	.42	-.49	-.82	-1.26	-.05	-.81	-.51	-1.12	- .89	...
N3887	Sc	3′	24"	.56	1.06	.01	.57	-.56	-.87	-1.14	-.07	-.91	-.58	...	- .94	1162
						-.15	.46	-.46	-.71	-1.04	-.05	-.74	-.46	...	- .79	...
N3893	Sc	6′	20"	.70	1.86	-.11	.43	-.44	-.72	-1.10	.00	-.73	-.47	-1.01	- .80	1001
						-.05	.47	-.48	-.78	-1.20	.00	-.79	-.51	-1.06	- .86	...
N3893	Sc	3′	20"	2.69	.93	-.02	.43	-.46	-.78	-1.14	-.04	-.79	-.49	-1.07	...	1001
						.04	.47	-.50	-.83	-1.24	-.04	-.85	-.53	-1.12	...	...
N3893	Sc	3′	20"	2.00	.93	-.03	.44	-.47	-.75	-1.14	...	-.78	...	- .99	...	1001
						.02	.48	-.50	-.81	-1.24	...	-.84	...	-1.03	...	...
N3953	Sb	4.2′	20"	1.51	.88	.40	.81	-.66	-1.02	-1.14	-.08	-1.09	-.73	-1.10	-1.00	958
						.40	.81	-.66	-1.02	-1.15	-.08	-1.09	-.73	-1.10	-1.01	...
N3953	Sb	3′	20"	1.90	.63	.53	.88	-.70	-1.06	-1.16	...	-1.12	...	-1.06	...	958
						.53	.88	-.70	-1.06	-1.17	...	-1.12	...	-1.06	...	...
M51	Sc	6′	20"	2.97	.71	.07	.55	-.56	-.85	-1.18	-.03	-.84	-.59	-1.00	- .91	445
						.07	.55	-.55	-.84	-1.17	-.02	-.84	-.58	-1.00	- .90	...
M51	Sc	1′	24"	10.52	.12	.15	.66	-.60	-.97	-1.30	-.03	-1.01	-.64	...	...	445
						.14	.66	-.60	-.96	-1.30	-.03	-1.01	-.64	...	...	...
M51	Sc	3′	24"	3.47	.35	.10	.62	-.57	-.93	-1.24	-.04	-.98	-.63	...	- .97	445
						.10	.62	-.57	-.92	-1.24	-.04	-.97	-.63	...	- .96	...
M51	Sc	3′	24"	3.14	.35	.15	.62	-.56	-1.06	...	...	...	...	...	...	445
						.14	.61	-.56	-1.05	...	...	...	...	...	...	...
N5248	Sc	1′	24"	2.17	.17	.21	.74	-.60	-1.00	-1.32	-.10	-1.07	-.76	...	-1.05	1181
						.24	.75	-.61	-1.03	-1.41	-.10	-1.09	-.77	...	-1.07	...
N5248	Sc	2′	24"	1.20	.34	.13	.65	-.59	-.94	-1.18	-.06	-.99	-.61	...	- .98	1181
						.15	.67	-.60	-.96	-1.25	-.06	-1.02	-.63	...	-1.00	...

TABLE 2 (CONT'D)

Name	Type	AP	Tel.	(G/S)	d	u	b	o	r	Hα	Mg	IR	Ti	Hα′	66	V_R
						"corrected" colors										
N5364	Sc	3′	24"	.52	.52	-.02	.63	-.75	- .97	-1.16	-.05	- .98	-.68	...	- .98	1393
						.04	.66	-.78	-1.02	-1.27	-.06	-1.04	-.72	...	-1.03	...
N5457	Sc	3′	24"	2.24	.14	.20	.69	-.59	- .92	-1.11	-.04	- .98	-.65	...	- .92	266
						.27	.74	-.64	- .98	-1.17	-.05	-1.05	-.70	...	- .98	...
N6503	Sc	4.2′	20"	1.55	1.14	.18	.64	-.63	- .96	-1.32	-.13	-1.04	...	...	...	26
						.00	.51	-.51	- .78	-1.13	-.10	- .84	...	...	...	...
N6503	Sc	3′	20"	2.54	.81	.16	.62	-.58	- .92	-1.22	-.06	- .99	-.61	-1.05	...	26
						-.02	.49	-.46	- .74	-1.04	-.03	- .79	-.48	- .89	...	...
N6946	Sc	4.2′	20"	.82	.30	.53	.88	-.94	-1.38	-1.70	-.18	-1.44	...	...	...	80
						.14	.57	-.69	-1.00	-1.34	-.12	-1.02	...	...	...	...

TABLE 3

ERRORS IN GALAXY OBSERVATIONS

G/S	N′	N	Δu	Δb	Δo	Δr	ΔHα	ΔMgb	ΔIR	ΔTiO	ΔHα′	Δ66
G/S≥1.0	12	38	.022 (.021)	.019 (.013)	.020 (.018)	.034 (.025)	.035 (.025)	.025 (.022)	.028 (.040)	.026 (.028)	.047 (.059)	.024 (.050)
.5≤G/S<1.0	8	23	.049 (.070)	.041 (.039)	.010 (.032)	.028 (.041)	.040 (.069)	.016 (.020)	.078 (.082)	.042 (.068)	.044 (.072)	.050 (.075)
G/S < .5	6	17	.080 (.085)	.044 (.060)	.041 (.072)	.052 (.076)	.045 (.049)	.042 (.060)	... ...	.05 (.07)	... ...	... ...

TABLE 4

ADOPTED CLUSTER COLORS

Time Slot	log t_{iMAX}	u	b	o	r	Hα	Mgb	IR	TiO	Hα′	66	$-m_g$
1	6.0	-.08	.74	1.42	.09	-2.38	1.98	2.29	2.18	-1.96	-1.17	15.35
2	6.1	-.17	.67	1.36	.00	-2.45	1.90	2.22	2.11	-2.03	-1.25	15.44
3	6.2	-.25	.61	1.28	-.08	-2.51	1.82	2.10	2.02	-2.09	-1.31	15.53
4	6.3	-.49	.44	.53	-.40	-2.46	1.05	.48	.83	-2.07	-1.35	15.44
5	6.4	-.73	.25	.33	-.48	-2.45	.75	.25	.56	-2.07	-1.37	15.09
6	6.5	-.94	.08	.14	-.52	-2.37	.47	.03	.30	-2.02	-1.35	14.69
7	6.6	-1.11	-.07	-.03	-.51	-1.99	.22	-.20	.06	-1.69	-1.10	14.32
8	6.7	-1.19	-.16	-.15	-.44	-1.21	.03	-.37	-.29	-1.03	- .65	14.04
9	6.8	-1.20	-.19	-.17	-.39	- .71	-.04	-.39	-.17	- .61	- .43	13.77
10	6.9	-1.13	-.15	-.16	-.41	- .58	-.06	-.47	-.22	- .52	- .42	13.46
11	7.0	-1.17	-.22	-.11	-.22	- .35	-.05	-.25	-.12	- .31	- .22	13.21
12	7.1	-1.03	-.15	-.16	-.29	- .38	-.05	-.33	-.19	- .34	- .27	13.17
13	7.2	-.91	-.11	-.21	-.34	- .40	-.06	-.39	-.24	- .37	- .31	13.12
14	7.3	-.85	-.14	-.14	-.31	- .29	-.06	-.26	-.18	- .27	- .22	13.05
15	7.4	-.66	-.06	-.19	-.35	- .34	-.07	-.32	-.23	- .32	- .27	13.02
16	7.5	-.54	-.02	-.21	-.36	- .35	-.07	-.33	-.26	- .33	- .28	12.88
17	7.6	-.39	+.05	-.23	-.31	- .37	-.06	-.35	-.28	- .35	- .30	12.82
18	7.7	-.34	.13	-.26	-.37	- .42	-.07	-.42	-.32	- .40	- .36	12.63
19	7.8	-.32	.20	-.30	-.41	- .47	-.08	-.48	-.36	- .44	- .40	12.31
20	7.9	-.31	.19	-.27	-.39	- .45	-.07	-.46	-.34	- .43	- .38	11.99
21	8.0	-.30	.16	-.26	-.39	- .44	-.07	-.44	-.32	- .41	- .37	11.74
22	8.1	-.31	.11	-.22	-.37	- .42	-.05	-.42	-.29	- .39	- .35	11.55
23	8.2	-.28	.11	-.21	-.37	- .42	-.05	-.42	-.28	- .39	- .35	11.37
24	8.3	-.24	.11	-.21	-.36	- .41	-.05	-.41	-.28	- .34	- .39	11.19
25	8.4	-.19	.12	-.21	-.36	- .41	-.04	-.41	-.28	- .38	- .34	11.02
26	8.5	-.13	.14	-.21	-.37	- .41	-.04	-.41	-.28	- .38	- .34	10.86
27	8.6	+.01	.22	-.27	-.43	- .48	-.04	-.49	-.34	- .46	- .42	10.70
28	8.7	+.12	.28	-.33	-.52	- .56	-.04	-.59	-.39	- .54	- .50	10.54
29	8.8	.06	.22	-.25	-.42	- .46	-.04	-.48	-.31	- .43	- .40	10.15
30	8.9	.10	.26	-.27	-.45	- .48	-.04	-.51	-.33	- .46	- .43	9.90
31	9.0	.16	.35	-.33	-.53	- .59	-.04	-.60	-.38	- .57	- .51	9.70
32	9.1	.19	.43	-.36	-.60	- .67	-.05	-.67	-.43	- .64	- .58	9.53
33	9.2	.20	.49	-.39	-.63	- .70	-.05	-.70	-.46	- .69	- .61	9.33
34	9.3	.09	.44	-.34	-.55	- .61	-.05	-.61	-.40	- .59	- .53	8.95
35	9.4	.25	.62	-.48	-.75	- .82	-.05	-.82	-.54	- .79	- .71	8.91
36	9.5	.25	.66	-.58	-.86	- .95	-.05	-.94	-.62	- .92	- .82	8.68
37	9.6	.31	.71	-.60	-.93	-1.00	-.05	-.99	-.65	- .98	- .87	8.57

TABLE 4 (CONT'D)

Time Slot	log t_{iMAX}	u	b	o	r	Hα	Mgb	IR	TiO	Hα′	66	$-m_g$
38	9.7	.38	.78	-.62	-.96	-1.03	-.05	-1.02	-.69	-1.00	- .91	8.30
39	9.8	.45	.83	-.65	-.99	-1.05	-.06	-1.06	-.71	-1.03	- .92	8.21
40	9.9	.53	.90	-.69	-1.02	-1.10	-.06	-1.11	-.76	-1.07	- .98	7.84
41	10.0	.61	.95	-.70	-1.05	-1.14	-.06	-1.13	-.79	-1.11	-1.00	7.65

TABLE 5

LARGEST EIGEN VALUES AND THEIR EIGEN VECTORS FOR 10-COLOR ANALYSIS

λ	F	u	b	o	r	Hα	Mgb	IR	TiO	Hα'	66
5.641	80.01	0.286	0.184	-0.436	-0.372	0.114	-0.237	-0.514	-0.403	0.085	-0.228
2.300	27.56	.157	-.122	.053	.064	.738	-.107	.054	.007	.520	.352
1.529	20.88	.749	.538	.288	.069	.032	.229	.053	.057	.00	.044
.160	2.24	.099	-.255	.504	-.667	-.294	.202	-.237	.011	.195	.074
				6-Color Analysis							
3.193	42.61	.457	.272	-.566	-.491	.231	-.320				
1.512	19.39	.688	.541	.350	.113	-.117	.291				
1.021	18.70	.222	-.113	.255	.230	.905	-.035				
.147	2.36	.216	-.282	.665	-.654	-.048	.034				

TABLE 6

LARGEST EIGENVALUES FOR SETS OF FOUR FILTERS

Filters	λ_1	λ_2	λ_3	F_1	F_2	F_3	$F_1F_2F_3$
u,b,g,o	1.923	.792	0.285	25.54	5.83	4.95	737.
u,b,g,Hα	1.616	1.242	.142	26.29	9.25	1.73	421.
u,b,o,Hα	1.345	1.291	.362	37.91	11.92	5.26	2377.
u,b,r,Hα	1.455	1.314	.230	35.80	12.26	3.39	1488.
u,g,o,Hα	1.527	.838	.634	32.35	17.30	13.58	7600.
u,g,r,Hα	1.648	.877	.475	30.67	15.10	9.00	4168.
u,g,Hα,IR	1.707	.830	.463	39.01	16.87	11.01	7246.
b,g,o,r	2.067	.793	.140	32.82	9.73	2.39	763.
b,g,o,Hα	1.310	1.008	.682	20.96	15.89	10.90	3630.
b,o,Hα,IR	1.717	.986	.297	48.07	5.68	8.98	2452.
b,o,r,Hα	1.985	.692	.323	35.27	5.75	11.87	2407.
b,g,Hα,IR	1.521	1.006	.472	24.70	17.36	7.67	3289.
u,o,r,Hα	1.979	.804	.217	41.97	6.64	7.57	2110.

TABLE 7

CONTRIBUTIONS TO LIGHT IN BURSTS OF STARS OF DIFFERENT MASSES

Star Masses	u	b	g	o	r	Hα	Mgb	IR	TiO	Hα'	66
					B_1 burst (log t ≤ 6.4)						
> 40 $M_\odot$	34.55%	39.38	52.58	52.22	50.92	47.19	42.40	65.95	54.68	44.75	47.87
20-40	36.06	35.91	36.34	26.55	38.95	47.19	22.16	13.17	17.33	44.32	45.22
10-20	18.05	14.35	6.74	11.89	7.18	5.19	18.32	10.77	14.32	5.32	5.79
5-10	9.01	7.85	3.25	6.97	2.20	.32	12.78	7.51	10.19	.42	.83
2.5-5.0	2.32	2.51	1.10	2.38	.75	.10	4.35	2.60	3.51	.14	.29
Total Lum.	4.66(5)	2.01(5)	3.38(5)	1.37(5)	3.93(5)	3.20(6)	8.85(4)	1.12(5)	9.29(4)	2.32(6)	1.09(6)
					B_2 burst (6.4 < log t ≤ 8.0)						
> 40 $M_\odot$	.46%	.36	.37	.43	.44	.32	.39	.47	.44	.35	.39
20-40	9.83	7.66	8.84	8.36	12.49	32.12	6.65	9.80	7.64	27.27	19.14
10-20	19.75	15.71	14.38	15.01	16.13	16.04	14.46	16.12	14.78	16.26	15.87
5-10	35.51	37.42	40.19	43.82	41.68	30.16	41.65	43.49	44.34	33.20	37.75
2.5-5.0	29.17	30.96	28.85	26.38	24.04	17.61	29.44	24.84	26.78	19.29	22.00
1.0-2.5	5.24	7.84	7.26	5.83	5.05	3.63	7.31	5.10	5.87	3.99	4.68
< 1.0	.04	.05	.11	.15	.17	.12	.11	.17	.16	.13	.15
Total Lum.	2.18(6)	1.11(6)	1.20(6)	1.40(6)	1.59(6)	2.30(6)	1.16(6)	1.58(6)	1.40(6)	2.04(6)	1.71(6)
					Constant Formation (8.0 < log t ≤ 10.0)						
2.0-5.0 $M_\odot$	17.19	16.04	14.25	14.24	13.62	13.72	14.34	13.60	14.12	13.71	13.65
1.0-2.5	72.88	74.89	73.31	71.76	71.88	71.58	73.52	72.07	71.54	71.77	71.78
< 1.0	9.84	8.85	12.43	14.24	14.61	14.62	11.92	14.34	14.36	14.61	14.55
Total Lum.	3.06(6)	2.27(6)	3.41(6)	5.17(6)	6.33(6)	6.51(6)	3.55(6)	6.66(6)	5.27(6)	6.34(6)	6.06(6)

TABLE 8. FITS OF GALAXIES TO MODELS

		Closest Model				C. E. V.				
Name	d	β	B_1	B_2	E_{min}	β	B_1	B_2	E'	N_c
N1140	0.87	5	6	7	0.008	3.5	5.0	6.0	0.013	2
N1156	0.42	6	6	7	.020	5.0	6.0	6.0	.021	3
N1569	0.88	6	7	7	.116	4.5	6.0	5.75	.097	4
N2366	0.57	3	7	1	.419	3.0	7.0	1.0	.419	1
N2366	0.57	1	6	1	.274	1.0	6.0	1.0	.274	1
N2537	0.67	5	4	5	.004	5.0	4.0	4.5	.004	4
N2537	1.33	3	3	3	.016	3.57	3.00	3.57	.012	7
N2552	0.46	4	1	5	.037	5.00	1.75	5.88	.038	8
N2552	0.66	1	2	1	.129	1.0	2.0	1.0	.129	1
N2552	0.33	2	2	5	.003	2.33	2.33	5.00	.002	3
N3109	0.43	3	2	4	.008	2.75	2.25	3.50	.007	4
N3396	0.88	3	4	5	.019	2.5	3.5	4.5	.019	2
N3396	0.88	5	5	7	.056	4.5	4.5	6.5	.059	2
N3447B	1.71	1	2	1	.506	1.0	2.0	1.0	.506	1
N3738	0.31	3	3	5	.007	3.0	2.62	4.62	.002	8
N3738	0.62	4	2	5	.021	3.75	1.62	5.00	.016	8
N4032	1.40	5	2	5	.012	4.14	1.57	3.86	.010	7
N4038	0.85	6	6	7	.019	5.0	5.0	6.0	.012	3
N4190	1.18	2	2	3	.005	2.67	2.0	4.0	.005	3
N4214	0.16	5	6	7	.047	4.0	5.5	6.5	.043	2
N4214	0.67	6	6	7	.018	5.0	5.0	6.5	.012	2
N4214	0.22	4	5	6	.014	4.75	5.75	6.25	.008	4
N4449	1.22	5	6	7	.017	3.67	4.67	6.0	.020	3
N4449	0.29	3	4	6	.015	4.0	4.75	6.25	.010	4
N4449	0.41	5	5	7	.013	4.0	4.5	6.5	.013	2
N4449	0.41	5	5	7	.020	4.0	4.33	6.0	.016	3
N4485	0.40	3	2	5	.008	3.17	1.83	5.0	.005	6
N4532	1.01	6	6	7	.102	6.0	6.0	7.0	.102	1
N4532	0.50	4	5	7	.101	3.6	5.2	6.8	.086	5
N4532	1.01	4	4	6	.033	5.0	5.0	6.67	.029	3
N4656	0.32	1	6	7	.055	1.0	6.0	7.0	.055	1
N4657	0.48	3	5	5	.019	3.67	5.67	6.0	.025	3
N4657	0.16	3	4	6	.009	3.5	4.5	6.5	.013	2
N4657	0.48	3	4	5	.015	3.17	3.83	4.83	.008	6
N4668	1.72	3	2	4	.010	3.2	2.2	4.8	.008	5
N5253	....	2	5	6	.014	3.5	6.0	6.0	.026	2
A0957	0.29	3	2	5	.007	2.75	1.75	4.75	.004	4
A0957	0.41	1	1	2	.380	1.0	1.0	2.0	.380	1
I2574	0.48	5	5	7	.144	4.67	4.33	7.0	.138	3
I1613	0.37	5	4	7	.194	4.5	3.5	7.0	.189	2

TABLE 8 (CON'T)

Name	d	Closest Model β	B_1	B_2	E_{min}	C. E. V. β	B_1	B_2	E'	N_c
N3259	0.99	6	4	6	0.023	5.67	3.67	5.00	0.022	3
N3259	0.99	6	4	6	.010	5.6	4.2	5.0	.008	5
N3259	1.41	7	4	7	.043	6.62	2.62	5.88	.053	8
N4861	0.55	2	3	4	.022	3.25	4.0	5.5	.020	4
N4861	0.55	5	5	6	.006	4.75	4.75	5.5	.007	4
N5204	0.50	5	5	7	.009	5.0	5.0	7.0	.009	1
M33	0.16	5	3	6	.013	5.2	2.8	6.0	.012	5
N628	0.40	6	2	6	.023	6.0	2.2	5.6	.022	5
N672	0.66	4	3	4	.051	4.4	3.2	4.8	.051	5
N1084	1.14	6	6	7	.034	5.0	5.0	6.0	.039	3
N1637	1.08	4	3	1	.055	3.5	2.5	2.0	.050	2
N2403	0.36	3	2	2	.007	3.5	2.5	3.0	.007	4
N2903	0.69	6	4	5	.006	5.8	4.0	4.2	.006	5
N3184	0.77	6	4	5	.009	5.71	3.57	4.14	.009	7
N3198	1.17	3	2	3	.003	4.0	2.4	4.4	.005	5
N3198	0.82	5	3	5	.005	4.0	2.17	3.67	.001	6
N3486	0.50	5	4	5	.021	5.0	4.0	5.5	.019	2
N3486	0.50	4	4	4	.016	4.71	4.43	5.43	.009	7
N3521	0.63	4	2	1	.003	4.25	3.0	2.5	.004	8
N3631	0.84	5	3	5	.013	5.33	3.67	5.33	.009	3
N3631	0.84	5	3	5	.010	4.8	3.6	4.6	.008	5
N3810	1.24	5	4	6	.022	4.75	3.5	5.25	.019	4
N3887	1.06	5	3	6	.005	5.0	2.67	5.83	.008	6
N3893	1.86	5	4	5	.005	4.67	3.67	5.0	.006	3
N3893	0.93	6	5	6	.016	5.17	3.83	5.83	.011	6
N3893	0.93	5	4	5	.011	5.0	4.0	4.5	.010	4
N3953	0.88	7	2	7	.003	7.0	2.5	5.5	.003	8
N3953	0.63	7	1	1	.013	7.0	1.88	1.88	.015	8
M51	0.71	6	4	6	.004	5.67	3.33	5.33	.005	3
M51	0.12	7	6	7	.011	6.33	4.67	5.33	.014	3
M51	0.35	6	4	5	.010	6.0	4.0	5.2	.009	5
M51	0.35	6	1	5	.067	6.2	1.2	5.2	.071	5
N5248	0.17	7	6	6	.038	6.71	5.86	4.71	.033	7
N5248	0.34	7	6	7	.010	6.4	4.4	5.6	.013	5
N5364	0.52	7	5	7	.084	7.0	4.0	7.0	.087	5
N5457	0.14	7	4	7	.009	6.75	3.12	5.88	.007	8
N6503	1.14	5	3	5	.012	5.0	3.0	4.5	.014	4
N6503	0.81	5	3	5	.003	4.33	2.33	5.17	.001	6
N6946	0.30	7	6	7	.056	6.5	4.5	6.0	.063	4

TABLE 9

AVERAGE MODEL NUMBERS OF GALAXIES

Class of Galaxy	N	$\langle\beta\rangle$	$\langle B_1\rangle$	$\langle B_2\rangle$
Irr's ($d > 0.6$)	18	3.75	3.84	4.92
Irr's ($d \leq 0.6$)	22	3.36	4.06	5.24
Irr's (all)	40	3.54	3.96	5.10
Sc-Irr's (all)	6	5.15	4.04	5.65
Sc's ($d > 0.7$)	15	4.79	3.28	4.57
Sc's ($d \leq 0.7$)	15	5.83	3.66	5.29
Sc's (all)	30	5.31	3.47	4.93
Sb's (all)	3	6.08	2.46	3.29
Spirals (all)	33	5.39	3.38	4.78
Irr's ($3.0 \leq \beta \leq 6.0$)	30	4.12	4.24	5.68
Sc's ($3.0 \leq \beta \leq 6.0$)	23	4.95	3.32	4.70
Spirals ($3.0 \leq \beta \leq 6.0$)	24	4.92	3.31	4.61

CAPTIONS FOR FIGURES

Figure 1: Plot of galaxy colors in (b-g) and (g-o). Irregulars are plotted with circles, Sc-Irr's by triangles, Spirals (mostly Sc's) by squares.

Figure 2: Plot of galaxy colors in (b-o) and (u-b). Symbols are same as in Figure 1.

Figure 3: Plot of galaxy colors in (b-o) and (Hα-r). Symbols are same as in previous Figures.

Figures 4 a, b, c: Galaxy colors as a function of aperture/ size ratio. Figures 4a, 4b, and 4c are plots of log d versus (b-o), (u-b), and (Hα-r) respectively. Symbols are same as in previous Figures.

Figure 5: Plot of galaxy colors in (u-g) and (o-g). Symbols are same as in previous Figures.

Figure 6: Plot of galaxy colors in (u-g) and (Hα-o). Symbols are same as in previous Figures.

Figure 7: Overall comparison of model and observed galaxy colors in (b-g) and (o-g), the same colors used in Figure 1. Filled circles represent (β, 2, 3) models; open circles, models with various "bursts" of star formation. (See text.) Dotted line denotes loci of observed galaxies.

Figure 8: Overall comparison of model and observed galaxy colors in (b-o) and (u-b), the colors used in Figure 2. Symbols same as in Figure 7.

Figure 9: Overall comparison of model and observed galaxy colors in (b-o) and (Hα-r), the colors used in Figure 3.

Symbols same as in Figure 7.

Figure 10: Fit of galaxies to models in β and B_1. Symbols for types of galaxies same as in Figures 1 to 6, except that filled and open symbols denote galaxies with higher and lower aperture/size ratios respectively. Dotted areas are typical error volumes.

Figure 11: Fit of galaxies to models in β and B_2. Symbols same as in Figure 10.

Figure 12: Fit of galaxies to models in B_1 and B_2. Symbols same as in Figure 10.

FIG. 1

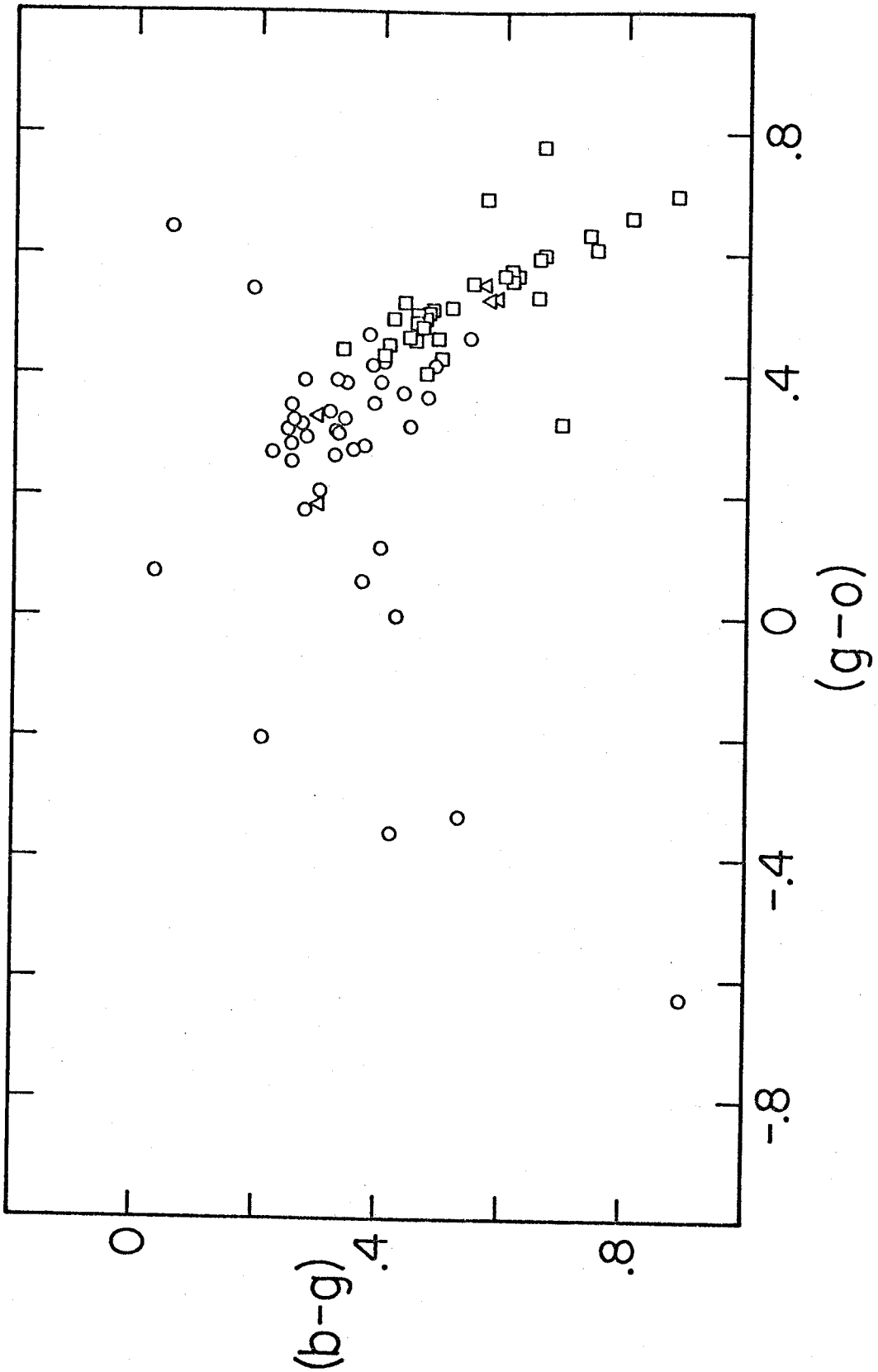

FIG. 2

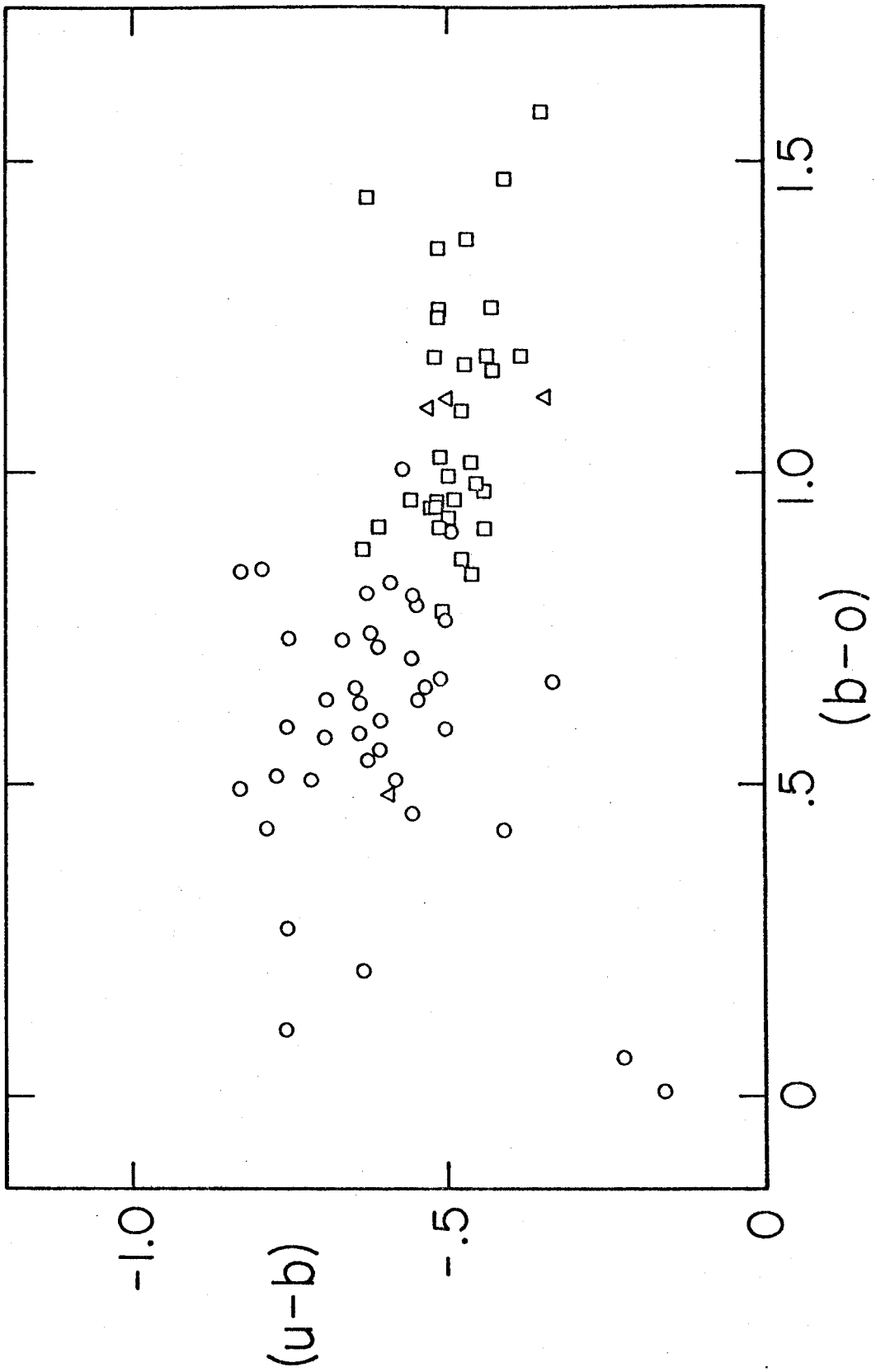

FIG. 3

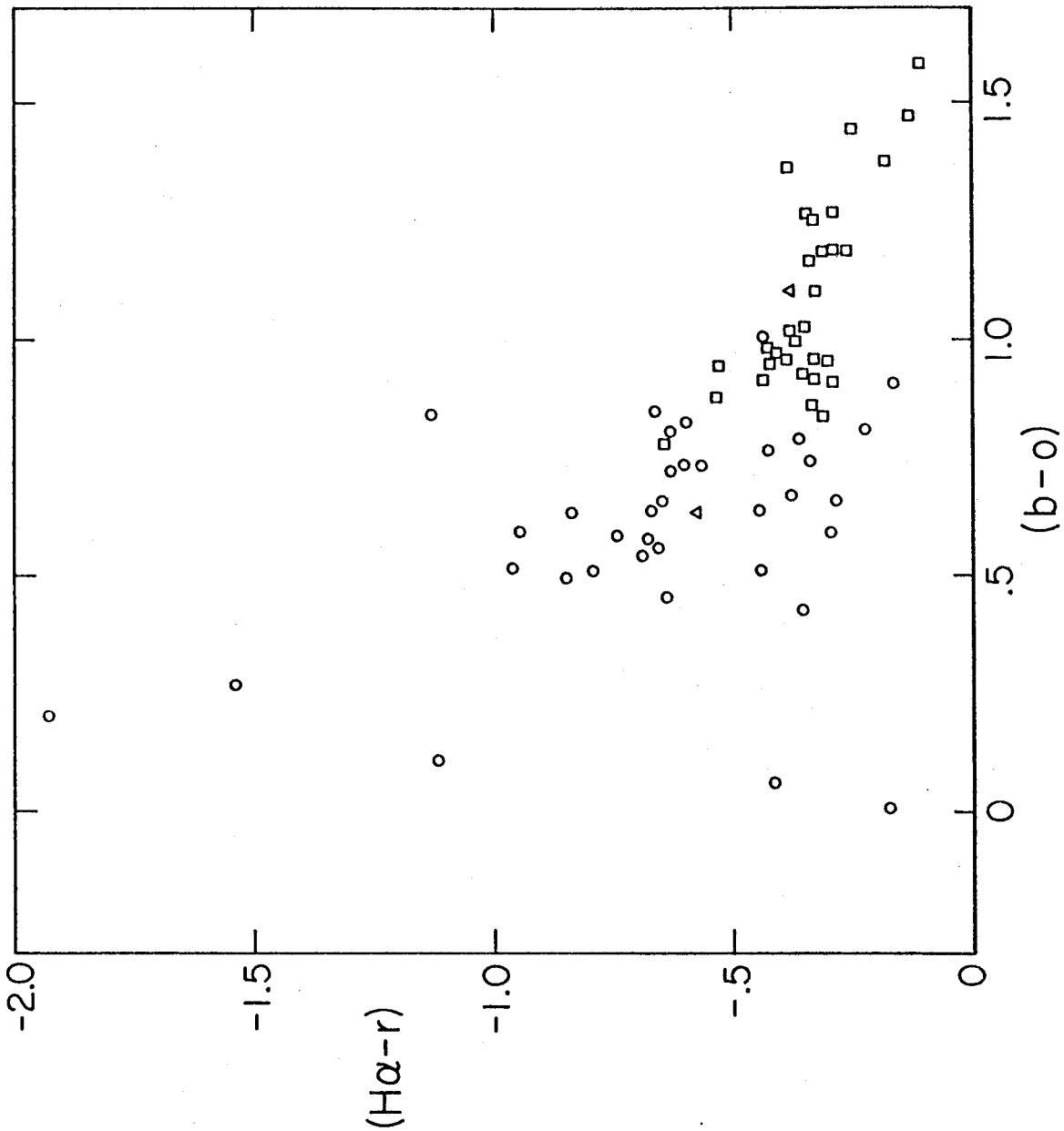

FIG 4a,b,c

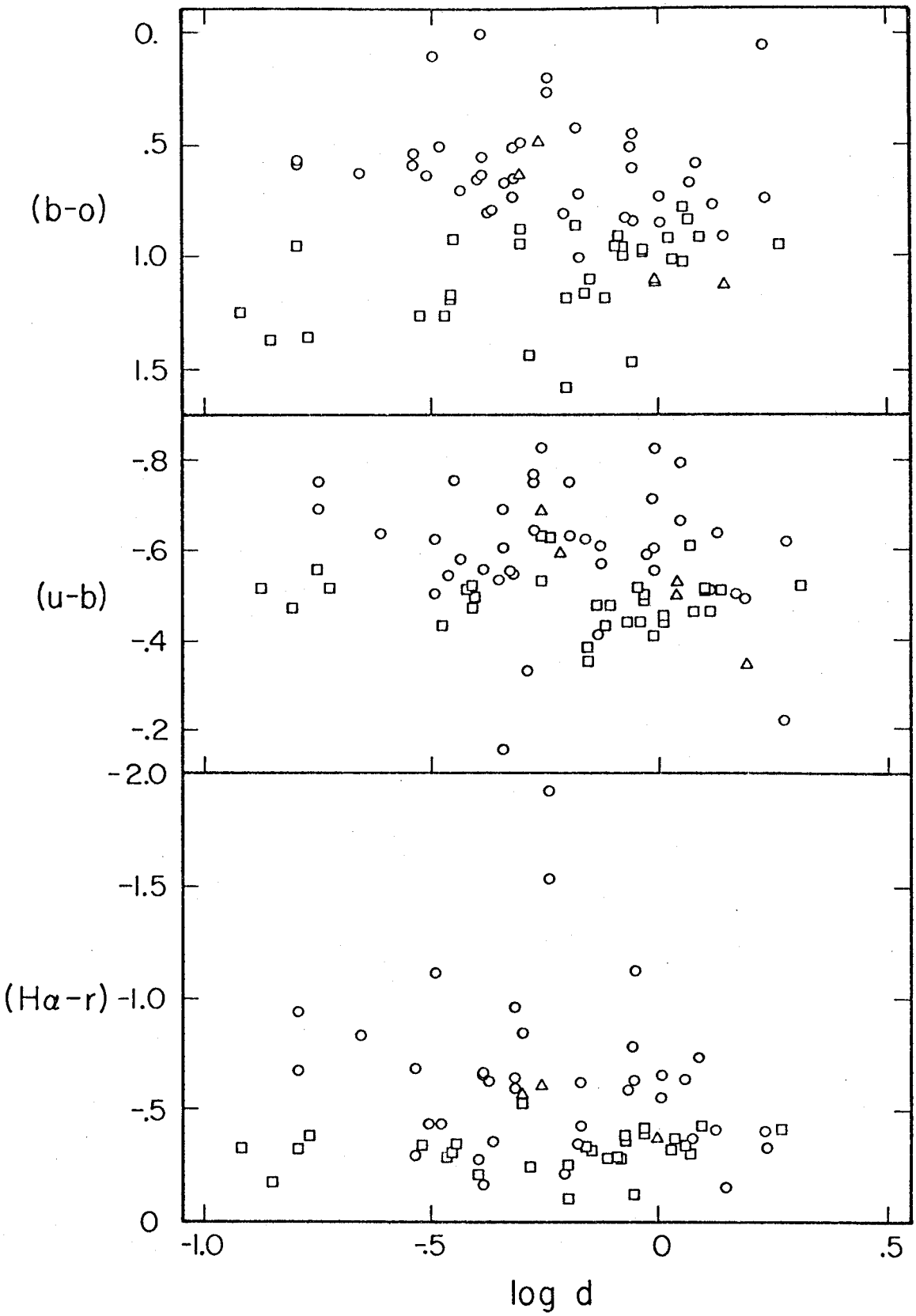

FIG. 4

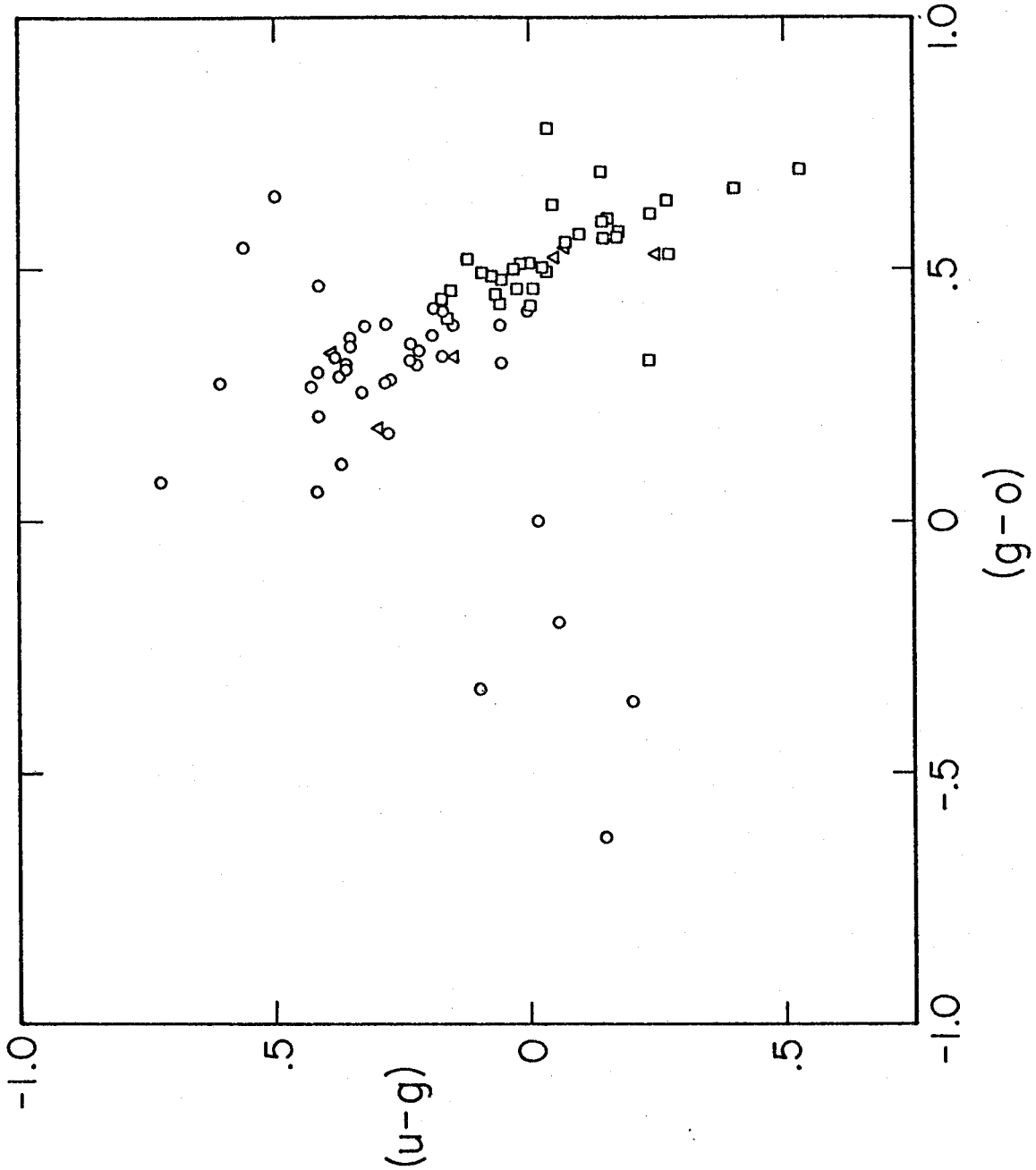

FIG. 6

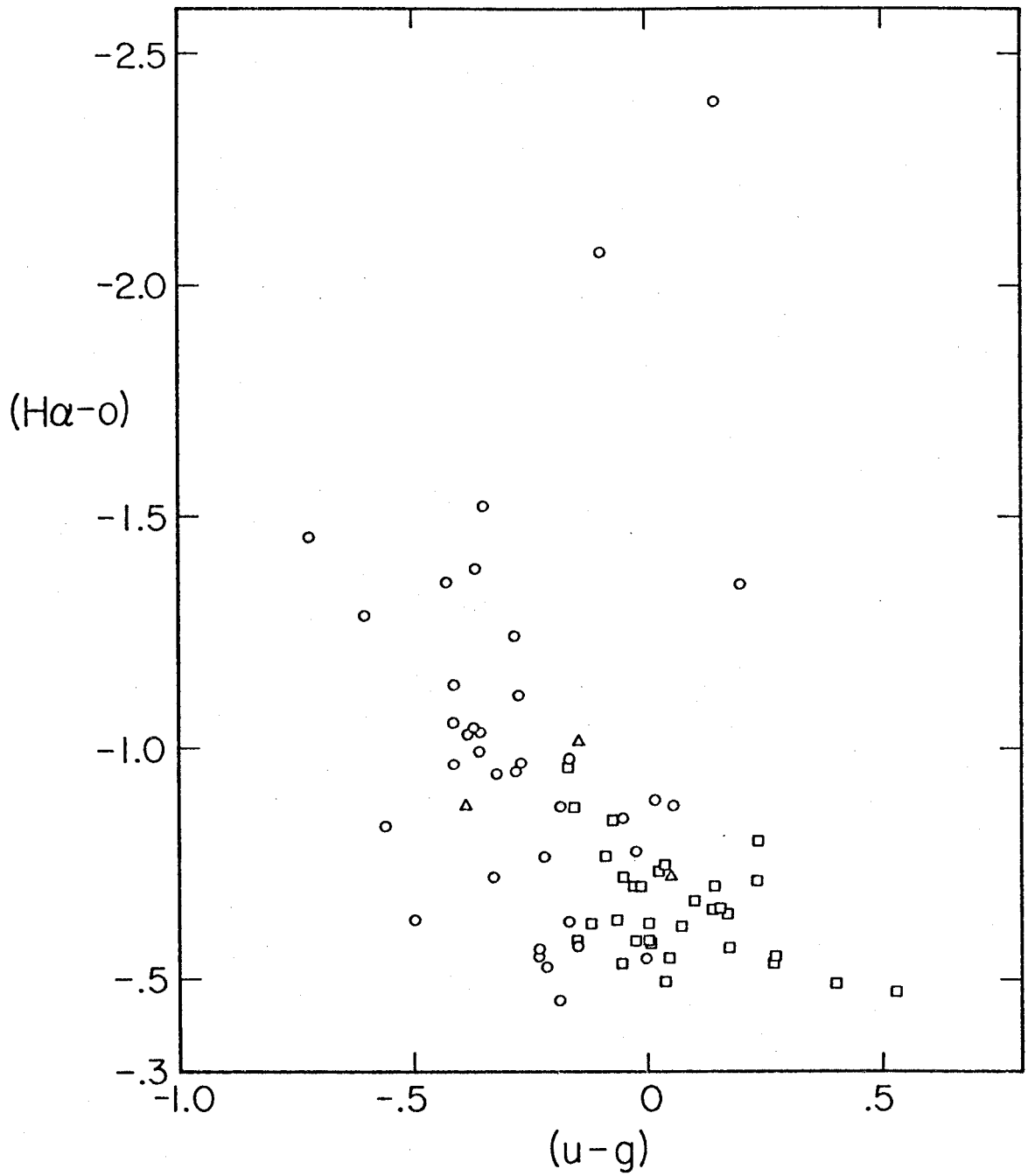

FIG. 7

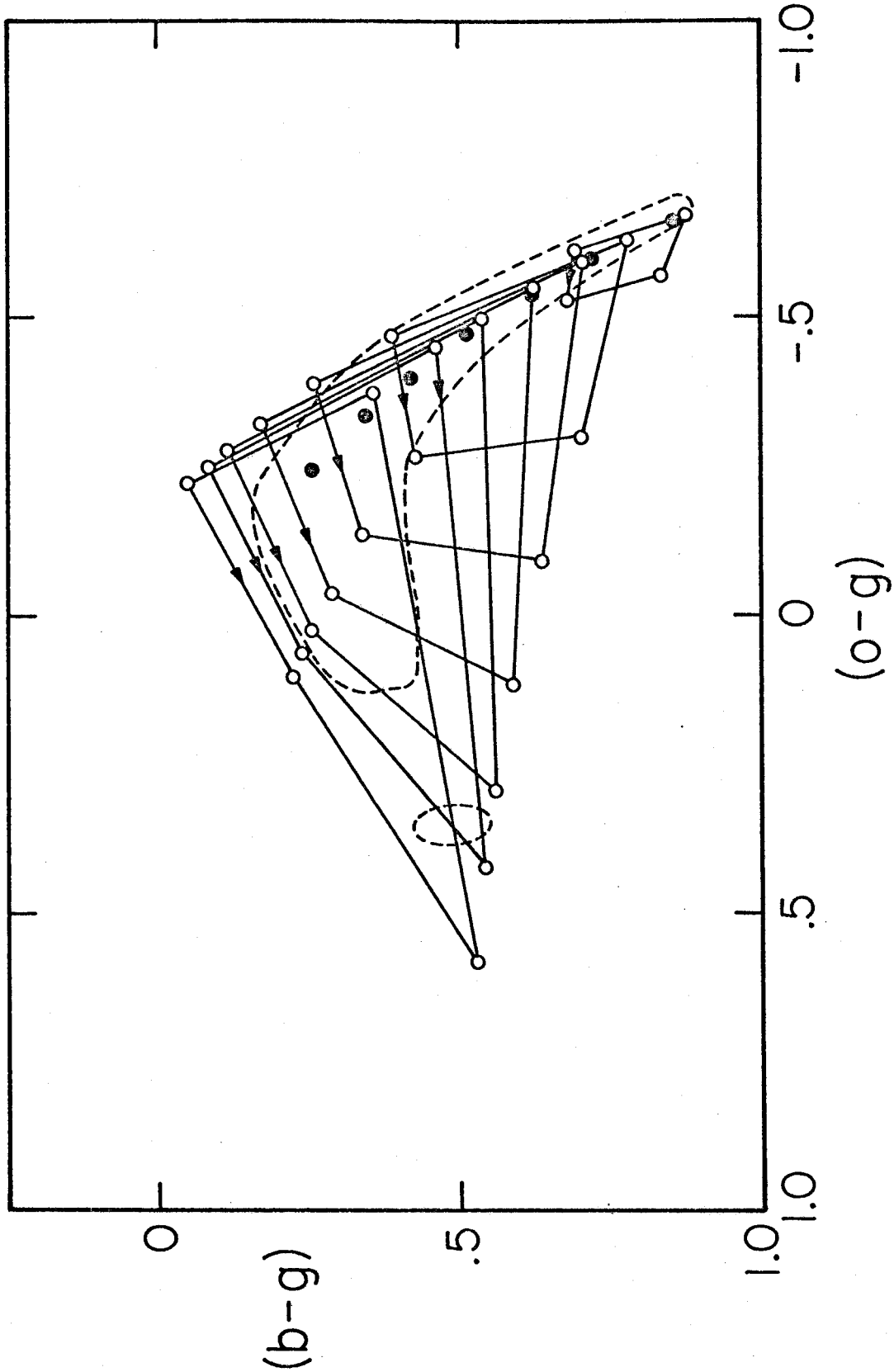

FIG. 8

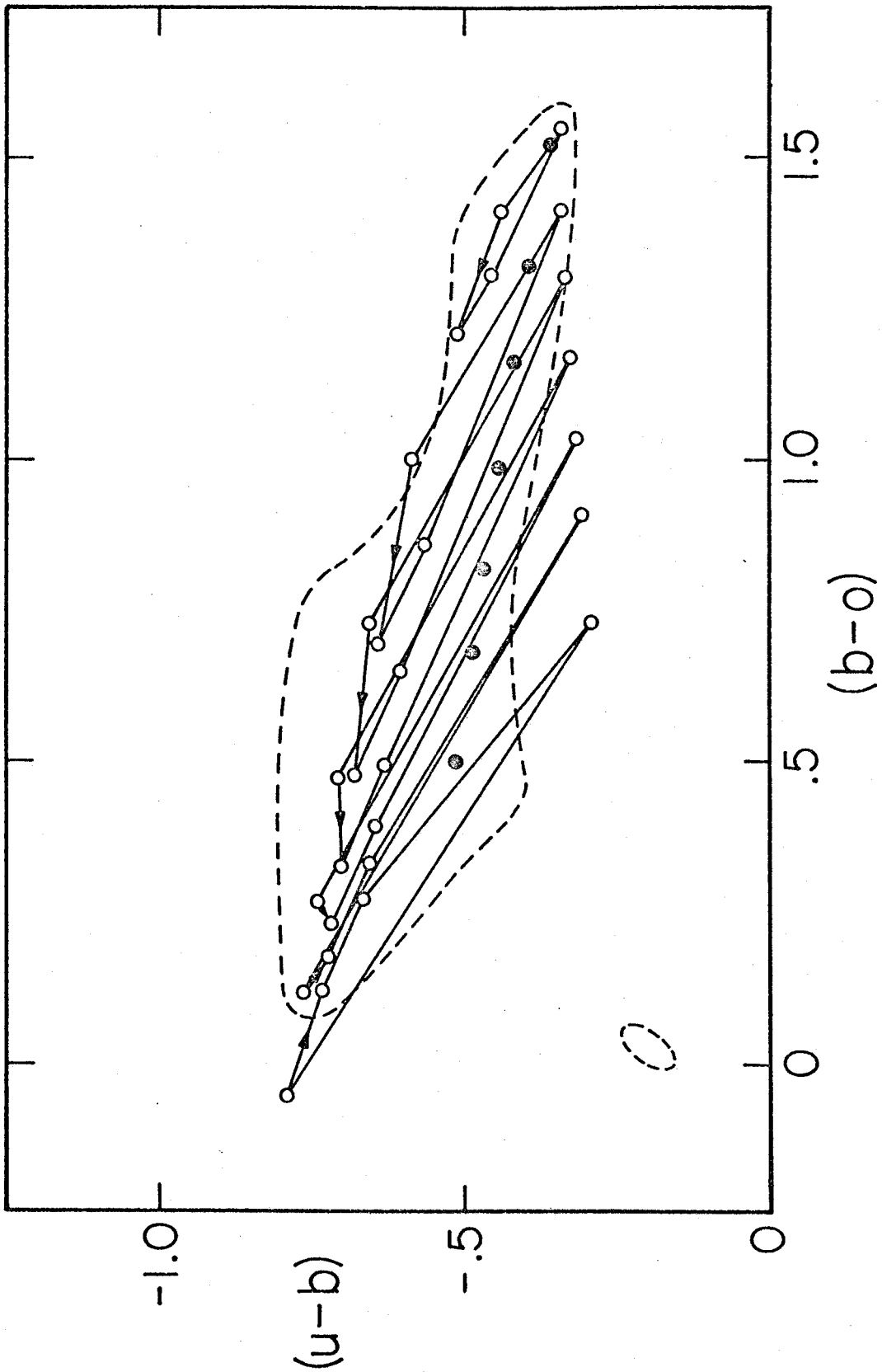

FIG 9

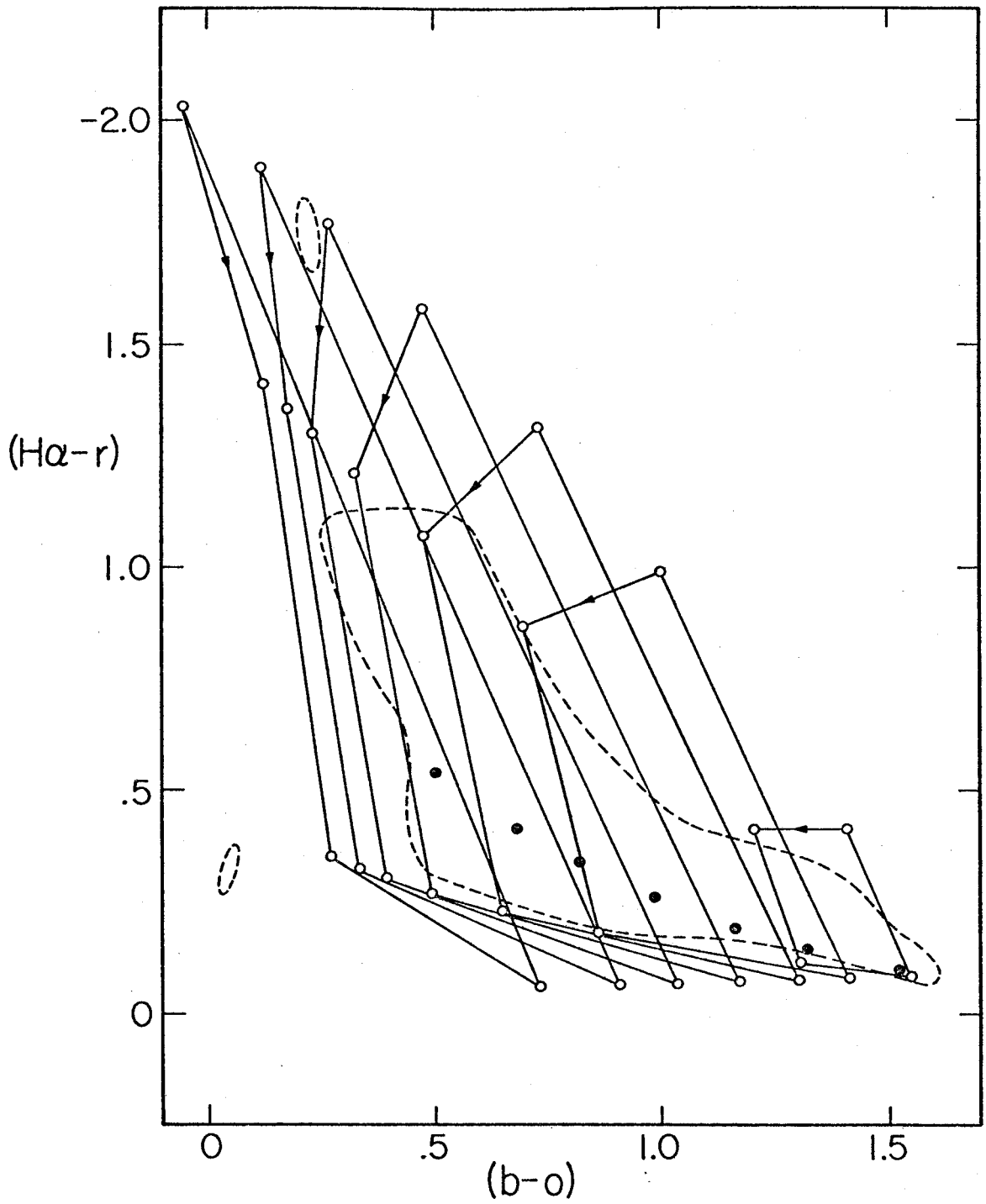

FIG 10

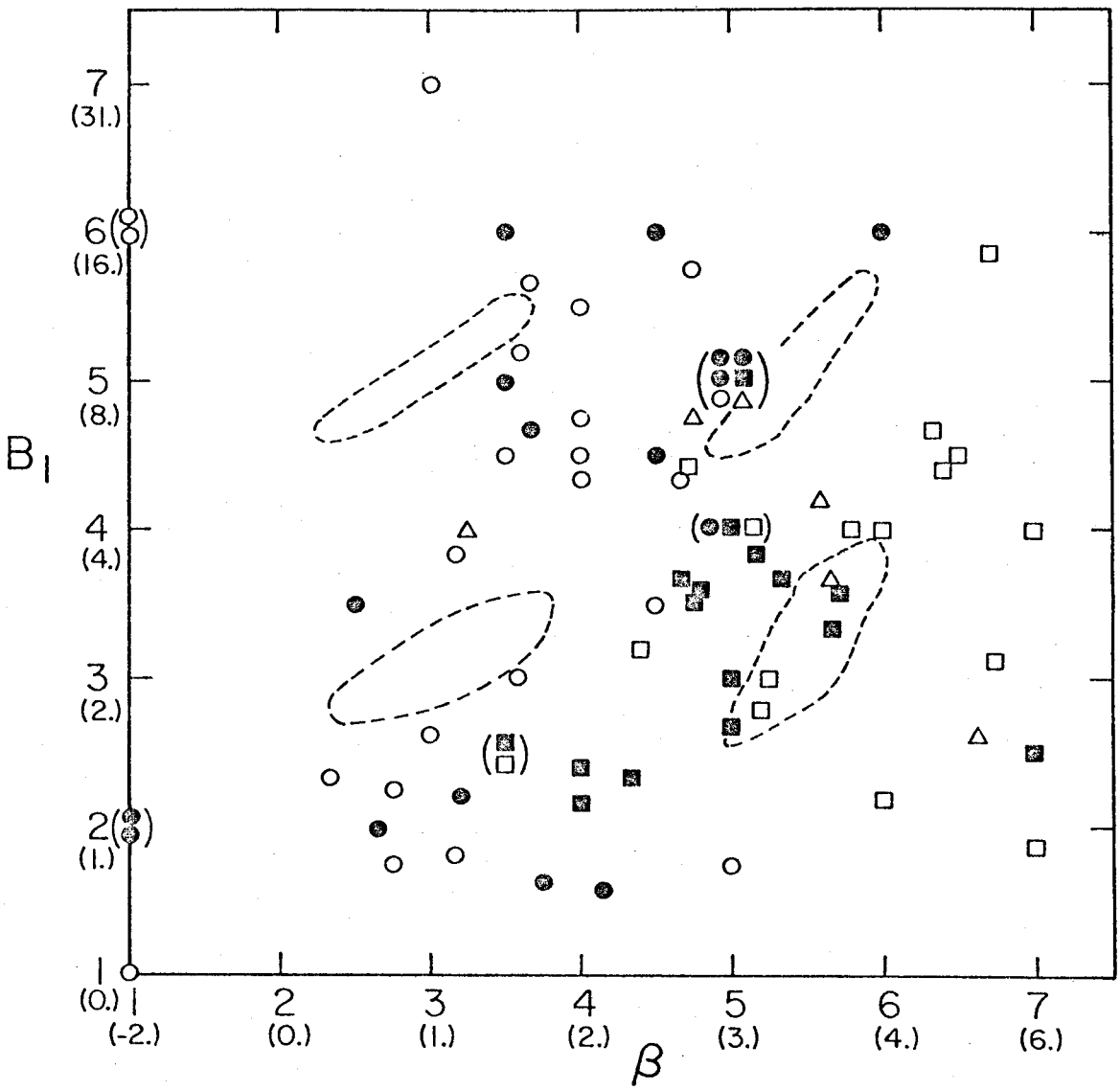

Fig. 11

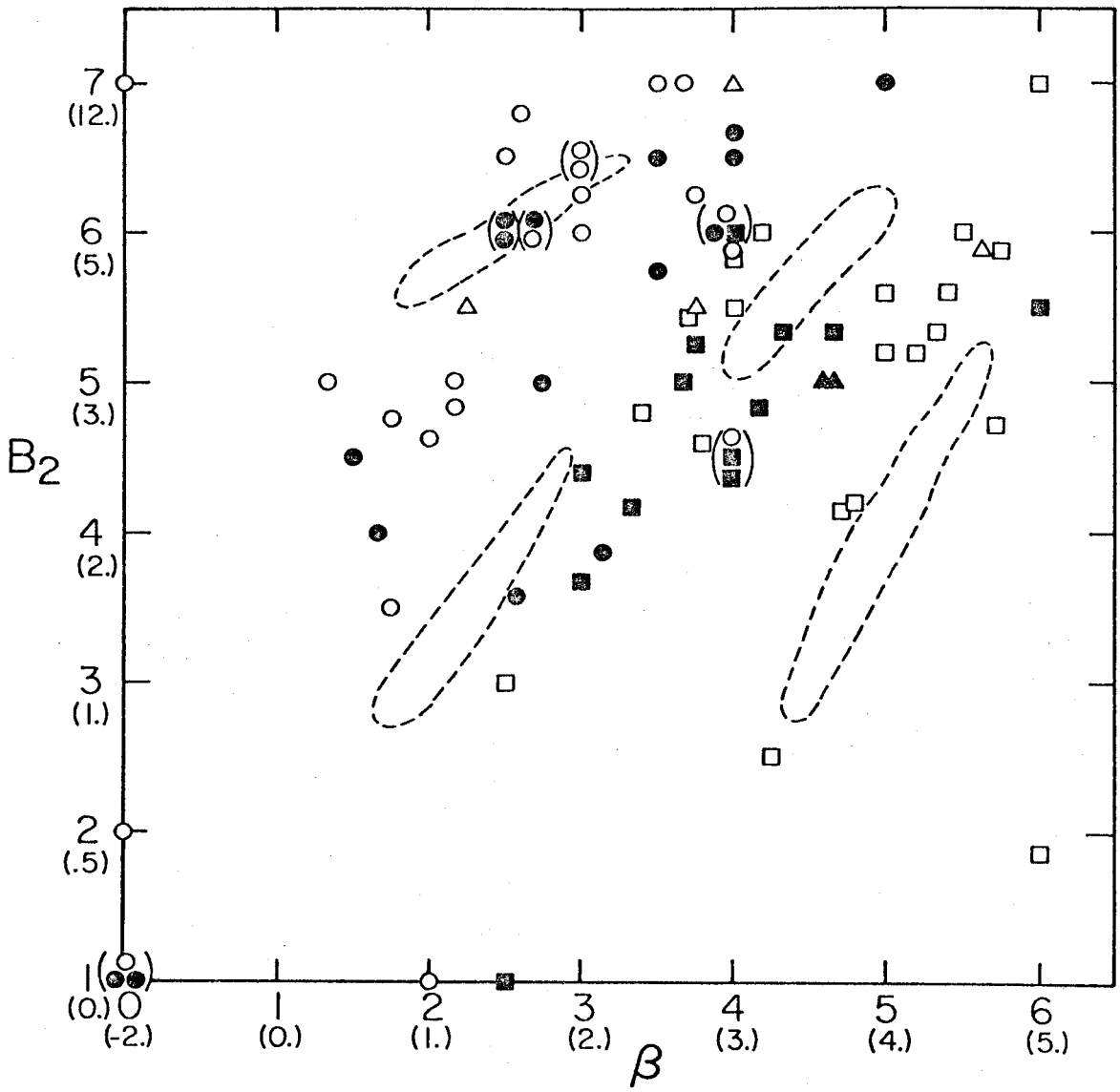

FIG 12

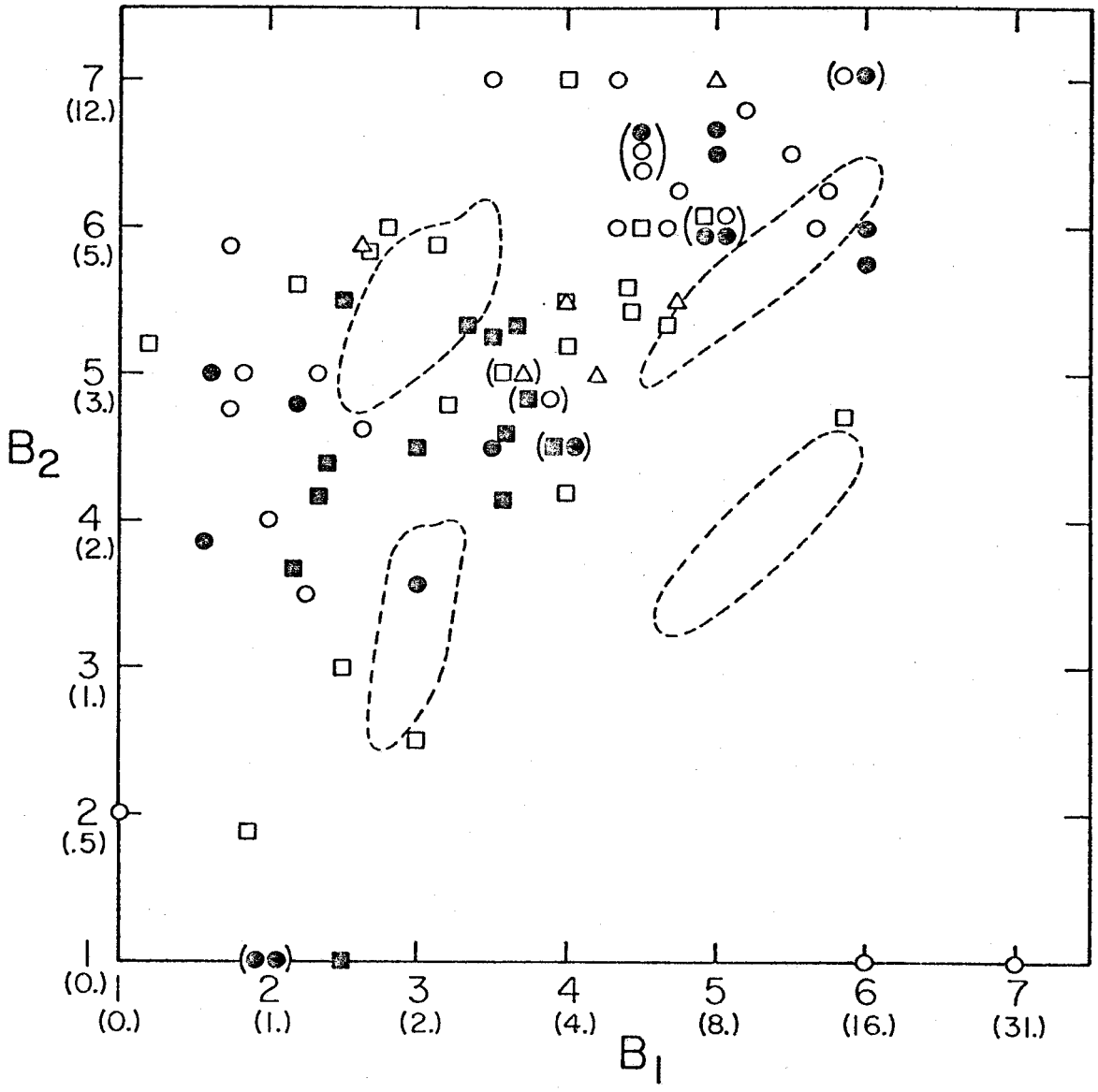

CHAPTER 2

COLORS AND THE STELLAR CONTENT OF CLUSTERS IN THE MAGELLANIC CLOUDS

I. INTRODUCTION

The four-color photometery and modeling of the stellar content of clusters in the Magellanic Clouds was undertaken for several reasons. First, because the cluster models could be used to construct models of the stellar content of late-type galaxies (see Bagnuolo (1976a)). Galaxies can be regarded as being composed of "clusters" of various ages. Colors of galaxies calculated directly from stellar-evolutionary tracks would be necessarily less accurate, because of various uncertainties in the tracks.

Secondly, because interesting properties of the stellar composition of the clusters themselves might be inferred. In particular, the ratio of blue to red supergiants, n_b/n_r, might be estimated in clusters dominated by stars of 3 to 30 solar masses. n_b/n_r varies appreciably in calculated evolutionary tracks, especially for stars of over 5 $M_\odot$, according to the composition assumed, treatment of semiconvection, and neutrino emission. Schild (1970) and others have examined individual stars in clusters to determine this ratio empirically. It was thought that photometery of the integrated light of a larger number of rich clusters might provide additional independent information about n_b/n_r.

Also, differences in the initial mass formation function, f(m), of the clusters might be detected. f(m)

is the relative number of stars of mass m to m+dm in a newly formed cluster. In a previous paper by Searle, Sargent and Bagnuolo (1973), hereafter referred to as SSB, it was found that:

$$f(m) = C\, m^{-\alpha} \quad , \text{ if } \quad .25\ M_{\odot} \leq m \leq 35\ M_{\odot} \qquad (1)$$

$$= 0 \quad , \text{ otherwise}$$

where $\alpha = 2.45$ and C is a constant, is a reasonable approximation to the initial mass formation functions (IMFF's) of Saltpeter (1955) and Limber (1960). Clusters enriched or depleted in massive stars, with lower or higher values of α in f(m), might be expected to show differences in the colors.

Finally, some degree of interstellar reddening may be expected. With the five filters chosen it would be possible to obtain three "reddening-free" parameters, one more than with the UBVR color system.

II. OBSERVATIONS

Forty-six clusters in the Magellanic Clouds were by Searle in November 1973 at the 40" Cassegrain reflector at Las Campanes Observatory in Chile. A photometer with the five "Gunn" filters u, b, g, o, r and an S-20 tube were used. Table 1 lists the essential properties of the photometric system. (λ_{max} in the Table is the wavelength of maximum response.)

A set of equatorial standards, given by Haug et al. (1967) was used, and the color system was standardized by setting the (u-g), (b-g), (o-g), (r-g) colors equal to 0.00 and g equal to 7.00 for "Z4a," an A0 V star. In order to compute cluster colors 102 different stars of all luminosity classes and spectral types from O5 to M6 were observed by Bagnuolo (1976b) at Palomar and Table Mountain Observatories. A simple linear transformation between the colors observed by Searle and Bagnuolo (denoted by subscripts with s and b respectively) was obtained by a least-squares fit of observations of six standards:

$$
\begin{aligned}
(u-g)_s &= 1.007\ (u-g)_b - 0.018 \\
(b-g)_s &= 1.004\ (b-g)_b - 0.001 \\
(o-g)_s &= 1.043\ (o-g)_b - 0.002 \\
(r-g)_s &= 1.030\ (r-g)_b - 0.002 \\
g_s &= g_b + 0.032\ (o-g)_b - 0.020
\end{aligned}
\qquad (2)
$$

Hereafter all colors discussed will be in the Searle (cluster) system. Table 2 is a list of the cluster colors. (The significance of the Q's will be discussed later.)

III. CLUSTER MODELS

The general scheme followed in the construction of the cluster models was to assemble a reasonable set of stellar-evolutionary tracks, with an adjustable n_b/n_r for those with $m \geq 3\ M_\odot$. Next, calculate the light

contributions of a number of places along the tracks in the filters and in regions of time. Finally, sum up the light contributions in all filters for each region of time. The approximate colors of average star clusters of various ages will then be obtained.

The first step is to assemble the evolutionary tracks in the log T_e, log L plane. In order to calculate the colors of clusters with different n_b/n_r, we assume that the evolutionary tracks above 3 $M_\odot$ have the same topology: Model stars move off the Main Sequence, enter a red giant region, then move through a blue loop, ending again in the red giant region. Nevertheless, models with the same n_b/n_r, but a different topology, such as blue supergiants first, would produce similar cluster colors. The 15 and 5 $M_\odot$ evolutionary tracks are from Robertson (1972, 1971) respectively. These models (Robertson's case I, A) were also used in Dixon, Ford, and Robertson (1972) to calculate the UBV colors of model clusters. The 15 $M_\odot$ track has $n_b/n_r \simeq 1$, and was adopted intact. The 5 $M_\odot$ track was modified somewhat to get $n_b/n_r \simeq 1$ and to better agree with Arp and Thackeray's (1967) observations of NGC 1866. The other tracks used are modifications of those used in SSB. The 3 $M_\odot$ model was taken from Iben (1966) and modified to get a reasonable track in the blue loop phase and so that $n_b/n_r \simeq 1$. Small changes in the luminosities and times along the track were also made in order to approximate

models with the chemical composition, (X,Z) = (0.604, 0.04), of the 15 and 5 $M_\odot$ models. The 30 solar mass track, originally from Strothers (1963), was suitably modified as above. The 60 $M_\odot$ track was obtained from the results of Hartwick and Vanden Bergh (1972) and extrapolation. In both the 30 and 60 $M_\odot$ tracks blue loops similar to those of the 15 $M_\odot$ track were assumed.

For the tracks of stars less massive than 3 $M_\odot$ a different topology is assumed and evolution after He ignition is ignored. The 2.25 - 1.0 $M_\odot$ models are from Iben (1967a, 1967b); although the positions and times along the red giant tips were modified to agree with Sandage's (1962) observation of NGC 188 and Johnson and Sandage's (1955) of M 67. The lowest mass models ($m < M_\odot$) are the same as those of SSB. Table 3 gives the luminosity (log L), temperature (log T_e), and time (t in units of 10^7 yrs.) at various points along the adopted tracks with $m \geq M_\odot$.

In order to obtain the color intensities produced by a point along an evolutionary track in the log T_e, log L plane, the following procedure was adopted. Color, spectral type plots were produced from the 102 stars observed, including 18 supergiants corrected for reddening. The color, spectral type plots were transformed into color, log T_e plots by assuming the log T_e, spectral type relations from Johnson (1966), Morton (1969), Morton and Adams (1968), and Lee (1970). Bolometric corrections as a function of log T_e were similarly obtained from

these sources and Bradley and Morton (1969). Finally, (g-V), log T_e relations were obtained from over 60 stars that have listed V magnitudes in the Bright Star Catalog (1964). For the purposes of color computation stars are regarded as belonging to luminosity classes V, III, or I; thus, for each color three relations in color, log T_e were generated. From the above relations a point in the log T_e, log L plane corresponds to color intensities in the five filters.

A large number (up to 60) of stellar-evolutionary tracks were interpolated between the model tracks above in log L, log T_e, and log t. The time between t = 0 and t = 10^{10} years ago was divided into 41 "time slots," the upper boundaries of which are given by: log t_{imax} = 6.0 + 0.1 (i-1) , where t_{imax} is the upper boundary in time of the i^{th} time slot. As an approximation, the average color intensities along each segment of the evolutionary track are assumed to be those of the midpoint. The upper and lower times of each segment determine the contributions of color intensity by the segment to each time slot. Up to 21 points (20 segments) were used in the tracks. It was found that using twice this number changed the computed cluster colors by less than 0.02 mag at most. The color intensities of a cluster of a particular age can then be regarded as the sum of the color intensity contributions of all segments of all tracks to

the appropriate time slot. An advantage of using time slots in the calculation is that, unlike in SSB, there are no large excursions in the computed cluster colors that must be averaged.

In the cluster color calculations the initial mass formation function is first assumed to be that of Limber (1960). We assume modifications to this function in the form: $f(m) = f_L(m)\ m^{-\delta}$, where $f_L(m)$ is the Limber function. Here $\delta = 0$ corresponds to the standard case $\alpha = 2.45$ of SSB. Similarly $\delta = 0.45$ corresponds to the case $\alpha = 2.0$, which is enriched in higher mass stars.

The ratio of n_b/n_r for model clusters can be changed by varying the time intervals of red or blue supergiant segments of the tracks, assuming the sum of supergiant times to be constant.

The colors of the youngest clusters ($t < 10^7$ yrs) were expected to be strongly affected by the presence of emission lines arising from the absorption of ultraviolet photons of the most massive stars ($m \geq 15\ M_\odot$) by the surrounding gas. Contributions to emission lines from within the stellar atmosphere were neglected. Also, perfect efficiency in the degredation of the photons by the gas is assumed. Since only two clusters with significant emission were observed, the main effect of emission lines in the interpretation of the cluster colors will be

to cause limits or turnoffs in the predicted colors.

It can be shown (Searle (1975)) that:

$$F_i' \simeq F_i\left[1 + \sum_L (s_L/S_i)(1.27\times10^{11}/\Delta\upsilon_i)(F_\beta/F_i)\ W_\beta I_L\right] \quad (3)$$

where F_i' is the average flux density in the filter band i including the emission lines and is proportional to the number of counts per second. F_i and F_β are the mean continuum flux densities at the filter i band and Hβ respectively. W_β is the equivalent width of the Hβ emission line in $\mathring{A}$, and I_L is the intensity of emission line L relative to Hβ. $\Delta\upsilon_i$ is the bandwidth of the filter and 1.27×10^{11} is a conversion factor. s_L/S_i is the ratio of the sensitivity of the photometer at line L to the average sensitivity in the filter band i. Summation is taken over the number of lines that can affect the count in the filter. Relation (3) gives a corrected flux density in the presence of emission lines, and for no emission lines obviously $F_i' = F_i$.

The emission lines used in the calculations and other data are given in Table 4. Estimates of W_β produced by O stars with $30{,}000 \leq T_e \leq 50{,}000\ ^\circ K$ were obtained by Searle (1971). Values of I's for H II regions of different temperatures are given in the last three columns of Table 4. The three H II regions used in the calculation of the youngest cluster models are M 101 #2, NGC 604, and

NGC 5471, given by (Ibid.), Aller, Czyzak, and Walker (1968), and Searle and Sargent (1972) respectively.

IV. ANALYSIS OF CLUSTERS

A series of nine sets of cluster models were computed with $n_b/n_r = 0$, 1, and infinity, and $\delta = -0.55$, 0, and 0.5 (i.e. $\alpha \simeq 3.0$, 2.45, and 1.95). In addition to the u, b, g, o, r intensities, three "reddening independent" parameters were computed, based on the Whitford reddening law as given by Miller and Matthews (1972):

$$\begin{aligned} Q_1 &= (u-g) - 1.050\ (g-r) \\ Q_2 &= (b-g) - 0.725\ (g-r) \\ Q_3 &= (g-o) - 1.703\ (o-r) \end{aligned} \tag{4}$$

We can now compare the computed cluster colors to observations. Figure 1 is a plot of some of the models and the clusters in the (u-g), (g-r) plane. It was found that this plot gives some of the widest separations in colors of models. Portions of 5 sets of model clusters are plotted in Figure 1 from time slots 4 to 21 ($\sim 10^8$ yrs). After time slot 21 only the "standard" case ($n_b/n_r = 1$, $\delta = 0$), denoted by a small dashed line, is plotted. Two sets of models denoted by dotted and dot-dashed lines are those of model clusters enriched in massive stars ($\delta = 0.5$, $\alpha \simeq 1.95$) with $n_b/n_r = 1$ and 0 respectively. The solid line, small dotted line, and large dotted line denote sets of models with $\delta = 0$, the Limber IMFF, and

n_b/n_r = 0, 1, and infinity respectively. Not shown are sets of models for the (δ =-0.55, α =3.0) case, but they would be almost symmetrically placed on the opposite side of the "Limber" cases from the (α = 1.95) cases. For the sets of models with n_b/n_r = infinity the difference in the plotted colors for different mass functions is minimal, so that only the set with the Limber function is plotted.

In Figure 1 the plots reach a maximum in (u-g) and then turn over for very low log t due to the effects of emission lines, mainly [O III] and Hβ in filter g. Previously constructed model colors without emission continue upward some 0.3 mag in (u-g). Similar turnoffs are noticeable in other diagrams.

Also from the Figure it is apparent that the model colors for younger clusters depend much more on the n_b/n_r ratio than on the mass formation function. This is to be expected, since the light of the clusters is dominated by the higher mass stars. Varying the relative amounts of lower mass stars compared to higher mass stars should have a relatively small effect on the cluster colors. The main difference in sets of models with different mass formation functions occurs, as in SSB, in the rate of decline of the integrated luminosity of clusters with time. Table 5 gives the change in g in magnitudes from the time $t = 10^7$ years, Δg, where $\Delta g = 0.00$ at $t = 10^7$. Values of Δg for the three different mass functions are listed,

assuming $n_b/n_r = 1$. As expected, the clusters with more massive stars ($\delta = 0.5$) decline fastest in g with time.

The observed clusters in Figure 1 appear generally to agree reasonably well with the models. Some of the oldest clusters, at the lower right, lie above the predicted cluster colors. In a forthcoming paper Searle (1976) will discuss the colors of the globulars. From the Figure it appears that the best fit of the younger clusters, bluer than (u-g) $\sim$-0.4, is roughly $n_b/n_r \sim 1$ for clusters between $10^8 \geq t \geq 3 \times 10^7$ ($-0.4 \geq (u-g) > -0.7$), and $n_b/n_r \sim .7$ for clusters with $3 \times 10^7 > t \geq 10^7$ ($-0.7 \geq (u-g) > -1.2$). The two clusters observed in emission suggest that n_b/n_r may be greater than 1 for very massive stars, but obviously there are not enough data here. In the preceding it was assumed that differential absorption was small ($E(B-V) \sim$ 0.05 or less), but this seems plausible because of the good agreement of older clusters with the models.

We next consider relations with the reddening independent parameters. Figure 2 is a plot in Q_1, Q_2 of the clusters and the three models having the Limber IMFF with $n_b/n_r = 0$ (dashed line), 1 (solid line), and infinity (dotted line). The models with different IMFF's are not shown, but are close to the models above having the same n_b/n_r. The main observational difference in the younger cluster models is the position of the turnoff caused by emission lines. There is a difference in the maximum

Q_1 reached of 0.4 between the n_b/n_r = infinity and n_b/n_r = 0 cases. In Figure 2 it can be seen that a good overall agreement exists between the clusters and models. For the younger clusters ($t \sim 10^7$) it appears that we can eliminate the n_b/n_r = infinity case, since three clusters have higher values of Q_1 than the highest value of this case. It seems likely that n_b/n_r is less than ~2. Finally, the two clusters with strong emission lines agree with the models.

Another comparison of the cluster colors can be made by comparing the models and clusters in a plot of Q_3 and Q_2. Generally speaking, Q_3 is a measure of the change in slope of the energy distribution between filters g and o, and o and r. Q_3 should have a value close to zero for most clusters, but should be strongly influenced by emission lines in filters g and r, such as [O III] and Hα. For individual stars, Q_3 rises from 0. at A0 to 0.3 for K3 giants, then drops to -0.3 or less for the coolest stars. Figure 3 is a plot of Q_2 and Q_3 similar to previous plots. (Here the case n_b/n_r = 0, δ = 0.5, dot-dash line, has been added for the youngest clusters.) In this Figure there is a reasonable agreement between clusters and models, especially considering that a change in assumed (o-r) results in a change nearly three times as great in Q_3. The main conclusion to be drawn from Figure 3 is the same as that of Figure 2- the case n_b/n_r = 0 cannot account for the clusters ~10^7 yrs old. The "loops" in the model

colors, considered "non-physical," are caused by the transition in tracks between 3 and 2.25 $M_{\odot}$ where a different topology is assumed. The two clusters in emission appear to lie above the predicted colors in Q_3; however, possibly the aperture used collects more of the [O III] than Hα emission.

Finally the ages of twelve of the clusters have been obtained, based on color-magnitude (CM) diagrams and Cepheids. The CM ages were obtained from the Main Sequence termination in CM diagrams of twelve clusters from Robertson (1974), Hodge and Flower (1973), and Gascoigne (1969) (from several sources). The age- M. S. termination relations used are from Dixon, Ford, and Robertson (1972), based on cluster models similar to those of this paper. The distance moduli of the Clouds assumed, 18.7 and 19.2, are from Graham (1973). Cepheid ages for two of the clusters were obtained from the periods of 13 Cepheids from Gascoigne (1969) and the log t, ⟨log P⟩ relation of Tammann(1970), where ⟨log P⟩ is the average period of Cepheids in a cluster. There is a fairly good agreement between the Cepheid and CM ages for the two clusters (see Table 3).

Figure 4 is a plot of the twelve clusters above and the same five models as in Figure 1 in Q_1 and log t.

From Figure 4 it can be seen that for the younger clusters $n_b/n_r \sim 0.6$, while for the older clusters $n_b/n_r \sim 1.4$. (Some calculations were done for models with $n_b/n_r = 0.5$ and 2.0, and the colors were close to half-way between those of the $n_b/n_r = 0$ and 1, and 1 and infinity cases respectively. Thus, intermediate values of n_b/n_r can be estimated.) These values of n_b/n_r are in reasonable agreement with those estimated from the (u-g) and (g-r) colors in Figure 1.

V. SUMMARY AND CONCLUSIONS

The following conclusions seem consistant with the above data from computed clusters and observations:

i) Cluster models were found to agree reasonably well with the 5-filter observations of clusters in the Magellanic Clouds. We can present in Table 6 some "semi-empirical" colors as a function of time, based on a smoothed fit of the clusters with the models. These colors can be used in calculating colors of galaxies.

ii) Enrichment or depletion of clusters in massive stars compared to the Limber IMFF does not affect calculated colors very much. Clusters with different IMFF's will have different slopes in the g, log t or g, (u-g) planes.

iii) Some information about n_b/n_r ratios of younger clusters (in the region in log t between ~6.7 to ~7.9) can be obtained, which pertain to evolutionary tracks of stars between 20 and 3 $M_\odot$. Comparison of the cluster observations to the models in the (u-g), (g-r) plane suggests a lower limit of n_b/n_r of ~ 1 for clusters ~ 5 x 10^7 yrs old to ~0.6 for clusters ~ 6 x 10^6 yrs old. Plots in the reddening-independent colors, in Q_1 and Q_2, and Q_2 and Q_3, suggest an upper limit for the younger clusters (t ~6x10^6) of n_b/n_r about 1 to 2. Finally a plot in the Q_1, log t

plane for 12 clusters and the models gives a value of $n_b/n_r \sim 1.3$ for clusters with $t \sim 5 \times 10^7$ yrs to ~ 0.6 for clusters with $t \sim 6 \times 10^6$ yrs. The reasonable agreement between the various plots indicates that there is relatively little absorption in the clusters ($E(g-r) \lesssim 0.05$) and that the best values of n_b/n_r run from ~ 1.3 to ~ 0.6 for clusters in the region ($6.7 \leq \log t < 7.9$). Thus, n_b/n_r is estimated roughly to run from slightly more than 1 to ~ 0.6 for stellar-evolutionary tracks from $\sim 3\ M_\odot$ to $\sim 20\ M_\odot$.

iv) Globular clusters can be distinguished in some plots. Their properties will be discussed in a later paper by Searle.

REFERENCES

Aller, L. H., Czyzak, S. J., and Walker, M. F. 1968, Ap. J., 151, 491.

Arp, H., and Thackeray, A. D. 1967, Ap. J., 149, 87.

Bagnuolo, W. G. 1976a, b, to be published.

Bradley, P. T., and Morton, D. C. 1969, Ap. J., 156, 687.

Bright Star Catalogue, 1964, Hoffeid, ed.; New Haven, Yale U. Press.

Dixon, M. E., Ford, V. L., and Robertson, J. W. 1972, Ap. J., 174, 17.

Gascoigne, S. C. B. 1969, in The Magellanic Clouds, Muller, ed.; Berlin, Springer Press, p. 25.

Graham, J. A. 1973, I. A. U. Coll. No. 21, Fernie, J. D., ed.; Dordrecht, Holland, D. Reidel Co., p. 120.

Hartwick, F. D. A., and Vanden Bergh, D. A. 1972, Ap. J., 176, 677.

Haug, U., Dachs, T., Pesch, J., and Pfleiderer, J. 1967, Z. Astrophys., 66, 433.

Hodge, P. W., and Flower, P. J. 1973, Ap. J., 185, 829.

Iben, I. Jr., 1966, Ap. J., 142, 1447.
———. 1967a, Ap. J., 147, 624.
———. 1967b, Ibid., 650.

Johnson, H. L. 1966, Ann. Rev. Astr. and Ap., 4, 193.

Johnson, H. L., and Sandage, A. 1955, Ap. J., 121, 616.

Lee, T. A. 1970, Ap. J., 162, 217.

Limber, D. N. 1960, Ap. J., 131, 168.

Miller, J. S., and Matthews, W. G. 1972, Ap. J., 172, 593.

Morton, D. C. 1969, Ap. J., 158, 629.

Morton, D. C., and Adams, T. F. 1968, Ap. J., 151, 611.

Robertson, J. W. 1971, Ap. J., 170, 353.

Robertson, J. W. 1972, Ap. J., 177, 473.
———. 1974, Astrophys. Supp., 15, 261.

Saltpeter, E. E. 1955, Ap. J., 121, 161.

Sandage, A. 1962, Ap. J., 135, 333.

Schild, R. E. 1970, Ap. J., 161, 855.

Searle, L. 1971, Ap. J., 168, 327.
———. 1975, private communication.
———. 1976, to be published.

Searle, L., and Sargent, W. L. W. 1972, Ap. J., 173, 25.

Searle, L., Sargent, W. L. W., and Bagnuolo, W. G. 1973, Ap. J., 179, 427.

Strothers, R. L. 1963, Ap. J., 138, 1074.

TABLE 1

PROPERTIES OF THE PHOTOMETRIC SYSTEM

Filter	$\bar{\lambda}$(Å)	λ_{MAX}(Å)	h.p. Bandwidth (Å)
u	3545	3570	375
b	3970	3945	455
g	4930	4910	723
o	5975	5850	542
r	6750	6505	765
Hα	6572	6572	65
Mgb	5175	5173	66
IR	7005	6950	253
TiO	6210	6197	109
Hα′	6587	6590	95
66	6583	6583	207

TABLE 2. CLUSTER COLORS

Name	(u-g)	(b-g)	(g-δ)	(g-r)	Q_1	Q_2	Q_3	Ages: CM, Cep
121	0.23	0.68	0.60	0.92	-0.73	0.01	0.06	
256	-.30	.12	.20	.31	-.62	-.11	.01	
330	-.78	-.04	.21	.37	-1.16	-.31	-.06	7.05,....
L56	-.90	-.12	.05	.12	-1.02	-.21	-.07	
346	-1.03	.15	-.55	-.07	-.96	.20	-1.37	
L72	-.62	.05	.30	.51	-1.15	-.32	-.06	
416	.21	.66	.59	.89	-.73	.02	.08	
419	.32	.59	.54	.84	-.57	-.02	.03	
458	-.35	.05	.14	.24	-.60	-.12	-.03	7.67,....
1466	.11	.55	.55	.82	-.75	-.04	.09	
S33	.22	.57	.46	.69	-.51	.07	.07	
1711	-.71	-.04	.13	.23	-.96	-.21	-.04	
1755	-.44	-.02	.16	.28	-.73	-.22	-.04	
1774	-.48	.03	.25	.43	-.94	-.28	-.06	
1783	-.27	.59	.50	.76	-.53	.04	.06	
1805	-.96	-.10	.59	.49	-1.48	-.45	-.24	
1818	-.80	-.04	.24	.44	-1.26	-.36	-.10	7.27,....
1835	.24	.60	.58	.89	-.70	-.05	.05	
1831	.07	.29	.27	.42	-.37	-.01	.01	
1850	-.47	.02	.17	.32	-.80	-.21	-.09	7.38,....
1854	-.53	.04	.17	.31	-.85	-.18	-.07	7.40,....
1856	.04	.24	.29	.46	-.44	-.09	.00	
1872	.04	.23	.29	.51	-.49	-.14	-.08	
1866	-.23	.13	.21	.36	-.61	-.13	-.05	7.70,7.84
1903	-.44	.02	.18	.32	-.77	-.21	-.06	
1943	-.36	.14	.20	.39	-.77	-.14	-.12	
S53	-.94	-.09	.15	.29	-1.25	-.30	-.09	
1987	.21	.42	.42	.70	-.53	-.09	-.06	
1986	-.55	.04	.18	.30	-.87	-.18	-.02	
1978	.35	.72	.60	.90	-.60	.07	.09	
2004	-1.14	-.14	.24	.48	-1.64	-.49	-.17	7.03,...
2019	.26	.65	.60	.91	-.70	-.01	.07	
2041	-.36	.06	.21	.33	-.71	-.18	.01	
2058	-.31	.12	.21	.35	-.68	-.13	-.03	
2065	-.30	.15	.22	.36	-.68	-.11	-.02	
2070	-.91	.14	-.06	.27	-1.19	-.06	-.62	
2100	-.94	-.05	.24	.45	-1.41	-.38	-.12	7.11,....
2107	.09	.26	.28	.46	-.39	-.07	-.03	
2134	-.07	.18	.22	.36	-.45	-.08	-.02	
2136	-.27	.12	.26	.41	-.71	-.18	.00	7.61,7.53
2157	-.38	.12	.21	.33	-.73	-.12	-.05	7.31,....
2164	-.50	.00	.11	.18	-.69	-.13	-.01	7.55,....
S69	.13	.55	.55	.84	-.76	-.06	.06	
2214	-.54	-.02	.12	.24	-.79	-.19	-.08	7.48,....
47 Tuc	.48	.92	.67	1.00	-.57	.20	.11	
ω Cen	.15	.69	.64	.96	-.86	-.01	.10	

TABLE 3. PROPERTIES OF ADOPTED STELLAR-EVOLUTIONARY TRACKS

Property	Pt. #	$60M_\odot$	$30M_\odot$	$15M_\odot$	$5M_\odot$	$3M_\odot$	$2.25M_\odot$	$1.5M_\odot$	$1.25M_\odot$	$1.0M_\odot$
log L	1	5.99	5.16	4.44	2.90	1.97	1.47	0.74	0.36	-0.12
	5	6.39	5.52	4.69	3.04	2.14	1.62	0.87	0.53	0.14
	6	6.36	5.54	4.76	3.12	2.21	1.78	0.96	0.61	0.23
	10	6.52	5.66	4.84	3.06	2.32	1.74	1.08	0.85	0.55
	11	6.36	5.49	4.66	2.93	2.13	1.90	1.30	1.10	0.78
	17	6.56	5.69	4.86	3.19	2.30	2.57	2.17	2.12	2.02
	19	6.57	5.70	4.88	3.19	2.29	2.78	2.54	2.50	2.46
	21	6.28	5.41	4.58	3.18	2.28	....	....	....	.....
log T_e	1	4.712	4.630	4.515	4.260	4.135	4.043	3.898	3.819	3.743
	5	4.640	4.550	4.430	4.189	4.062	3.970	3.852	3.807	3.765
	6	4.620	4.569	4.479	4.228	4.096	3.996	3.891	3.829	3.768
	10	3.546	3.546	3.546	3.626	3.620	3.678	3.679	3.675	3.680
	11	3.565	3.565	3.565	3.645	3.650	3.668	3.668	3.669	3.671
	17	4.450	4.350	4.246	3.776	3.675	3.607	3.605	3.607	3.611
	19	4.315	4.230	4.150	3.701	3.650	3.580	3.575	3.574	3.575
	21	3.580	3.580	3.580	3.626	3.620	.....	.....	.....	.....
t (10^7 yr)	1	0.00	0.00	0.001	0.01	0.24	0.57	1.8	2.95	5.1
	5	0.1466	0.3416	0.680	4.24	22.37	48.50	157.1	283.2	671.1
	6	0.1520	0.3543	0.7053	4.467	23.41	52.02	165.2	301.4	808.1
	10	0.1530	0.3566	0.7099	4.734	25.31	55.66	219.9	434.3	1045.7
	11	0.1606	0.3744	0.7453	5.180	27.81	56.17	226.3	445.0	1065.2
	17	0.1640	0.3821	0.7607	6.728	31.59	58.73	240.56	475.55	1102.96
	19	0.1728	0.4027	0.8018	7.252	34.05	59.47	242.26	477.81	1105.81
	21	0.1747	0.4072	0.8107	7.511	35.26	.....	.....	.....	.....

TABLE 4

DATA FOR EMISSION LINE EFFECTS

Filter	Lines	$f_e/\langle f \rangle$	I_{hi}	I_{med}	I_{lo}
u	3727	.56	.25	2.14	1.38
b	3727	.52	.25	2.14	1.38
	3880	.94	.18	.34	.58
	3970	.99	.18	.22	.58
	4101	.73	.28	.28	.29
	4340	.175	.47	.48	.46
g	4340	.04	.47	.48	.46
	4861	1.00	1.000	1.000	1.000
	4959	.98	.04	.64	1.78
	5007	.96	.13	1.90	5.75
o	5876	.96	.00	.03	.11
	6563+[NII]	.14	4.61	3.71	2.95
r	6563+[NII]	.98	4.61	3.71	2.95
	6750	.77	.08	.15	.26

TABLE 5

BRIGHTNESS IN g AS FUNCTION OF TIME

log t	$\delta = -.55$ ($\alpha \sim 3.0$)	$\delta = 0$ ($\alpha \sim 2.45$)	$\delta = +.5$ ($\alpha = 1.95$)
6.0	-1.30	-2.08	-2.92
6.5	-0.73	-1.24	-1.79
7.0	0.00	0.00	0.00
7.5	0.20	0.44	0.71
8.0	1.08	1.63	2.22
8.5	1.75	2.50	3.31
9.0	2.72	3.66	4.68
9.5	3.55	4.63	5.75
10.0	4.50	5.71	7.01

TABLE 6

SEMI-EMPIRICAL CLUSTER COLORS

log t	(u-g)	(b-g)	(o-g)	(r-g)
6.4	-0.86	0.17	0.25	-0.53
6.6	-1.17	-0.11	-0.09	-0.50
6.8	-1.19	-0.17	-0.17	-0.41
7.0	-1.12	-0.18	-0.14	-0.27
7.2	-0.90	-0.13	-0.18	-0.33
7.4	-0.62	-0.04	-0.21	-0.37
7.6	-0.39	0.09	-0.25	-0.35
7.8	-0.34	0.19	-0.29	-0.42
8.0	-0.33	0.14	-0.25	-0.38
8.2	-0.28	0.11	-0.22	-0.37
8.4	-0.18	0.13	-0.22	-0.38
8.6	0.02	0.25	-0.30	-0.47
8.8	0.07	0.24	-0.27	-0.47
9.0	0.14	0.38	-0.36	-0.58
9.2	0.16	0.47	-0.38	-0.62
9.4	0.24	0.64	-0.55	-0.83
9.6	0.33	0.74	-0.64	-0.93
9.8	0.49	0.86	-0.67	-1.00
10.0	0.61	0.95	-0.71	-1.06

CAPTIONS FOR FIGURES

Figure 1:

Comparison of observed and model clusters in (u-g) and (g-r). The numbers along the "tracks" are values of log t. The sets of cluster models are denoted as follows: (from left to right) large dashed line, (n_b/n_r= infinity, δ= 0); small dashed line, (n_b/n_r= 1, δ= 0); dotted line, (n_b/n_r=1, δ = 0.5); solid line, (n_b/n_r= 0, δ= 0); dot-dashed line, (n_b/n_r= 0, δ= 0.5). Observed cluster colors denoted by open circles here and in following figures.

Figure 2:

Comparison of observed and model clusters in Q_1 and Q_2. The numbers along the "tracks" are values of log t. The sets of cluster models are denoted as follows: dashed line, n_b/n_r= 0; solid line, n_b/n_r= 1; dotted line, n_b/n_r= infinity.

Figure 3:

Comparison of observed and model clusters in Q_2 and Q_3. The lines have the same significance as in Figure 2, except that the added dot-dash line denotes the case, (n_b/n_r=0, δ=0.5).

Figure 4:

Comparison of models and twelve clusters with known ages in Q_1 and log t. The sets of cluster models are denoted as follows: (from low to high Q_1) dot-dashed line, (n_b/n_r= infinity, δ= 0); solid line, (n_b/n_r= 1, δ= 0); dotted line, (n_b/n_r= 1, δ= 0.5); small dashed line, (n_b n_r=0, δ =0); large dashed line, (n_b/n_r= 0, δ= 0.5).

FIG 1

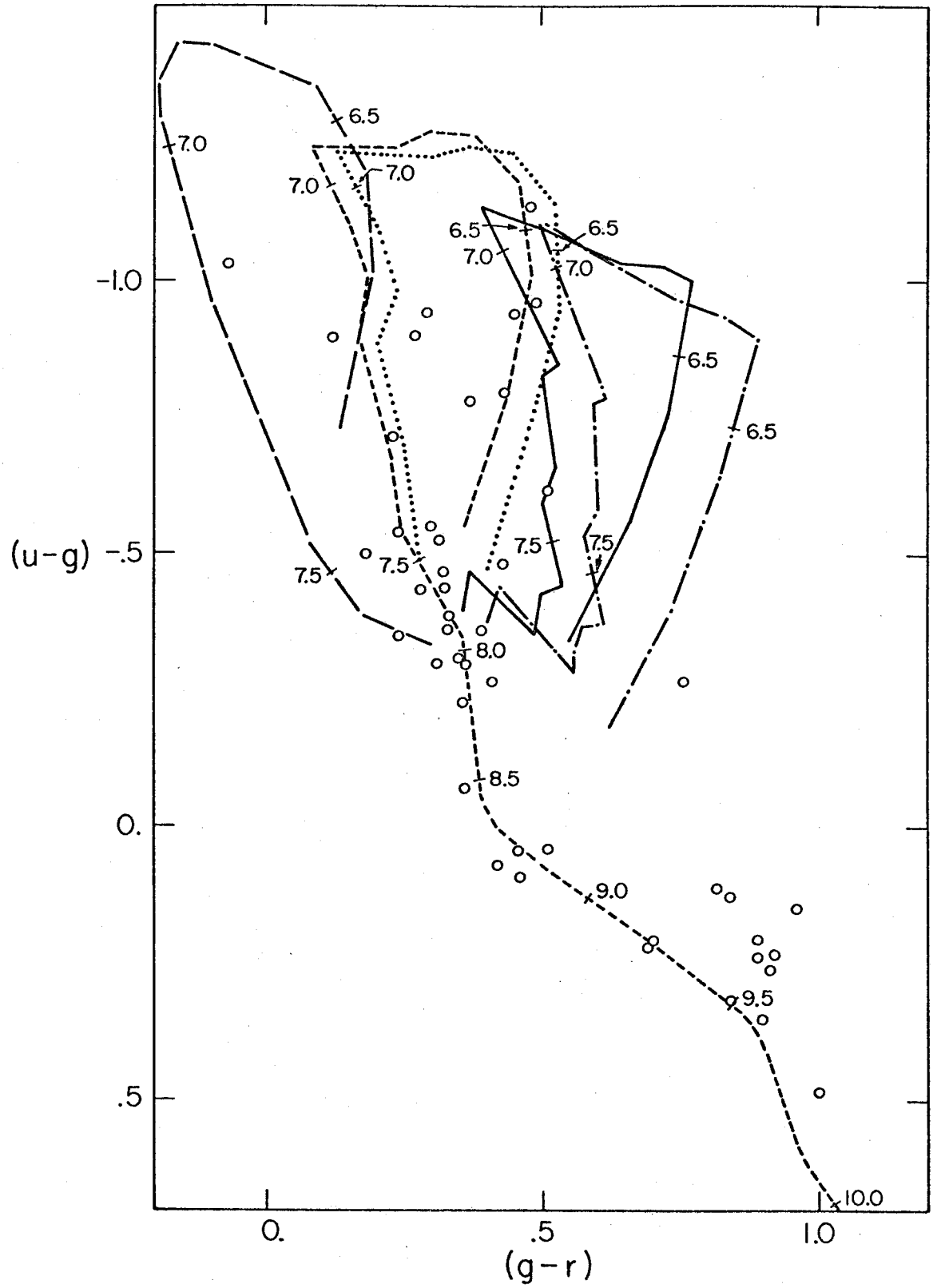
6.5
7.0
7.0
7.0
6.5
6.5
7.0
7.0
6.5
6.5
7.5
7.5
7.5
7.5
8.0
8.5
9.0
9.5
10.0
-1.0
(u-g) -.5
0.
.5
0.
.5
1.0
(g-r)

FIG. 2.

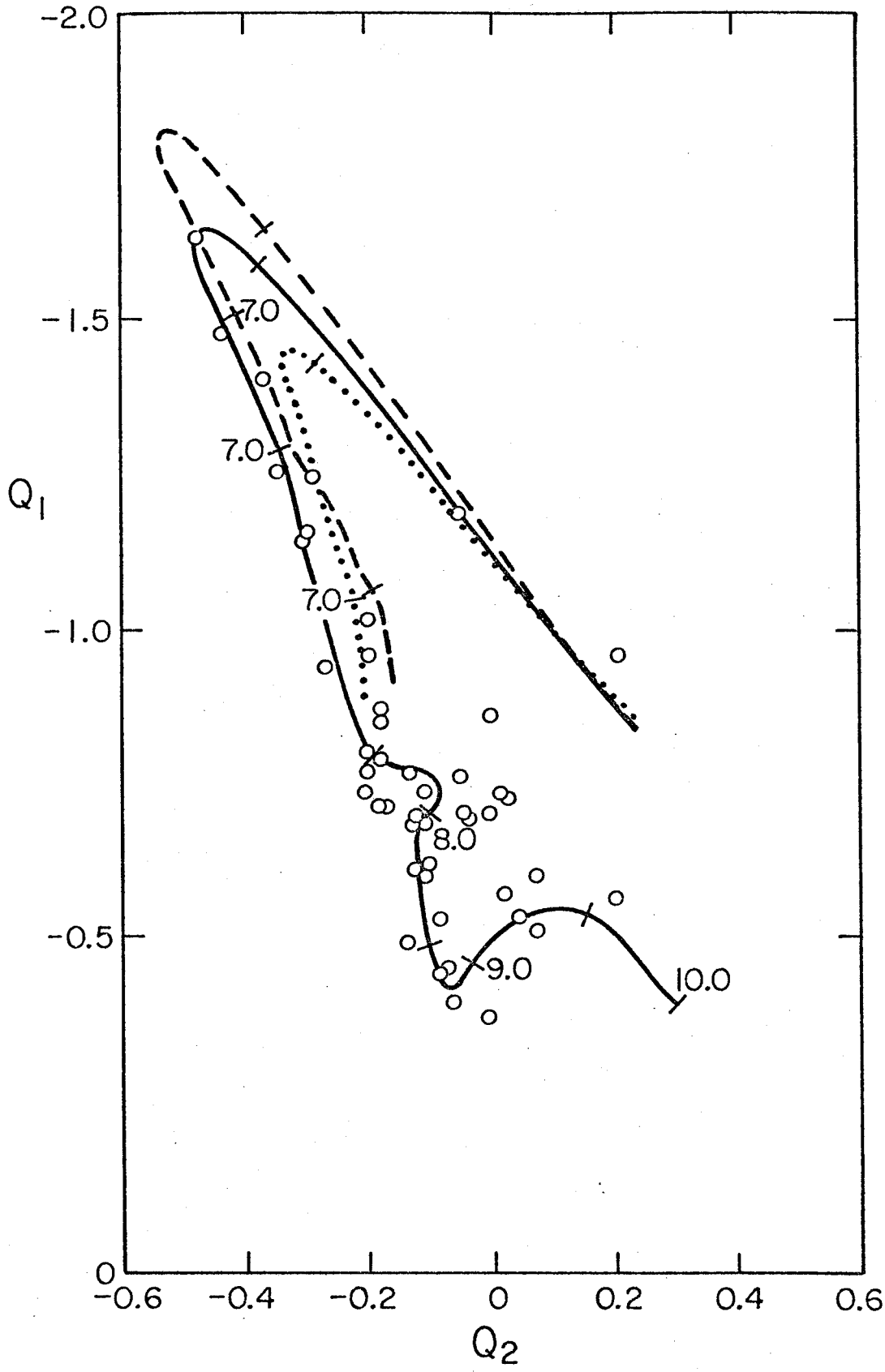

Fig 3

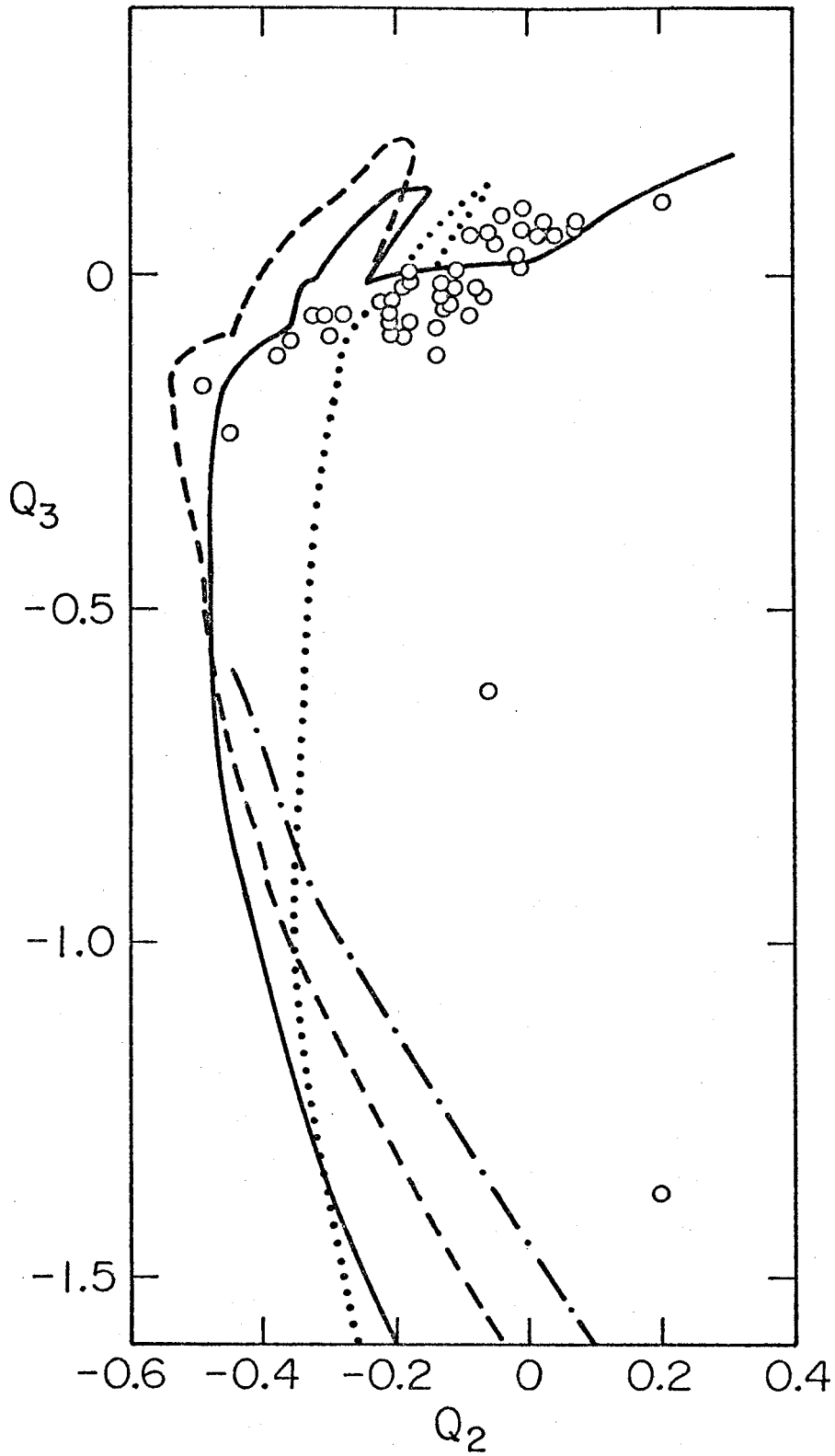

Fig. 4

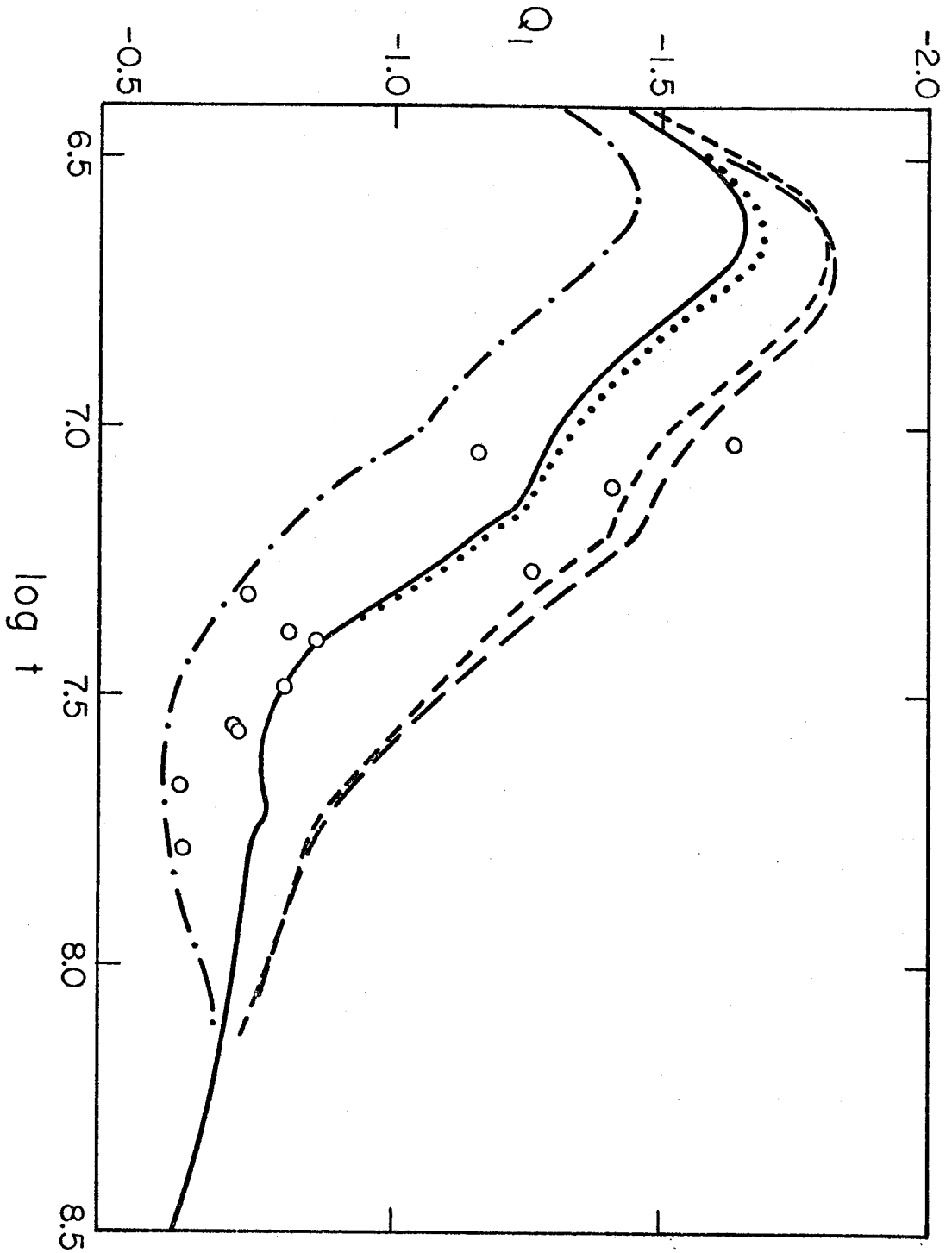

CHAPTER 3

TEN-COLOR PHOTOMETRY OF 102 STARS OF VARIOUS SPECTRAL TYPES AND LUMINOSITY CLASSES

I. INTRODUCTION

This paper presents the results of photometry of a number of stars in a ten-color system. The photometry of Irregular and Sc galaxies in the same system is described in another paper (Bagnuolo (1976), hereafter referred to as "paper I.") The observations of stars described in this paper were made in order to calibrate the color system so that the colors of model clusters and galaxies could be computed and compared with observations. Cluster models and observations are presented in Searle and Bagnuolo (1976). In this paper the observed star colors and also average star colors as a function of assumed log T_e will be presented. The overall behavior of average colors as functions of log T_e and spectral type will be discussed.

II. OBSERVATIONS

A set of eleven filters was used for the photometry of the stars, and also for the galaxies presented in paper I. Five medium bandwidth filters designed originally by J. E. Gunn, designated by u, b, g, o, and r respectively, were used to measure the overall continuum over a wide frequency range and the Balmer Jump. The Gunn filters were constructed from a collection of Schott glass and Wratten filters. Figure 1 contains plots of the transmission curves

of these five filters, determined by a Cary 14 spectrophotometer. The dashed line is a relative response curve, given by Aaronson (1972) of the S-20 phototube at Table Mountain Observatory, used for much of the observations. The largest effect of the phototube sensitivity is to eliminate almost all of the response form the third transmission peak in the r filter.

Three of the most prominent spectral features in the late-type galaxies that were observed (paper I) were expected to be the Mg b triplet, TiO bands, and the Hα line in emission and absorption. A set of filters was used to measure these features. The Mgb filter, centered on the Mg b triplet near λ5175 is similar to that of Wood (1965). The filter designated by TiO was intended to measure the TiO band at about λ6200. The filters designated by Hα, Hα', and 66 measure Hα emission, the latter two being especially useful for large redshifts. Finally, the IR filter, centered at about λ7005, measures an emission-free continuum region somewhat redder than the r filter. Table 1 lists the properties of the photometric system defined by the above filters and S-20 phototubes. The fourth column lists also the maximum transmission of the filters also found by the Cary 14.

One hundred and nine different stars were observed. In order to determine color-type and color-temperature relations, stars of all luminosity classes between spectral

types O5 and M6 were observed. Most of the stars were taken from papers by Mc Clure and van den Bergh (1968), Wood (1965), and Spinrad and Taylor (1971). Also, most of the stars have visual magnitudes between 3.5 and 7.0. The first and second columns of Table 2 list the star name (an HD number unless otherwise indicated), and spectral type and luminosity class. The last column gives the visual magnitudes listed by the Bright Star Catalogue (1964). (In a few cases the magnitude is given by the S.A.O. Catalogue (1966); the magnitude of HD 14442 is from Kraft and Hiltner (1961).) Uncertain measurements or variable stars are marked with a colon.

The observations of the stars were made on six nights in July- August 1972 and two nights in June 1973 with the 24" reflector at Table Mountain Observatory, and on eight nights in July- September 1973 with the 20" reflector at Palomar. A two-tube S-20 photometer was used for the Palomar observations and another S-20 photometer was used at Table Mountain. In both cases the numbers of counts were recorded digitally on paper tape. At the Palomar 20" apertures of 1.5 to 3.0 mm diameter were used, corresponding to 1.5' to 3.0'. Four to eight readings of five to twenty seconds were used. Readings of the star and sky were obtained, usually by taking successive readings with the star in one tube, then the other. Typically, about 50,000 net counts per second (star minus sky) in the g filter were obtained for a 7.0 magnitude A star. At Table Mountain a similar procedure

was followed. Apertures of 0.67 mm to 4.0 mm (20" to 2.0' at the 24" telescope) were used. Measurements were made in the pattern star-sky-star, except in the four July 1972 nights on which stars were observed only once.

Eighty-two different stars were observed in the 1972 Table Mountain runs in which filters u, b, g, o, r, Mgb, and 66 only were used. The 1973 observations at Table Mountain and Palomar were made in order to observe stars in filters Hα, IR, TiO, and Hα' and to obtain greater accuracy in colors already measured. A total of sixty-three different stars were observed in 1973, including thirty-six of the 1972 stars. Fifty-five different stars were observed at Palomar, twenty-two at Table Mountain. Overall, 56 stars were observed only once, 25 twice, and 28 more than twice. The third column of Table 2 gives the total weight, w, of observations in which the 1973 observations are given a weight of 1.0 and the 1972 observations (considered more inaccurate) a weight to 0.7. From the listed w the number of times a star was observed in 1972 or 1973 can be readily obtained.

A set of standard stars, comprised of seven equatorial standards of Haug, Dachs, Pesch, and Pfleiderer (1967) and 5 other stars, was used to correct the 1973 observations for atmospheric extinction and variations in tube sensitivity. Almost all of the stars were observed with an airmass, z, less than 1.5, and second order extinctions were neglected.

(Aaronson (1972) showed that second-order extinction effects are negligible for $z < 2.0$, which is confirmed by observations of stars with high z.) The reduction of the Table Mountain and Palomar stars was done separately. The determination of extinction is a modification of that of Hardie (1962) and can be briefly described as follows. We first assume that the extinction on each night is given by an average extinction coefficient, which can be estimated from observations in which the same stars were observed at different airmasses. Using these average extinctions we estimate the unextinguished ($z = 1.00$) colors and g magnitudes of stars on each night, which we will denote by $(i-g)'_x$ and g'_x respectively for star x. We can define an average color ratio by: $R_{xy}(i-g) = (1/m)\sum[(i-g)'_x - (i-g)'_y]$, where summation is taken over all m nights on which both stars x and y were observed. $R_{xy}(g)$ can be similarly defined. Obviously, $R_{xx}(i-g) = 0$. For any two observations of stars x and y on a given night, $(i-g)_x$ and $(i-g)_y$, an observed color ratio may be defined by: $r_{xy}(i-g) = (i-g)_x - (i-g)_y$.

The observed color ratios are insensitive to moderate changes in tube sensitivity; thus, variations in r_{xy} are due to extinction. Let $e_{xy}(i-g)$ be the difference between an observed and average color ratio: $e_{xy}(i-g) = |r_{xy}(i-g) - R_{xy}(i-g)|$. Similarly, let $\Delta z = |z_x - z_y|$ be the difference in airmass of the stars. Points for all

different pairs of observations can be plotted in the $(e_{xy}, \Delta z)$ plane. (If n stars are observed, the number of points is $n(n-1)/2$.) The extinction coefficient is then the slope of a least-squares line fitted through the points and the origin, the points being weighted according to the estimated accuracies of e_{xy}'s. Thus, the colors of all the stars are used to estimate extinction. The extinctions obtained were reiterated to get slightly better estimates of the R_{xy} and the extinctions.

The mean colors on each night of a certain star ("Z4A" for the Palomar observations) can be estimated from the unextinguished colors of all stars observed by means of the R_{xy}. Thus, the nightly sensitivities can be estimated. The 1972 observations were reduced in a similar way, except that extinctions in the August run were obtained by repeated observations of the same stars. The colors of about thirty stars obtained in the August run were then used as standards to estimate extinctions and sensitivities in the July run.

Simple linear transformations, obtained from a least-squares estimate from some 19 stars observed at both Table Mountain and Palomar, were used to transform the 1972 and 1973 Table Mountain colors to the Palomar system, adopted as standard:

$$(i-g)_P = a_i(i-g)_T + b_i \; ; \quad g_P = a_g\, g_T + b_g(o-g)_T + c \qquad (1)$$

where i is an arbitrary filter, P and T refer to Palomar and Table Mountain quantities respectively, and the a's, b's, and c are constants. The coefficients obtained for the 1972 Table Mountain stars are very close to those of the 1973 stars, as expected. No deviations from linearity in the plots defining the empirical transformations above could be detected, which is not surprising for transformations between similar systems. In the standard Palomar system, the colors of the A0 V star "Z4A" of Haug et al. are set at (i-g)= 0.00 for all i $\neq$ g, and g = 7.00.

The colors of 18 supergiants were corrected for interstellar reddening. Estimates of the reddening, E(B-V), were obtained for eight of the stars from McClure and van den Bergh (1968), Kraft and Hiltner (1961), and Wood (1965). The reddening of the stars was also determined from the use of two-color plots in (u-g)-(b-g), (b-g)-(g-o), and (g-o)-(g-r), and comparing the supergiant colors with the mean colors of giants. Whitford's (1958) reddening law, as quoted by Miller and Mathews (1972), was used to determine the slopes of reddening lines and to convert color excesses in (g-o) or (B-V) into color excesses for all colors. (If E(o-g) = 1.00, then E(B-V)=-1.30, E(u-g)=-1.62, E(b-g)=-1.10, E(r-g)=1.54, E(Mgb-g)=0.27, E(IR-g)=1.69; E(Hα-g), E(Hα'-g), and E(66-g) = 1.44; and E(V-g)=0.56.) The colors of the stars are listed in Table 2. Under the column headed "i", color (i-g) appears, except for the g magnitude, designated by m_g.

For the 18 supergiants, the colors corrected for reddening are listed immediately below the observed colors. The g magnitude is corrected by E(g-V) so that a relation between g and V can be determined. The colors of seven equatorial standards are listed last, because their spectral classifications are uncertain.

Estimates of the observational errors of the 1973 star colors were obtained from the mean of the standard deviations of the colors of the standards. Table 3 gives these estimated mean standard errors. ("Median errors," defined as the median of the standard deviations of colors, are generally somewhat smaller; "probable errors" are about 0.7 times as large as those of the Table.) Errors of the 1972 stars were similarly estimated from stars observed several times. In Table 3 the errors in the 1973 stars are generally smaller, particularly in the g magnitude. The smaller 1973 errors are probably due to the improved observational and reduction techniques. The lower part of Table 3 lists the differences in average color between Table Mountain and Palomar observations of the six most frequently observed standards. These systematic differences are generally smaller than the estimated observational errors.

III. DISCUSSION OF RESULTS

The temperatures of the stars listed in the fourth column of Table 2 were obtained by assuming temperature-

spectral type relations from Johnson (1966), Morton and Adams (1968), and Lee (1970). Table 4 gives average colors as a function of log T_e for stars of luminosity classes V, III, and I. The average colors were obtained from plots of the star colors of Table 2 against log T_e. Table 4 can be used to compute cluster or galaxy colors from stellar evolutionary tracks in the (log L, log T_e) plane. Plots of the colors of Table 2 against spectral type were also produced. Color separations of stars of different luminosity classes and deviations from smooth black body- like curves are considered the interesting features of the plots of colors versus log T_e or spectral type. The features discussed for color- log T_e plots can be seen in Table 4. The most interesting features of the color plots seem to be the following:

1) In plots of (u-g) versus log T_e or spectral type the biggest feature is due to the Balmer Jump as one might expect. There is a minimum in the plot at log T_e= 3.9 (type A2) where (u-g)= 0.0, and a maximum at log T_e= 3.8 (F5), where (u-g)= 0.15. The depression in (u-g) compared to what a black body would be appears to be roughly 0.4 to 0.5 mag.

Another feature of the (u-g)- log T_e plot is that late B- early A giants and supergiants are bluer than dwarfs of the same temperature by up to 0.2 mag. (at log T_e =4.1). This separation is more noticeable in the plot of (u-g) with

log T_e than that with spectral type, because lower temperatures were assumed for giants and supergiants than dwarfs of the same spectral type. Finally, there is a separation between cool stars of different luminosity classes, most noticeable around M0 (log T_e = 3.6), which diminishes for the coolest stars. For cool stars dwarfs are generally bluest in (u-g).

2) In the plot of (b-g) versus spectral type there is a separation of stars of classes I and III from dwarfs between spectral types K1 to M2. The separation, similar to that in (u-g), reaches a maximum of 0.5 mag. at K4. On the color- temperature plot a similar separation exists, except that there is also a difference between giants and supergiants. The separation of supergiants from dwarfs is significant at log T_e= 3.75, reaches a maximum at log T_e= 3.65 to 3.60, then diminishes rapidly. The separation of giants from dwar occurs at cooler temperatures and is greatest between log T_e = 3.60 and 3.55. There is also a small separation of giants and supergiants from dwarfs in the color- temperature plot from log T_e= 4.1 to 3.8, similar to that for (u-g).

3) The main feature of the (o-g) plots is that stars cooler than log T_e= 3.6 (~K7) do not become much redder in (o-g). This is probably due to absorption bands in the o filter. There are little differences between stars of different luminosity classes in the (o-g) plots, except that supergiants between 4.0 and 3.65 in log T_e seem slightly

redder than the class III or V stars.

4) In the (r-g)- log T_e plot there is generally little luminosity separation, except that the coolest dwarfs are up to 0.15 mag. bluer that giants or supergiants (at log T_e= 3.55). On the (r-g)- spectral type plot dwarfs later than G0 are 0.1 to 0.2 mag. bluer than giants or supergiants. Finally, the rise in (r-g) appears to slow for stars cooler than log T_e= 3.55, although to a much lesser degree than in (o-g).

5) The plots of (Hα-r) are virtually flat. The dip in (Hα-r), mainly for dwarfs , centered at log T_e= 3.95 is due to the Hα absorption line. The depth of the absorption dip is about 0.06 mag.

6) In the plot of (Mgb-g) the main feature is a luminosity separation for stars later than about G7. This luminosity separation is described by Wood (1965) who used a similar "Mgb" filter. In the color- temperature plot luminosity separation begins at about log T_e= 3.75 and reaches a maximum of 0.3 mag. between supergiants and dwarfs at log T_e= 3.60. This separation diminishes to about 0.12 mag. for log $T_e \leq$ 3.50. Giants have (Mgb-g) between that of supergiants and dwarfs , though somewhat closer to the latter. (See Table 4.) In the color- spectral type plot there is a maximum separation of 0.2 mag. between classes III and V and 0.35 mag. between I and V at about K4.

7) (IR-r) becomes gradually redder for cooler stars as expected. There appears to be no noticeable luminosity separation.

8) (TiO-o) varies from 0.06 at log T_e= 4.5 to -0.08 at log T_e= 3.65, then drops because of TiO bands to 0.15 at log T_e= 3.50.

9) (Hα'-r) has a behavior similar to that of (Hα-r). The dip at log T_e= 3.95 is about 0.04- 0.05 mag.

10) (66-r) has a flat plot with a small dip at log T_e = 3.95. The decline to 0.10 at log T_e= 3.5 is probably due to a TiO band.

We may summarize the results presented above as follows. First, generally speaking, there appear to be larger differences in color due to luminosity effects between stars of the same spectral type than the same temperature. Late B- early A stars in the (u-g) plots are an exception to this rule. Secondly, the most important features appear to be: the effect of the Balmer Jump on (u-g), the luminosity separation in (u-g) and (b-g) for stars later than G5 (or log T_e= 3.75) and the smaller luminosity separations in (u-g) and (b-g) for late B- early A stars. There is a leveling- off of (o-g) for stars later than K4 (log T_e= 3.6), and a small luminosity separation for supergiants from log T_e = 4.0 to 3.65. A luminosity separation in (Mgb-g) exists for stars later than G7 (log T_e= 3.75). The color (TiO-o) drops for M stars cooler than log T_e= 3.6. Finally, the Hα, Hα',

and 66 filters provide little information about stars, except for the dip in (Hα-r) and (Hα'-r) around A2 (log T_e= 3.95). These colors were later used for measurements of Hα emission in galaxies.

REFERENCES

Aaronson, M. 1972, unpublished B. S. Thesis, Caltech.

Bagnuolo, W. G. 1976, to be published.

Bright Star Catalogue 1964, Hoffeid, ed.; Hew Haven, Yale U. Press.

Hardie, R. H. 1962, in Astronomical Techniques, Hiltner, W.A., ed.; Chicago, U. of Chicago Press, Chapter 8.

Haug, U., Dachs, T., Pesch, J., and Pfleiderer, J. 1967, Z. Astrophys., 66, 433.

Johnson, H. L. 1966, Ann. Rev. Astr. and Ap., 4, 193.

Kraft, R. P. and Hiltner, W. A. 1961, Ap. J., 134, 850.

Lee, T. A. 1970, Ap. J., 162, 217.

Mc Clure, and van den Bergh, S. 1968, A. J., 73, 313.

Miller, J. S., and Mathews, W. G. 1972, Ap. J., 172, 593.

Morton, D. C., and Adams, T. F. 1968, Ap. J., 151, 611.

S. A. O. Catalog, 1966, reprint 1971; Washington, D. C., Smithsonian Astrophys. Obs.

Searle, L., and Bagnuolo, W. G. 1976, to be published.

Spinrad, H., and Taylor, B. J. 1971, Ap. J. Supp., 22, 445.

Whitford, A. E. 1958, A. J., 63, 201.

Wood, D. B. 1965, A. J., 74, 177.

TABLE 1

PROPERTIES OF THE PHOTOMETRIC SYSTEM

Filter	$\bar{\lambda}$ (A)	λ_{max}	$\Delta\lambda$ (bandwidth)	T_{max}
u	3545	3570	375	0.51
b	3970	3945	455	0.54
g	4930	4910	723	0.53
o	5975	5850	542	0.60
r	6750	6505	765	0.89
Hα	6572	6572	65	0.82
Mgb	5175	5173	66	0.59
IR	7005	6950	253	0.60
TiO	6210	6197	109	0.59
Hα'	6587	6590	95	0.53
66	6583	6583	207	0.67

TABLE 2

Star Colors

Name	Type	W	log T_e	u	b	m_g	o	r	Hα	MgIb	IR	TiO	Hα′	66	m_v
14442....	05 III	1.0	4.675	-0.86	0.08	9.26	-0.44	-0.48	-0.58	-0.09	-0.52	-0.35	-0.52	-0.48	9.22
				-1.74	-0.53	8.95	0.11	0.37	0.21	0.06	0.40	0.30	0.27	0.32	
10 Lac...	09 V	1.7	4.505	-1.71	-0.47	4.56	0.17	0.30	0.19	0.01	0.29	0.20	0.23	0.23	4.88
222363...	09.5 III	1.0	4.451	-0.87	0.03	8.23	-0.27	-0.34	-0.42	-0.07	-0.36	-0.26	-0.39	-0.33	...
				-1.56	-0.45	7.98	0.17	0.34	0.21	0.05	0.39	0.26	0.25	0.29	
S12188...	B2 III	1.0	4.264	-0.58	0.12	8.43	-0.31	-0.49	-0.70	-0.08	-0.49	-0.36	-0.58	-0.50	7.8:
				-1.33	-0.40	8.17	0.16	0.23	-0.02	0.05	0.30	0.19	0.10	0.18	
S21803...	B2 IV	1.0	4.288	-1.12	-0.21	6.25	-0.03	-0.02	-0.08	-0.01	-0.03	-0.01	-0.07	-0.03	6.4:
				-1.43	-0.42	6.14	0.16	0.28	0.20	0.04	0.30	0.22	0.21	0.25	
3360.....	B2 V	1.4	4.312	-1.48	-0.46	3.37:	0.17	0.30	...	-0.04	...	...	...	0.20	3.61
198478...	B3 IA	1.0	4.182	-0.68	0.08	4.84	-0.32	-0.46	-0.55	-0.09	-0.50	-0.35	-0.51	-0.46	4.83
				-1.40	-0.42	4.58	0.14	0.25	0.11	0.03	0.28	0.19	0.15	0.20	...
53Psc....	B3 V	1.0	4.253	-1.15	-0.31	5.63	0.14	0.23	0.16	0.04	0.24	0.17	0.17	0.20	5.81
147394...	B5 IV	2.4	4.180	-1.04	-0.33	3.69	0.12	0.22	0.15	-0.04	0.21	0.14	0.14	0.14	3.82
Mu And...	B5 V	1.4	4.193	-1.10	-0.33	4.30	0.16	0.24	0.18	-0.02	0.43	0.15	0.16	0.16	4.53
29 Psc...	B8 III	3.4	4.054	-0.93	-0.27	4.85	0.12	0.20	0.15	0.02	0.22	0.16	0.17	0.18	5.10
222439...	B8 V	0.7	4.079	-0.52	-0.26	3.87	0.11	0.19	...	-0.04	...	...	...	0.11	4.13
Io Oph...	B8 V	9.7	4.079	-0.69	-0.24	4.12	0.09	0.17	0.13	-0.01	0.17	0.11	0.14	0.14	4.28
109 Vir..	A0 V	2.4	3.982	-0.22	-0.15	3.33	0.04	0.09	0.08	-0.06	0.05	0.04	0.09	0.02	3.74
123299...	A0 III	2.7	3.973	-0.29	-0.20	3.55	0.04	0.08	0.06	-0.02	0.09	0.00	0.08	0.08	3.64
Z4 A.....	A0 V	14.0	3.982	0.00	0.00	7.00	0.00	0.00	0.00	0.00	0.00	0.00	0.00	0.00	...
12953	A1 IA	1.0	3.960	0.08	0.35	5.77	-0.50	-0.73	-0.85	-0.12	-0.81	-0.55	-0.79	-0.72	5.68
				-0.76	-0.22	5.48	0.02	0.07	-0.10	0.02	0.07	0.06	-0.04	0.03	
207260...	A2 IA	1.4	3.954	0.20	0.25	4.31	-0.41	-0.57	...	-0.14	...	...	...	-0.60	4.28
				-0.49	-0.23	4.06	0.03	0.10	...	-0.02	...	...	...	0.03	
AL.Lac...	A2 V	0.7	3.958	-0.24	-0.17	3.54	0.04	0.14	...	-0.14	...	...	...	...	3.85
1280.....	A2 V	0.7	3.958	-0.17	-0.11	4.36	0.02	...	...	-0.04	...	...	...	0.05	4.44
161817...	H.B.A2	20.7	3.956	0.12	0.08	6.85	-0.09	-0.14	-0.15	-0.04	-0.16	-0.10	-0.15	-0.13	6.98
210221...	A3 I	1.0	3.942	0.43	0.21	6.13	-0.32	-0.46	-0.48	-0.08	-0.51	-0.34	-0.48	-0.43	6.14
				-0.02	-0.11	5.97	-0.03	-0.01	-0.06	0.00	0.02	0.00	-0.06	0.01	
122458...	A3 III	2.7	3.944	0.06	0.04	4.12	-0.04	-0.06	-0.06	-0.08	-0.08	-0.08	-0.07	-0.06	4.26
173880...	A3 V	4.4	3.946	-0.10	0.04	4.19	-0.04	0.00	0.03	-0.04	-0.03	-0.05	0.04	-0.01	4.30
5448.....	A4 III	0.7	3.935	-0.04	-0.03	3.69	-0.04	-0.02	...	-0.07	...	...	...	-0.02	3.93
HR 343...	A7 V	1.7	3.914	0.00	0.08	4.15	-0.06	-0.07	-0.10	-0.05	-0.11	-0.07	-0.08	-0.08	4.33
187726,..	A7 III	1.4	3.914	0.05	0.09	3.89	-0.10	-0.12	...	-0.03	...	...	...	-0.16	...
159876,..	F0 IV	0.7	3.876	-0.59	-0.19	5.77	-0.03	0.02	...	-0.06	...	...	...	-0.06	3.54
571.....	F2 II	0.7	3.860	0.34	0.28	4.90	-0.27	-0.38	...	-0.05	...	...	...	-0.44	5.05
				0.14	0.14	4.83	-0.14	-0.18	...	-0.03	...	...	...	-0.26	...
164136...	F2 II	2.1	3.860	0.11	0.23	4.49	-0.27	-0.36	...	-0.05	...	...	...	-0.37	4.48
				0.00	0.15	4.45	-0.20	-0.26	...	-0.07	...	...	...	-0.27	...

TABLE 2 (continued)

Name	Type	W	log T_e	u	b	m_g	o	r	Hα	Mg	IR	Ti	Hα′	66	m_v
S93824...	F2 V	1.0	3.860	-0.05	0.31	6.06	-0.24	-0.33	-0.35	-0.02	-0.38	-0.26	-0.34	-0.32	6.11
128167...	F2 V	1.7	3.860	-0.23	0.28	4.41	-0.26	-0.35	-0.38	-0.21	-0.40	-0.30	-0.38	-0.35	4.45
35 Peg...	F4 V	0.7	3.839	0.06	0.33	5.41:	-0.20	-0.27	...	-0.06	...	...	...	-0.33	4.80
110 Her..	F5 V	2.7	3.827	-0.12	0.36	4.18	-0.29	-0.40	-0.47	-0.08	-0.50	-0.30	-0.45	-0.44	4.20
140283...	F5 VI	0.7	3.827	-0.26	0.34	7.30	-0.39	-0.57	...	-0.13	...	...	...	-0.60	7.26
142860...	F6 V	1.7	3.813	-0.13	0.40	3.87	-0.32	-0.46	-0.50	-0.09	-0.51	-0.40	-0.50	-0.49	3.85
194598...	F6 V	0.7	3.813	0.01	0.26	5.70	-0.23	-0.34	...	-0.08	...	...	...	-0.38	...
222368...	F7 V	3.8	3.798	-0.12	0.38	4.11	-0.35	-0.47	-0.53	-0.11	-0.54	-0.40	-0.51	-0.48	4.13
Del.Equ..	F7 V	0.7	3.798	-0.13	0.40	4.44	-0.07	-0.07	...	-0.06	...	...	...	-0.42	4.51
36A UMA..	F8 V	0.7	3.786	-0.15	0.32	4.96	-0.29	-0.38	...	-0.07	...	...	...	-0.41	4.82
142373...	F9 V	11.7	3.780	-0.07	0.47	4.62	-0.55	-0.55	-0.61	-0.08	-0.63	-0.44	-0.58	-0.54	4.60
217476...	G0 IA	0.7	3.763	1.63	...	5.11	-1.19	-1.24	...	...	...	...	...	...	4.99
				0.64:	...	4.81:	-0.58:	-0.30:	...	...	...	...	...	...	...
122563...	G0 II	1.7	3.766	0.60	0.83	6.29	-0.64	-0.98	-0.99	-0.14	-1.04	-0.73	-0.99	-0.91	6.20
				0.30	0.62	6.18	-0.45	-0.69	-0.72	-0.10	-0.72	-0.52	-0.72	-0.64	...
176051...	G0 V	18.7	3.771	0.03	0.55	5.23	-0.40	-0.59	-0.62	-0.04	-0.64	-0.44	-0.60	-0.57	5.22
Nu And...	G0 V	3.1	3.776	-0.06	0.43	4.07	-0.35	-0.47	-0.54	-0.09	-0.55	-0.41	-0.52	-0.49	4.08
160693...	G0 V	1.4	3.771	-0.10	0.51	8.49	-0.38	-0.54	...	-0.07	...	...	...	-0.57	...
165401...	G1 V	10.7	3.766	0.00	0.56	6.81	-0.39	-0.58	-0.62	-0.03	-0.62	-0.43	-0.59	-0.56	...
Gam Ser..	G2 IV-V	3.4	3.758	0.06	0.57	4.50	-0.39	-0.54	-0.60	-0.08	-0.61	-0.42	-0.57	-0.58	4.43
179957-8.	G4 V	0.7	3.757	0.09	0.64	6.02	-0.40	-0.61	...	0.02	...	...	...	-0.56	5.90
206859...	G5 IB	4.1	3.710	1.27	1.35	4.54	-0.72	-0.99	-1.06	-0.13	-1.11	-0.79	-1.01	-0.98	4.35
				1.03	1.18	4.46	-0.57	-0.76	-0.85	-0.10	-0.86	-0.62	-0.80	-0.77	...
175305...	G5 III	0.7	3.700	0.22	0.71	7.09	0.50	0.78	...	-0.12	...	...	...	-0.78	...
31 Aql...	G5 IV	0.7	3.737	0.48	0.82	5.21	-0.49	-0.66	...	-0.05	...	...	...	-0.67	5.17
Mu Her...	G5 IV	0.7	3.727	0.40	0.76	3.48	-0.47	-0.66	...	-0.09	...	...	...	-0.70	3.35
51 Peg...	G5 V	2.4	3.753	0.20	0.67	5.45	-0.42	-0.57	-0.60	-0.05	-0.61	-0.45	-0.57	-0.61	5.53
219615...	G7 III	1.7	3.694	0.73	1.00	3.87	-0.58	-0.84	-0.96	-0.12	-0.98	-0.70	-0.92	-0.85	3.69
13611....	G8 III	1.0	3.691	0.73	0.98	5.24	-0.57	-0.82	-0.90	-0.12	-0.92	-0.63	-0.87	-0.82	4.44
Mu Peg...	G8 III	0.7	3.688	0.72	1.02	3.64	-0.57	-0.77	...	0.00	...	...	...	-0.77	3.50
129312...	G8 III	1.7	3.688	1.00	1.17	5.03	-0.63	-0.88	-0.93	0.17	-0.96	-0.72	-0.95	-0.88	...
88512....	G8 IV	0.7	3.711	0.50	0.88	3.82	-0.57	-0.83	...	-0.12	...	...	...	-0.89	...
199191...	K0 III	0.7	3.674	0.80	1.10	7.23	-0.47	-0.68	...	-0.02	...	...	...	-0.78	...
181276...	K0 III	0.7	3.674	0.90	1.07	3.86	-0.58	-0.84	...	-0.03	...	...	...	-0.87	3.84
59 Aql...	K0 III	2.4	3.670	1.13	1.24	4.87	-0.67	-0.94	-1.01	-0.07	-1.04	-0.75	-0.96	-0.91	4.73
212943...K0	III-IV	1.4	3.690	1.10	1.22	4.84	-0.69	-0.98	...	-0.08	...	...	...	-0.96	4.80
185144...	K0 V	2.1	3.719	0.43	0.86	4.65	-0.52	-0.78	...	-0.06	...	...	...	-0.79	4.68
54 Psc...	K0 V	1.7	3.719	0.68	0.99	5.97	-0.57	-0.79	-0.84	0.02	-0.85	-0.63	-0.82	-0.78	5.84
145675...	K0 V	1.7	3.719	0.81	1.03	6.65	-0.57	-0.81	-0.83	0.00	-0.84	-0.64	-0.84	-0.80	...
210745...	K1 IB	0.7	3.672	2.32	2.03	3.74	-1.03	-1.46	...	-0.17	...	...	...	-1.45	3.36
				1.87	1.73	3.59	-0.76	-1.04	...	-0.10	...	...	...	-1.06	...
6833.....	K1 III	0.7	3.660	1.22	1.33	6.96	-0.78	-1.12	...	-0.15	...	...	...	-1.10	...
36 And...	K1 IV	1.7	3.680	1.11	1.23	5.60	-0.67	-0.93	-0.98	-0.02	-1.00	-0.74	-0.96	-0.91	5.45
Gam Cep..	K1 IV	0.7	3.680	1.11	1.16	3.44	-0.68	-0.93	...	-0.07	...	...	...	-0.92	3.22

TABLE 2 (continued)

Name	Type	W	log T_e	u	b	m_g	o	r	Hα	Mg	IR	Ti	Hα′	66	m_v
139323...	K2 V	1.7	3.645	1.12	1.18	7.80	-0.53	-0.89	-0.80	-0.02	-0.86	-0.65	-0.85	-0.86	...
139341...	K25 V	1.7	3.642	0.85	1.06	6.91	-0.61	-0.87	-0.91	0.06	-0.93	-0.70	-0.93	-0.87	...
13686....	K3 IB	1.0	3.631	2.69	2.34	8.09	-1.34	-1.92	-1.89	-0.18	-2.02	-1.45	-1.86	-1.81	7.2:
				2.23	2.02	7.93	-1.05	-1.47	-1.47	-0.10	-1.53	-1.11	-1.44	-1.39	...
143107...	K3 III	1.7	3.624	1.60	1.54	4.39	-0.81	-1.12	-0.10	-0.10	-1.24	-0.90	-1.19	-1.13	4.15
Del And..	K3 III	0.7	3.624	1.75	1.59	3.79	-0.71	-0.75	...	0.28	...	...	...	-0.89	3.21
39 Cyg...	K3 III	0.7	3.624	1.96	1.74	4.71	-0.89	-1.24	...	-0.05	...	...	...	-1.27	4.40
20 Cyg...	K3 III	0.7	3.624	1.19	1.69	5.26	-0.85	-1.17	...	-0.01	...	...	...	-1.14	5.00
Mu Aql...	K3 III	0.7	3.624	1.57	1.48	4.67	-0.79	-1.08	...	-0.02	...	...	...	-1.07	4.44
16160....	K3 V	1.0	3.644	0.96	1.19	5.98	-0.72	-1.01	-1.03	0.12	-1.08	-0.77	-1.01	-0.96	5.82
219134...	K3 V	0.7	3.644	1.11	1.27	5.69	-0.72	-1.02	...	...	...	...	...	-1.02	5.57
13520....	K4 III	1.0	3.603	2.24	1.98	5.23	-1.04	-1.49	-1.48	-0.06	-1.61	-1.08	-1.47	-1.43	4.94
Nu Peg...	K4 III	1.7	3.603	2.30	2.00	5.20	-1.00	-1.40	-1.42	0.00	-1.51	-1.04	-1.41	-1.36	4.84
200905...	K5 IB	1.4	3.574	2.41	2.11	4.18	-1.10	-1.56	...	-0.16	...	...	...	-1.60	3.72
				2.18	1.96	4.11	-0.96	-1.34	...	-0.13	...	...	...	-1.40	...
189319...	K5 III	0.7	3.577	2.58	2.09	3.85	-1.06	-1.58	...	-0.08	...	...	...	-1.57	3.56
Gam Dra..	K5 III	0.7	3.577	2.37	1.93	2.69	-0.99	-1.46	...	-0.13	...	...	...	-1.48	2.22
154363...	K5 V	0.7	3.643	1.08	1.24	8.17	-0.96	-1.37	...	-0.04	...	...	...	-1.38	...
61 Cyg A.	K5 V	0.7	3.643	1.36	1.42	5.67	-0.85	-1.19	...	0.18	...	...	...	-1.17	5.19
61 Cyg A&B	K5-7 V	1.0	3.620	1.36	1.49	5.12	-0.98	-1.37	-1.41	0.11	-1.46	-1.04	-1.40	-1.34	4.78
157881...	K7 V	1.0	3.602	1.55	1.61	7.92	-1.14	-1.58	-1.61	...	-1.61	-1.19	-1.61	-1.55	7.54
147379...	M0 V	0.7	3.574	1.60	1.65	8.97	-1.17	-1.71	...	-0.05	...	...	...	-1.72	...
204724...	M1 III	0.7	3.556	2.56	2.11	4.89	-1.07	-1.66	...	-0.05	...	...	...	-1.60	4.61
1326A....	M1 V	1.7	3.556	1.67	1.71	8.58	-1.20	-1.84	-1.95	-0.02	-1.93	-1.10	-1.87	-1.77	...
208816...	M2 IA	0.7	3.544	...	1.94	5.44	-1.35	-2.16	...	-0.21	...	...	...	-2.09	4.9:
				...	1.67	5.31	-1.11	-1.79	...	-0.16	...	...	...	-1.74	...
13136....	M2 IB	1.0	3.544	3.02	2.59	9.15	-1.63	-2.53	-2.42	-0.26	-2.70	-1.63	-2.37	-2.29	...
				2.16	2.00	8.85	-1.10	-1.69	-1.65	-0.16	-1.78	-1.01	-1.60	-1.52	...
1013.....	M2 III	0.7	3.544	2.67	2.02	...	-1.07	-1.87	...	-0.15	...	...	...	-1.76	4.8:
175588...	M4 II	0.7	3.510	2.31	1.99	4.51	-1.01	-1.87	...	-0.20	...	...	...	-1.77	4.33
173739...	M3 V	1.4	3.527	1.52	1.60	9.52	-1.12	-1.87	...	-0.16	...	...	...	-1.85	...
173739-40	M3-4 V	1.0	3.480	1.60	1.65	8.49	-1.09	-1.92	-2.01	-0.07	-2.03	-0.85	-1.91	-1.80	8.47
B 1°-4774	M3 V	1.0	3.515	1.54	1.58	9.98	-1.14	-1.78	-1.89	-0.02	-1.84	-1.08	-1.80	-1.71	8.98
132813...	M5 III	1.7	3.470	2.39	1.83	4.84	-1.04	-1.93	-1.91	-0.23	-2.35	-0.88	-1.96	-1.81	4.69
R Lyr....	M5 III	1.7	3.470	2.07	1.48	4.56	-1.03	-2.00	-1.97	-0.22	-2.46	-0.90	-2.03	-1.84	4.0:
148783...	M6 III	1.0	3.430	1.84	1.16	5.37	-1.13	-2.28	-2.21	...	-2.79	-1.03	-2.29	-2.11	4.4:
Z3 A.....		12.0		0.65	0.07	8.67	-0.02	-0.04	-0.05	-0.01	-0.03	-0.02	-0.05	-0.02	...
Z3 K.....		9.0		2.54	2.16	7.49	-1.11	-1.67	-1.69	-0.03	-1.78	-1.07	-1.65	-1.58	...
Z4 K.....		13.0		1.79	1.72	7.14	-0.90	-1.31	-1.33	-0.06	-1.40	-0.99	-1.30	-1.26	...
Z5 A.....		14.0		-0.08	0.26	7.69	-0.20	-0.30	-0.28	-0.03	-0.31	-0.21	-0.28	-0.26	...
Z5 K.....		13.0		1.84	1.68	6.45	-0.84	-1.20	-1.24	-0.07	-1.28	-0.92	-1.21	-1.17	...
Z6 K.....		8.0		0.10	0.24	7.47	-0.13	-0.19	-0.16	-0.02	-0.21	-0.14	-0.17	-0.16	...
Z7 A.....		8.0		-0.12	0.04	7.81	-0.10	-0.14	-0.10	-0.03	-0.15	-0.10	-0.11	-0.11	...

TABLE 3

Estimated Errors of Observations

Year	u-g	b-g	g	0-g	r-g	Hα-g	Mgb-g	IR-g	TiO-g	Hα′-g	66-g
1973...	0.019	0.018	0.052	0.015	0.017	...	0.016	...	...	...	0.023
1974...	0.013	0.010	0.014	0.007	0.010	0.012	0.010	0.014	0.012	0.013	0.011
Systematic Difference between Observations at Palomar and Table Mountain:											
	0.011	0.019	0.010	0.008	0.009	0.007	0.005	0.006	0.011	0.018	0.012

TABLE 4

AVERAGE STAR COLORS

T_e	L.C.	(u-g)	(b-g)	(o-g)	(r-g)	(Hα-r)	(Mgb-g)	(IR-r)	(TiO-o)	(Hα'-r)	(66-r)	(V-g)
4.7	---	-1.89	-0.51	0.15	0.29	-0.11	-0.03	0.02	0.07	-0.06	-0.01	0.21
4.6	---	-1.83	-0.49	0.15	0.29	-0.10	-0.03	0.02	0.06	-0.06	-0.01	0.20
4.5	---	-1.69	-0.46	0.15	0.29	-0.09	-0.03	0.01	0.05	-0.05	-0.01	0.19
4.4	I	-1.58	-0.43	0.15	0.28	-0.08	-0.03	0.00	0.04	-0.05	-0.02	0.18
	III	"	"	"	0.28	"	"	"	"	"	"	"
	V	-1.56	"	"	0.28	"	"	"	"	"	"	"
4.3	I	-1.44	-0.40	0.14	0.26	-0.08	-0.03	0.00	0.04	-0.05	-0.02	0.17
	III	"	"	"	"	"	"	"	"	"	"	"
	V	-1.36	-0.38	"	"	"	"	"	"	"	"	"
4.2	I	-1.29	-0.37	0.13	0.24	-0.08	-0.04	-0.01	0.03	-0.05	-0.02	0.15
	III	-1.22	"	"	"	-0.07	"	"	"	"	"	"
	V	-1.11	-0.33	"	"	-0.06	"	"	"	"	"	"
4.1	I	-1.06	-0.32	0.12	0.20	-0.05	-0.04	-0.02	0.03	-0.03	-0.03	0.12
	III	-0.93	"	"	"	-0.04	"	"	"	"	"	"
	V	-0.79	-0.27	"	"	-0.03	"	"	"	"	"	"
4.0	I	-0.70	-0.24	0.07	0.13	-0.04	-0.04	-0.02	0.01	-0.03	-0.01	0.06
	III	-0.54	"	0.06	0.13	-0.02	"	"	"	-0.02	"	"
	V	-0.43	-0.16	0.07	0.13	0.01	"	"	"	0.00	0.00	"
3.95	I	-0.17	-0.11	-0.03	0.01	-0.04	-0.04	-0.02	0.00	-0.03	0.02	0.03

TABLE 4 (CON'T)

T_e	L.C.	(u-g)	(b-g)	(o-g)	(r-g)	(Hα-r)	(Mgb-g)	(IR-r)	(TiO-o)	(Hα'-r)	(66-r)	(V-g)
3.95	III	0.00	-0.08	-0.02	0.01	-0.01	-0.04	-0.02	0.00	-0.02	0.02	0.03
	V	-0.14	-0.03	-0.02	0.01	0.02	"	"	"	0.03	"	"
3.9	I	0.00	0.01	-0.20	-0.22	-0.04	-0.04	-0.04	-0.02	-0.03	0.01	-0.01
	III	0.00	0.04	-0.10	-0.16	-0.02	"	"	"	-0.02	"	"
	V	0.00	0.11	-0.10	-0.16	0.00	"	"	"	0.00	"	"
3.85	I	-0.00	0.17	-0.26	-0.34	-0.05	-0.05	-0.06	-0.03	-0.02	0.00	-0.05
	III	-0.07	0.22	-0.20	-0.31	"	"	"	"	"	"	"
	V	-0.07	0.27	-0.20	-0.31	"	"	"	"	"	"	"
3.8	I	-0.10	0.37	-0.40	-0.50	-0.06	-0.06	-0.07	-0.05	-0.03	-0.01	-0.09
	III	-0.15	0.40	-0.30	-0.47	"	"	"	"	"	"	"
	V	-0.15	0.40	-0.30	-0.47	"	"	"	"	"	"	"
3.75	I	0.37	0.85	-0.53	-0.67	-0.07	-0.11	-0.08	-0.07	-0.02	0.02	-0.14
	III	0.12	0.56	-0.44	-0.62	"	-0.07	"	"	"	0.01	"
	V	0.12	0.63	-0.44	-0.62	"	-0.03	"	"	"	0.01	"
3.7	I	1.18	1.28	-0.67	-0.84	-0.08	-0.14	-0.10	-0.08	-0.03	0.01	-0.23
	III	0.57	0.80	-0.56	-0.78	-0.08	-0.06	"	"	"	"	"
	V	0.66	0.93	-0.55	-0.78	"	0.00	"	"	"	"	"
3.65	I	1.96	1.84	-0.91	-1.06	-0.07	-0.16	-0.11	-0.08	-0.02	0.03	-0.32
	III	1.26	1.37	-0.73	-1.03	"	-0.05	"	"	"	0.02	"
	V	1.01	1.17	-0.73	-1.03	"	0.08	"	"	"	0.02	"
3.6	I	2.25	2.03	-1.03	-1.43	-0.06	-0.19	-0.12	-0.05	-0.02	0.06	-0.44
	III	2.29	2.01	-1.01	"	"	-0.06	"	"	"	0.04	"
	V	1.42	1.53	-1.01	"	"	0.10	"	"	"	0.05	"

T_e	L.C.	(u-g)	(b-g)	(o-g)	(r-g)	(Hα-r)	(Mgb-g)	(IR-r)	(TiO-o)	(Hα'-r)	(66-r)	(V-g)
3.55	I	2.15	1.83	-1.09	-1.70	-0.07	-0.21	-0.13	0.05	0.02	0.08	-0.56
	III	2.57	2.04	-1.09	-1.70	"	-0.08	"	"	-0.02	0.05	"
	V	1.61	1.65	-1.08	-1.56	"	0.05	"	"	-0.02	0.05	"
3.5	I	2.00	1.75	-1.14	-1.90	-0.07	-0.25	-0.14	0.12	0.03	0.10	-0.66
	III	2.40	1.90	-1.10	-1.90	"	-0.18	"	"	-0.01	0.08	"
	V	1.81	1.68	-1.10	-1.75	"	-0.11	"	"	-0.01	0.08	"
3.45	I	2.00	1.62	-1.15	-1.99	-0.08	-0.27	-0.15	0.17	0.02	0.12	-0.72
	III	2.04	1.45	-1.10	-1.99	"	-0.24	"	"	0.00	0.10	"
	V	2.01	1.68	-1.10	-1.95	"	-0.16	"	"	0.00	0.10	"

CAPTION FOR FIGURE

Figure 1:

Transmission curves for Gunn filters.

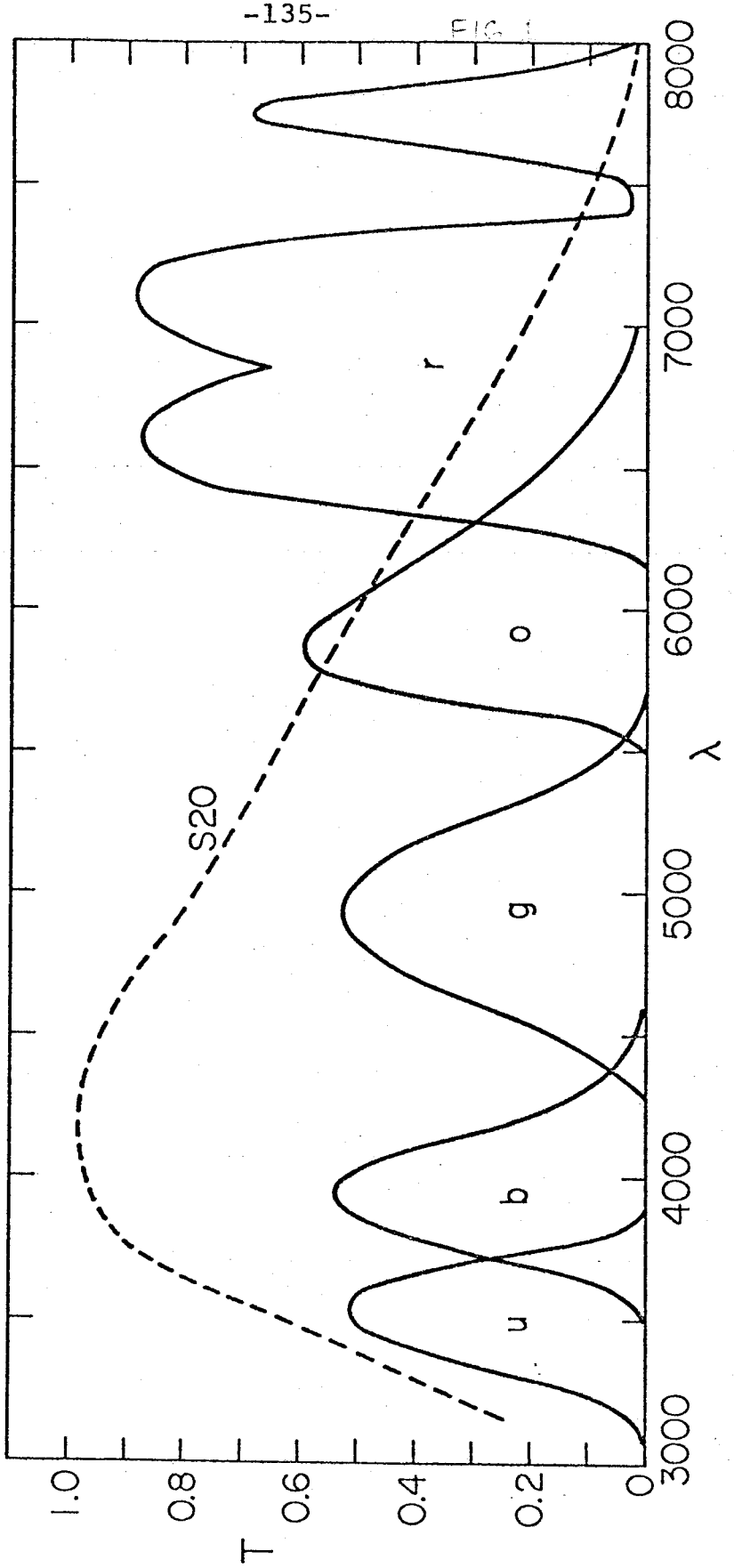
FIG. 1
T
λ
1.0
0.8
0.6
0.4
0.2
0
3000
4000
5000
6000
7000
8000
S20
u
b
g
o
r